COMMUNICATIONS QUARTERLY

THE JOURNAL OF COMMUNICATIONS TECHNOLOGY

Summer 1996 $9.95

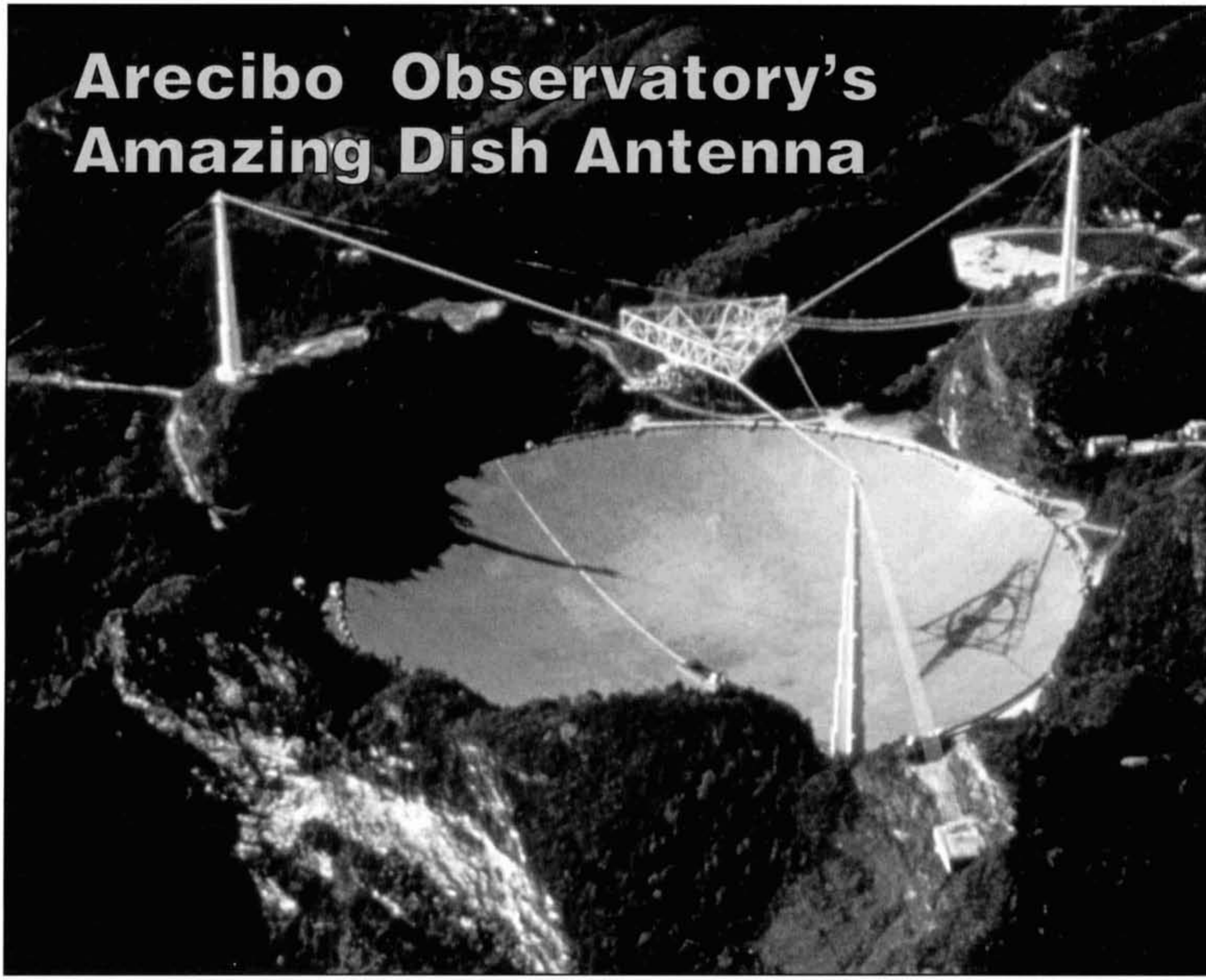

- Build a Tracking Generator for 0 to 2 GHz
- The Ultimate (and Transformerless!) Noise Bridge
- Fractal Antennas: Part 2
- The 2-Meter Discpole Antenna
- Anapoles: Toroidal Inductor Radiation
- A Yaesu FT-990/1000 Interface Circuit
- 4CX400A Russian Tubes
- Modeling and Understanding Small Beams: Part 4
- An Analysis of Long-Path Propagation Data at Solar Minimum
- The Wiltron Site Master: Return Loss/DTF Tester

ISSN 1053-9433


Svetlana DX Winners
4CX800A
4CX1600B
Conservative full legal output power of 1500W CW Key Down 4CX1600B (one) or 4CX800A (pair)
Simple low cost linear design
Low distortion
High stability
Rugged reliable Russian power tube quality
Svetlana quality backed by the best warranty in the business

COMMUNICATIONS QUARTERLY

THE JOURNAL OF COMMUNICATIONS TECHNOLOGY

CONTENTS

Volume 6, Number 3 Summer 1996

page 17

page 77

On the Cover: Arecibo Observatory, which boasts one of the world's most magnificent dish antennas, lies nestled in the hills of Puerto Rico. Turn to "Antennae Exotica" on page 17 to learn more. (Photo courtesy of Arecibo Observatory)

EDITORIAL

Is presentation everything?

I was cruising through the classifieds on AOL when a posting for some interesting antique radios caught my eye. The gentleman selling them turned out to be a ham in a neighboring state. I called and he invited me over, saying, "Come on up. The trip will be well worth your while!" When the next morning showed promise of becoming a beautiful New England day, I decided to make the drive and see for myself.

Now this fellow had some choice pieces, a 1931 Atwater-Kent model 80 cathedral and an early 1930's model 288 Zenith tombstone. This is the sort of stuff any radio collector would pay a hefty sum for—if the condition warranted! The AK 80, with its ornately spiraled side columns and detailed woodwork, is highly sought after by collectors.

When I head off on these trips, I always prepare for the worst. Mostly, I find old radios that have been stored in damp cellars for the last 50 years. The grille cloths are tattered and shredded, the chassis rusted, and the plywood and surface veneers long separated! Even the mice have lost interest and have long vacated these radios in search of better digs.

After a pleasant drive, I arrived at the owner's QTH in the Berkshire Mountains of rural Western Massachusetts. Following a brief exchange of introductions, he led me into a garage with a damp, earthen floor. As always, I was prepared for the worst. After some rummaging around, my host found the AK cathedral huddled away in a box of junk. I winced as he lifted the aged radio from its seclusion by grasping the top and giving it a hefty yank. The elderly cabinet obviously resented this rough treatment, and it responded with some loud creaks and groans in protest. I stepped back, expecting to get a good view of the arch-shaped upper cabinet section as it rocketed skyward, jettisoning its heavy chassis and wood base—leaving it to return and crash to earth. But, somehow, that resilient old fellow held together!

The Zenith was in equally poor condition. Layers of dirt, grime, and surface scratches covered its once finely polished and lacquered cabinet. Some recent abuse had also chipped away the edges of the front panel veneers. Sigh. To pique my interest, he continued to add items to the pile. There was a vintage Peerless cathedral-style speaker, several boxes of used TV tubes, piles of dusty early 1930's radio magazines, and a World War II German field telephone—with a section of the handset cord cut and missing.

We agreed on a fair price for the entire lot, although I was rather unhappy with the condition of the equipment. At least the radios hadn't been in the garage long enough for the glues to have weakened.

Upon arriving home, I unloaded my haul. Several days later, my XYL, normally tolerant of my penchant for adopting these vintage orphans, was beginning to mutter about the "trash" I had abandoned on her porch.

I set to work. After a few days of cleaning, combined with some furniture restoration tricks I've learned over the years, the radios started to look like themselves again. A final coat of shoe polish "wax" was applied and buffed...and there it was! The deep luster of the hand-rubbed lacquer finish the old stalwarts had sported over 60 years ago had returned!

So, what's my point? All too often at hamfests or antique radio meets, I see items—old and not so old—offered at premium prices. Sadly, most of this equipment usually looks about the same as the stuff I recovered from that garage in New England. Nicotine stains and years of grime, accented by burnt-out pilot lamps, mismatched knobs and missing rubber feet, are the first things I notice. If they exist at all, the manuals have torn covers, coffee stains, and other signs of neglect. To my mind, the seller is telling me: "I don't take pride in my equipment, but I want top dollar anyway! Take it or leave it!" I usually leave it, as do most other collectors, and the seller ends up carting the stuff home.

Had the owner of those radios taken a few days to make them more presentable, even displayed them proudly in his home, he probably could've tripled his asking price. No doubt he would have gotten it, eventually!

The same caveat goes for sellers at hamfests. A few hours spent cleaning the equipment, a few pennies for new pilot lamps, and replacements for those missing knobs and feet will reap the same rewards. Manuals in protective covers, even if torn, convey the message: "Hey, the gear is old, but well cared for. It's clean and worth my price!" This makes a sale more likely. At the least, more prospective buyers will stop, look, and haggle!

Here's where we can all learn a lesson from used car dealers. Even the oldest car on the lot is detailed, cleaned, and polished. Adorned with colorful pennants, they almost seem to yell out: "Buy me, I'm worth owning."

As *Communications Quarterly*'s senior technical editor, I face the same choices with our writers. For instance, an author submits a routine article for editorial review. His manuscript is double spaced, spell checked, and has undergone several rewrites before it arrives at our editorial offices. His footnotes and references are in order, the drawings and schematics are neatly drawn, and the captions are supplied. He's shown he cares, and takes pride in what he does, giving his work credibility.

Another author sends in a manuscript of far greater technical merit, but submits what is obviously a first rough draft. It's printed single space in small type with a worn ribbon and no margins. To top it all off, there are spelling errors. His drawings are rough sketches, with no tie ins to the text. Guess which manuscript I'll give my attention to first?

Of course, it's important to remember that even though something looks great, it may be just an empty shell. On the other hand, those scruffy old radios I bought from that guy in Massachusetts were beautiful under the years of accumulated grime. It's important to weigh each situation individually. After all, what good is a nice looking article with no substance?

Unfortunately, fair or not, in life presentation is often considered everything. People and objects are judged by the first impressions they make. Consequently, whether it be in the realm of our careers or our hobbies, the payback for that little extra effort is often well rewarded.

By the way, that wonderful old cathedral radio is now fully restored inside and out, playing away as I write this parable. 73.

Peter Bertini, K1ZJH
Senior Technical Editor

A publication of
CQ Communications, Inc.
76 North Broadway
Hicksville, NY 11801-USA

Editorial Offices: P.O. Box 465, Barrington, NH 03825. *Telephone/FAX: (603) 664-2515.* **Business Offices:** 76 North Broadway, Hicksville, NY 11801. Telephone: (516) 681-2922. FAX: (516) 681-2926.

Communications Quarterly is published four times a year (quarterly) by *CQ Communications, Inc. Communications Quarterly* is the philosophical successor of *Ham Radio Magazine* founded by T.H. "Skip" Tenney, Jr., W1NLB and James R. Fiske, W1HR. Subscription prices (all in U.S. Dollars): Domestic—one year $29.95; two years $56.95. Canada/Mexico—one year $34; two years $65. Foreign—one year $39.95; two years $76.95. Foreign Air Mail—one year $80; two years $155.

Second-class postage paid at Hicksville, NY and additional mailing offices.

Postmaster: Please send change of address to Communications Quarterly, CQ Communications, Inc., 76 North Broadway, Hicksville, NY 11801. ISSN 1053-9344.

Printed in U.S.A.

TECHNICAL CONVERSATIONS

Computer glitch shaves 30 years off life of sunspot cycle 22

Dear Editor:

I just noticed, in my letter on sunspots in the Winter 1996 issue, that the end of the present cycle is given as 1966.5. It should be 1996.5.

My word processor stuttered on the wrong key, and I didn't catch it. Sorry about that!

Bob Haviland, W4MB
Daytona Beach, Florida

Because we were unable to obtain reproduction permission from the author, the following article does not appear in the *ARRL Communications Quarterly Collection*...

Letter: Technical Conversations—A Reader Takes Note

By Nathan "Chip" Cohen, N1IR

2 Ledgewood Place
Belmont, MA 02178

Summary: The author comments briefly on several articles that appeared in the spring 1996 *Communications Quarterly*. The comments range from a discussion of photos submitted by W7DHD showing a number of radio pioneers, to the "Hex" antenna by Mike Traffie, to Paul Shuch's SETI article.

Summer 1996, page 5.

Please contact the author for additional information.

Author shares fan mail

Hi Wade:

Read your NMR article in the winter 1996 issue of *Communications Quarterly*.

Great! Really enjoyed it!

Will the author autograph my copy please?

Ben Zigun, KA1WA
Fairfield, Connecticut

Editorials: Great!—BWO's: Not so much!

Dear Mr. Bertini:

First, in your excellent editorial in the winter '95 issue, you mentioned spectrum analyzers-- last year I bought an HP8690A sweeper mainframe and a couple of solid-state plug-ins for same. When I worked in RF a while ago, HP's non-solid-state plug-ins used a Backward-Wave Oscillator tube whose acronym "BWO" we pronounced as "BeWoe"—a fitting description when one of these expensive little puppies ceased working. I recall that at least one military surplus spectrum analyzer used a BWO as its LO, but I don't recall which model. I'd steer clear of these unless I had a 100-percent money back guarantee!

Incidentally, the HP8690A uses an obscure pentode to regulate the high-voltage supply for its BWO plug-ins. The tube, a 7239, resembles a 6CL6 (i.e., a nine-pin, tall miniature envelope) with a plate cap. The going rate for this tube is in the $50 range—more than what I paid for the entire 8690A. Prospective purchasers of older instruments should be aware that spares of oddball tubes can get expensive (not to mention hard to find!).

Another case in point: I picked up a Marconi TF1066B signal generator for $10 at a fleamarket. This instrument features a precision-machined tuned-cavity oscillator that requires an obscure disk-seal triode—a TD03-10E--that sells for $200 via Richardson Electronics. I made one attempt to purchase one for $50 via mail-order from England, only to lose my money when the dealer cashed my check and refused to either honor the check or respond to repeated correspondence.

On another topic, I wonder whether we as radio amateurs and constructors need to divert our energies into using surface-mount methods? How many of our home-brew projects really demand that degree of miniaturization? Also, some discrete components are getting to be hard to find—that's an issue above and beyond SMT components in small quantities. As a hobby, we're better off encouraging construction in *any* form, and not discouraging new hams by presenting them with projects that demand special tools or hard-to-find parts.

Thanks again for your interesting editorials!

Brad Thompson, AA1IP
Meriden, New Hampshire

Dear Brad:

Thank you for your kind comments.

Regarding your test equipment purchases, I think you are due some sort of award for being the best bargain hunter I have ever had the pleasure of hearing from!

As for SMT, we are absolutely not attempting to discourage any ham builders by offering projects that involve this new technology. To the contrary, we are trying to do everything possible to ease the transition for readers—whether it be through worthy SMT parts kits covered in our "Quarterly Devices" column, or by showing Rick Littlefield's clever SMT component workstation.

As you noted, many discrete components with wire leads are getting hard to find. And, there are many interesting chips that are only available in SMT packages. Analog Devices' AD607 receiver-on-a-chip comes to mind, despite its being offered only in a 20-pin SSOP package that is the spawn of the devil to work with! We are considering doing a few feature articles using this device, and if we do we will have pc boards made available for this or any project involving SMT components.

Peter Bertini, K1JJH
Senior Technical Editor

Speaking of annunciators . . .

Dear Editor:

Please accept my compliments on providing a very good publication; I have been a subscriber since the first issue. I have not yet read all of the articles in the Spring 1996 issue, but I would like to submit the following comments.

1. Regarding Michael E. Gruchalla's excellent article "Using Inexpensive Digital Panel Meters," please consider the following correction to Figure 10 on page 74, and to Figures 11 & 12 (including the text) on pages 76–77:

The term "enunciator" is incorrect. An enunciator " . . . pronounces words in an articulate or precise manner." It does not appear that the subject device has a voice output.

I believe that the correct term is "annunciator"—defined as a " . . . signaling apparatus (which) displays a visual indication when engaged by an electric current."

[*Random House Dictionary of the English Language, 2nd Ed., 1987*]

2. It is gratifying that most of the authors have cited their sources. To enhance the quality of the publication, I suggest that those Bibliographies, Notes and References be printed in a larger, bolder font. An Appendix might be more appropriate (e.g., Paul Shuch's article).

3. Please provide a copy of the Author's Guidelines, as noted on page 110 of the Spring 1996 issue.

Thank you for your attention to my comments and request.

73,

Harold R. Jones, W6ZVV
San Mateo, California

Wayne Ryder, *W6URH*
Senior Design Engineer
Data Broadcasting Corporation
1900 South Norfolk Street
San Mateo, California 94403

A TRACKING GENERATOR FOR 0 TO 2 GHz

Build this handy spectrum analyzer add-on

Tracking generators are very useful devices. When outfitted with a tracking generator, your spectrum analyzer will provide a quick visual presentation of an amplifier's frequency response, let you peek at the performance of high, lowpass, or bandpass filters, align duplexers or cavities, or even perform swept antenna responses using a directional coupler. **Photo A** shows the performance of a 120-MHz notch filter using the tracking generator/spectrum analyzer combination. The tracking generator can also serve, with some limitations, as a sweep generator for such tasks as video IF alignment.

Unfortunately, few home workshops or small labs can justify owning such a device. But, I'll show you how to build your own for a fraction of what a used unit would cost!

The tracking generator discussed here is for use with spectrum analyzers with a first IF at around 2 GHz. It covers a range of about 300 kHz to 1.8 GHz. This particular unit is designed to work with analyzers that supply an output of from +9 to +13 dBm from the swept first local oscillator (LO). Fortunately, many popular analyzers, such as the Tektronix 7L13, 71L4, and the Hewlett Packard 8554, 8558, provide this needed LO interjection signal for use with external tracking generators. If you have a spectrum analyzer for the lower HF ranges that uses a first IF at around 200 MHz, you may be interested in reviewing my earlier article.[1] But before you build it, contact me for the latest information and updates on that circuit.

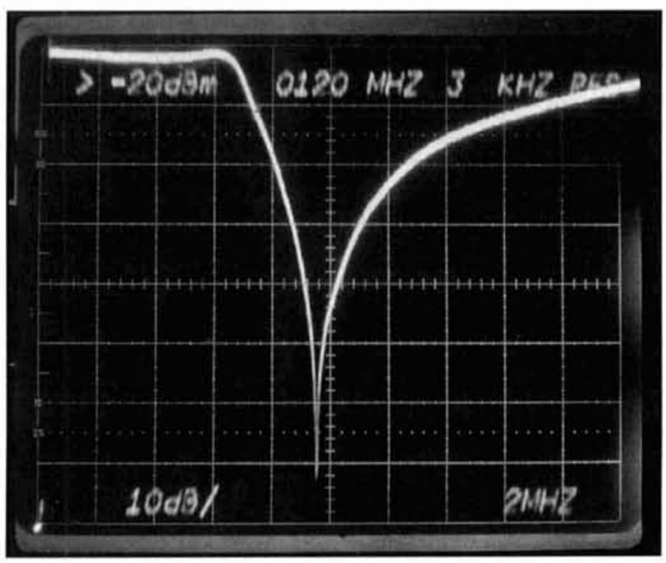

Photo A. Tracking generator used to display the performance of a 120-MHz notch filter.

Circuit description

The tracking generator must produce a CW signal centered on the frequency to which the spectrum analyzer is tuned. As the analyzer sweeps across a predetermined portion of the spectrum to be monitored, the tracking genera-

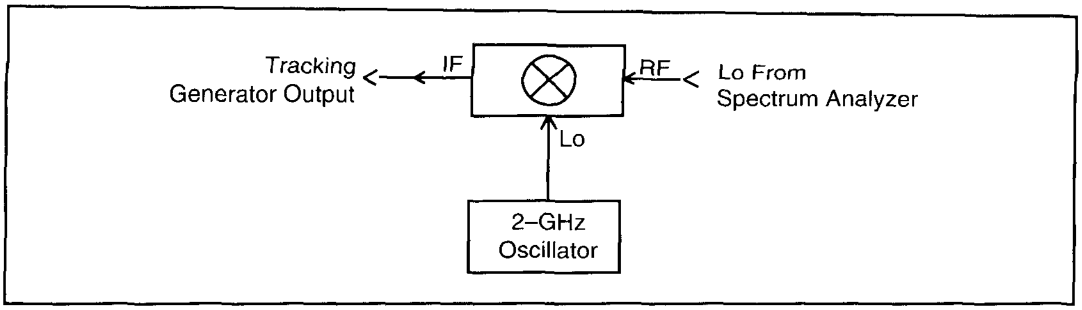

Figure 1. Basic diagram of what needs to be done to produce the centered CW signal.

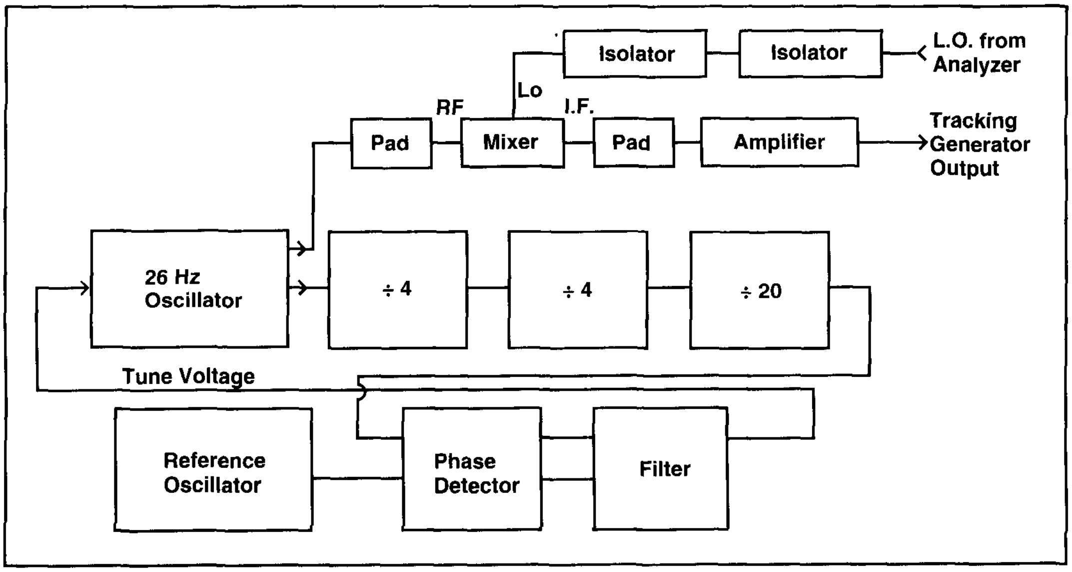

Figure 2. Tracking generator block diagram.

tor must accurately follow and generate an RF signal of constant amplitude on the analyzer's input frequency. The tracking generator RF output must be high enough to drive the analyzer display to over the 0 dB graticle, with enough power to comfortably handle the insertion loss of the device-under-test and associated fixed 50-ohm pads often used during these tests.

Figure 1 is a basic diagram of what needs to be done to accomplish this task. The LO output from the analyzer is mixed with a fixed oscillator 2-GHz signal that's centered exactly on the analyzer's first IF. Combined, these two signals produce an RF signal at the analyzer's input frequency over a range of about 0 to 1.8 GHz.

Unfortunately, in practice, things are a bit more complicated than what you see in **Figure 1**! **Figure 2** shows the actual tracking generator block diagram.

Two cascaded ferrite isolators (circulators with self-contained 50-ohm RF loads on the internal reject ports) are used to isolate the spectrum analyzer LO signal to prevent RF from the tracking generator feeding back into the analyzer. Each isolator should provide about 18 dB of isolation over the 2 to 4 GHz range with approximately 1 dB of insertion loss. Cascaded, the isolators will yield nearly 40 dB of isolation for about 2 dB insertion loss. Without the isolators, it would be possible for RF energy from the tracking generator to backfeed into the analyzer via its LO output jack.

Brand	Phone	Model	Isolation	Loss	Cost
UTE	908-922-1009	CT-3040-OT	18 dB	0.4 dB	$220
TRAK	813-884-1411	60A3001	18 dB	0.5 dB	$175
Loral	516-231-1700	4193	18 dB	0.5 dB	$265

Table 1. Currently manufactured isolators that meet the frequency, insertion loss, and isolation requirements for the tracking generator.

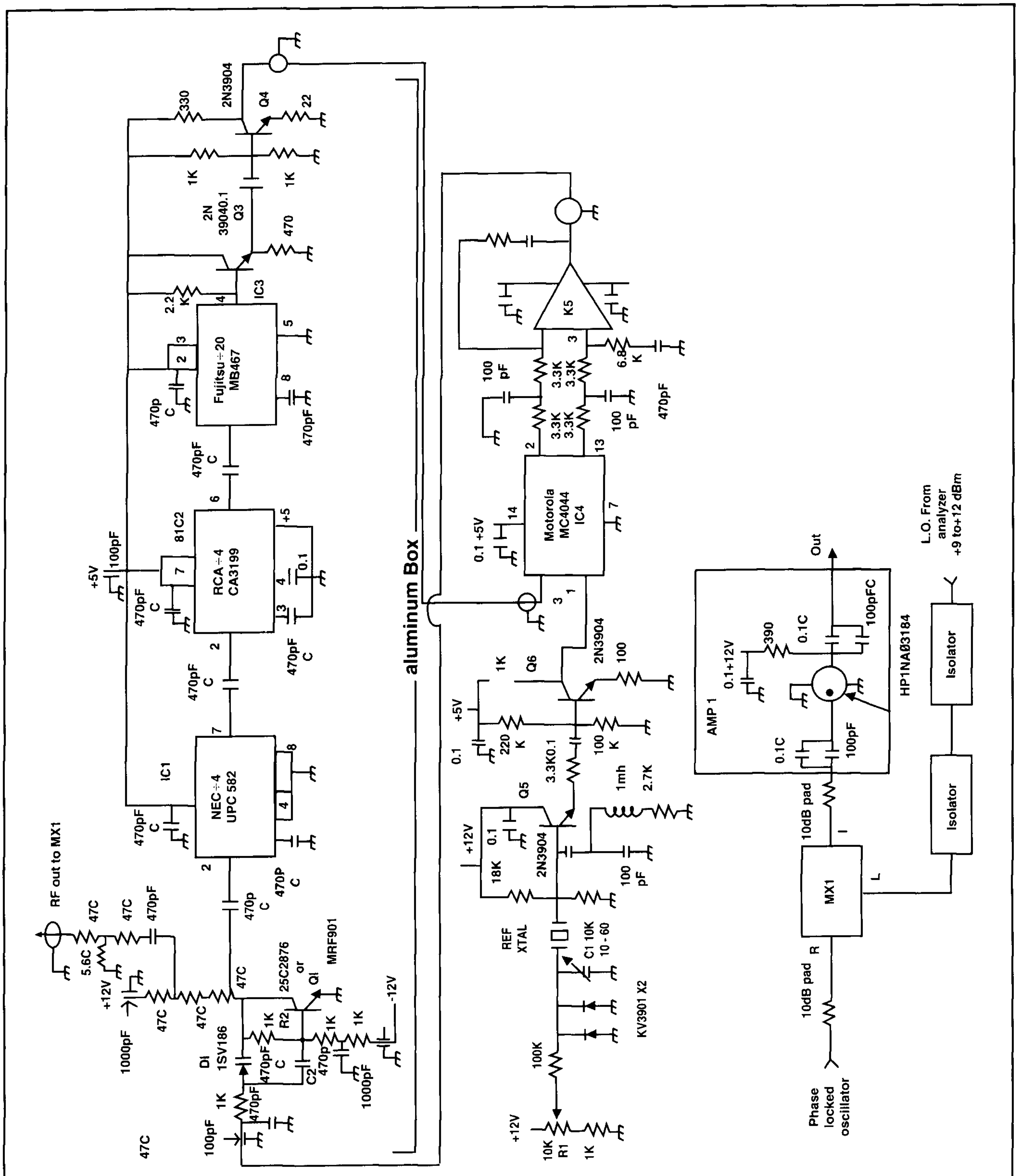

Figure 3. Tracking generator schematic. C equals chip part.

This could cause a rise in the analyzer's display base line, with a corresponding loss of usable dynamic range. For the same reason, the analyzer's input lowpass filter should be effective at rejecting spurious signals that fall on the analyzer's first IF.

I was fortunate to find two suitable isolators surplus at a good price! I used an Addington

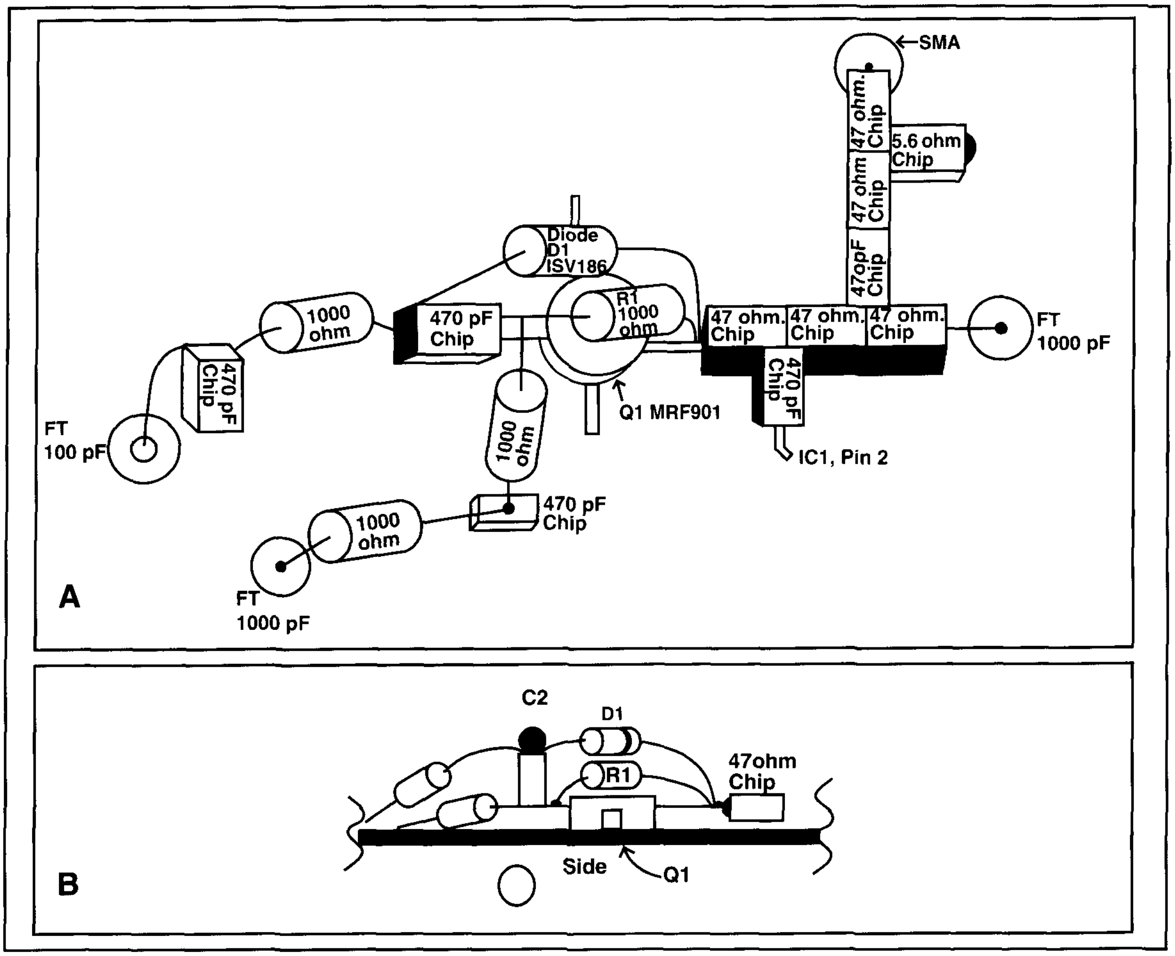

Figure 4. (A) The 2-GHz oscillator. (B) Side view.

model 217-0300, along with a UTE model CT3240. **Table 1** lists some suitable isolators that are currently available. Even if the isolators are purchased new, the total price for this generator is a bargain considering what an equivalent commercial model would cost new or used. Many mail-order surplus vendors carry microwave isolators.*

The LO output from the cascaded isolators feeds the LO point of a passive diode DBM (double-balanced mixer). I had a MiniCircuits Labs ZFM 4212 DBM on hand, so I tried it. Despite being rated to 1300 MHz (1.3 GHz), it still worked well at 1.8 GHz. The amplitude flatness of this tracking generator used with a Tek 7L14 was within 4 dB.

The required fixed 2 GHz injection signal is provided by a phase-locked oscillator circuit. Output from the oscillator is buffered by a fixed 10-dB pad (M/A Com 2082-6147-10, or equivalent). Tucker Electronics lists several such pads. Note that the attenuator after the mixer must be good to 4 GHz; the other must be rated to 2 GHz.

Phase locking system

Free running, the 2-GHz oscillator wouldn't be stable enough to maintain the tolerance needed. The oscillator is tuned via a 1SV186 varicap, permitting it to be phase locked to a reference crystal oscillator operating in the low HF range. Output from the oscillator is sampled and fed to IC1, a NEC 2-GHz divide-by-four prescaler chip. Extremely short lead lengths are needed for IC1! Chip bypass capacitors must be used where indicated. Again, short leads, careful bypassing, and a good groundplane will help alleviate any tendency towards self-oscillation in the first prescaler (see **Figure 3**).

Further prescaling is provided by an RCA CA3199 (divide-by-4) and Fujitsu MB467 (divide-by-20). The total prescaler provides for a divide by 320, producing an output of 6.5469

*Editor's note: I suggest that you give Tucker Electronics (1717 Reserve Street, Garland, Texas 75042; Telephone: 800-527-4642) a call about their surplus inventory. A recent Tucker catalog listed an E&M Labs S19P dual ferrite isolator rated for 2 to 4 GHz with 40-dB isolation for $200. No insertion loss data was given. That particular model also uses N rather than the smaller SMA fittings used on the author's isolators.

MHz at lock to correspond to an analyzer IF at 2.095 GHz.

$$2095 \text{ MHz} \div 320 = 6.5469 \text{ MHz} \quad (1)$$

A prescaler division by 256 would probably work, too, but would require a reference oscillator at around 8 MHz. Note that the upper limits of the MC4044 phase detector are around 8 MHz. The prescaler chips used in this circuit can get by with as little as 100 mV input.

2-GHz oscillator details

The circuit for the phase-locked 2-GHz oscillator is shown in **Figure 3**. Either a MRF-901 or 2SC2876 device may be used. Note that the oscillator is built "cordwood" style on a section of pc board (see **Figures 4A** and **B** for details). Very short lead lengths are used. The oscillator frequency is roughly "trimmed" by varying the soldered lead lengths of the varicap diode.

Preliminary VCO alignment

First, connect a variable 0 to 3-volt power supply (preferably a –6 to +6 volt) to the feedthrough supporting the 1SV186 varicap (the tuning voltage line to IC5 is temporarily disconnected). You'll need to supply power to the 2-GHz oscillator and prescalers. Monitor the prescaler output using a frequency counter. Varying the varicap supply voltage should cause a corresponding shift in the displayed frequency. If not, IC1, the first prescaler stage, may be self-oscillating.

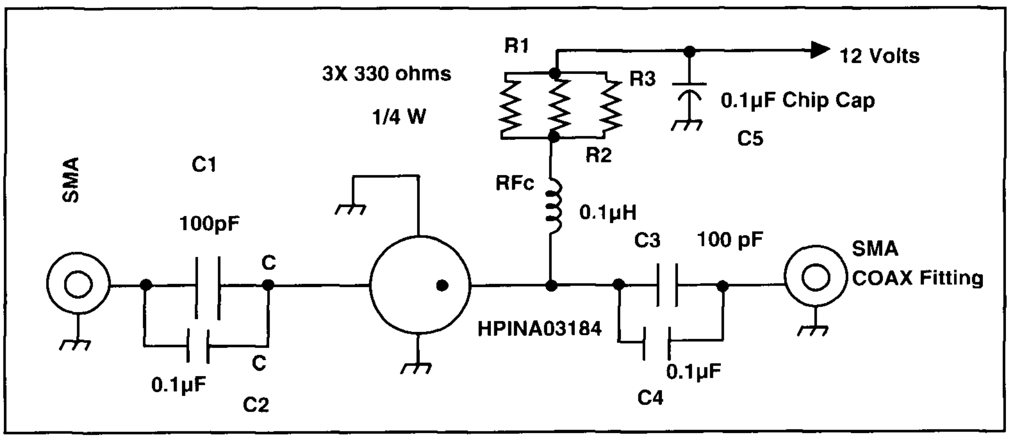

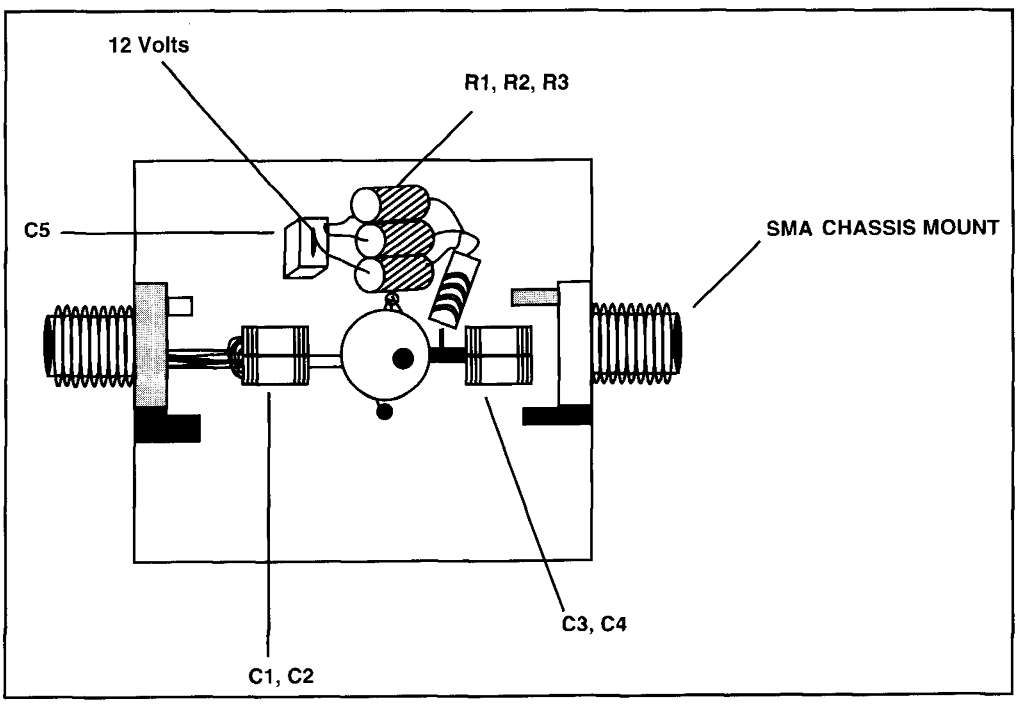

Figure 5. (A) Second amplifier stage circuit. (B) Construction (capacitors = chip and connectors = SMA 1104).

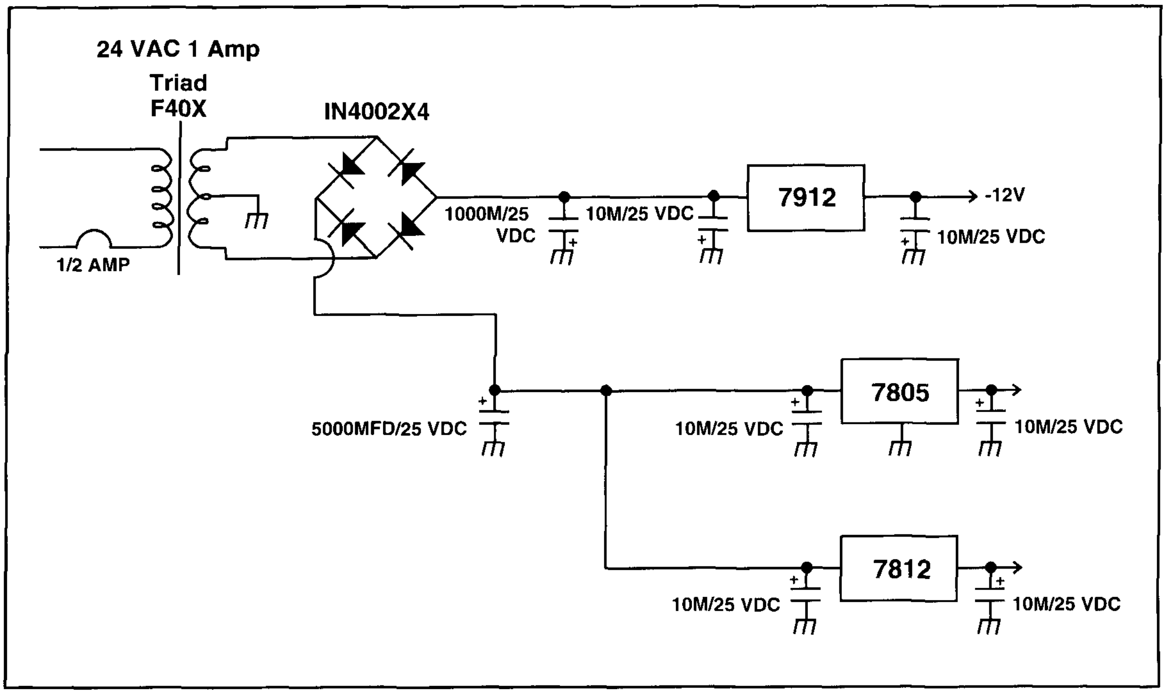

Figure 6. Tracking generator power supply.

Now, with the varicap tuning voltage set to within ±1 volt, check the frequency at the prescaler output. If it doesn't reach the desired 6.5469-MHz reference (or what's proper for the IF of your analyzer) within a ±1 volt tuning range, some adjustment is necessary. Do this by varying the lead length of the varicap diode. Be careful not to damage the 470-pF chip capacitor (C2), as several tries will likely be needed before the circuit is trimmed properly. Use of a 2 percent silver electronics-grade solder will help maintain the solder's bond to the ceramic chip capacitor during the stress of repeated resolderings.

Reference oscillator

A 2N3904 (Q5) is used in a Colpitts crystal oscillator to produce the 6.5469 MHz reference. The oscillator is trimmed by varicap tuning to the exact reference frequency via a 10 to 60 pF trimmer (with R1 at center rotation)! Front panel control R1 allows quick touch-ups of the reference frequency as needed. More details concerning the reference crystal oscillator will be given in the following paragraphs.

For initial alignment, first connect the tracking generator output to the analyzer input. Next set the analyzer to its narrowest usable IF bandwidth. With R1 set to the center of rotation, adjust the reference crystal trimmer capacitor for maximum upward deflection of the analyzer base line. Drift will be most noticeable when using the narrower IF bandwidths, and may be compensated for at this point by adjusting R1.

Because a drift at the crystal reference frequency is multiplied 320 times at the LO frequency, small shifts can become quite noticeable, especially when using narrow IF bandwidths! A mere 40-Hz drift at the 6-MHz reference frequency equates to a 13-kHz shift at 2 GHz! Depending upon the cut of the crystal, it may be necessary to play around with the oscillator circuit. You may have to use a variable capacitor (*or inductor—Ed.*) in series with the crystal to obtain the needed "rubbering" to reach the desired frequency. It might be a good idea to keep the oscillator circuit away from heat-producing components in the power supply. I've used this tracking generator with IF filter bandwidths as narrow as 30 kHz without being unduly bothered by drift.

The 6.5469-MHz reference signal is buffered by transistor Q6 and feeds the reference input (pin 1) of the MC4044 phase detector chip. The divide-by-N input (pin 3) is fed with the prescale output. An active filter/summing network, IC5 (a Philips NE5532 op-amp), follows. This circuit doesn't use the charge pump or Darlington pair that are part of the MC4044. The advantages of this potentially superior loop filter system are covered in **Reference 2**. **Reference 2** should also yield some good candidates for alternative prescaler chips, should some of the those used in this article prove hard to locate. The error tuning voltage from IC5 feeds the 1SV186 varicap tuning diode in the 2-GHz oscillator stage.

The 2-GHz oscillator and prescaler circuits should be housed in an RF tight aluminum enclosure. Feedthrough capacitors are used on the power supply voltages into the box. Once again, construction is cordwood style on a section of unetched pc board. An inexpensive die-cast aluminum box with dimensions of about 1.7 by 4 by 0.8 inches will do here. And, as in the rest of the tracking generator circuits, SMA fitted coaxial cables are used for interconnecting signal cables. Most of the components I've specified (isolators, fixed attenuators, and the MCL DBM) had SMA fittings, and this is what I used for RF interconnections in my unit. Note which signal cables are grounded on one end only, as indicated in the schematics, to prevent ground loops.

The circuitry associated with the 6-MHz reference oscillator and phase detector and filter may be built on unenclosed pc board material.

As mentioned earlier, a 10-dB fixed attenuator (M/A Com 2082-6147-10, or equivalent) is used at the MiniCircuits Labs RF port used for the 2 GHz oscillator injection.

Tracking generator output signal

The tracking generator output signal is taken from the IF port of the MCL mixer. I did so because this port is directly tied to the mixer diodes, without ferrite transformers, permitting operation down to as low as 0 MHz, and as high as 1.8 GHz, with low losses and a flat response. Because the IF port is most sensitive to mismatches, another M/A Com 10-dB fixed attenuator on this port provides isolation and matching. All other DBM ports have excellent 50-ohm terminations supplied by either isolator or fixed 10-dB pad loads.

To bring the tracking generator up to a useful output level of about –10 dBm, a broadband amplifier is needed. This is done via an HP 1NA03184 amplifier stage. The circuit is shown in **Figure 5A** and the construction details are given in **Figure 5B**. This amplifier stage is also constructed cordwood style on a small 0.5 by 0.5-inch section of pc board, which provides just enough room for SMA connectors, the amplifier, and the other several small parts used in this circuit. Extremely short lead lengths are used.

If desired, a second similar amplifier may be cascaded to provide an additional 10 dB of gain—but this will reduce the upper frequency limits to about 1.2 GHz. The front panel tracking generator output connector is a BNC or other suitable connector.

Power supply

The power supply is rather conventional and is shown in **Figure 6**. Either four 1N4002 diodes or a bridge rectifier package may be used. Three IC regulators provide the +12, –12, and +5 volts needed for the tracking generator circuits. These regulator ICs must be heatsunk.*

Acknowledgments

I wish to thank my son, Brian, KC6PFI, for his help in preparing this manuscript. ■

**Take care in placing the power transformer to avoid unwanted 60-Hz modulation of the 2-GHz oscillator from its magnetic field.—Ed.*

REFERENCES

1. Wayne Ryder, W6URH, "Spectrum Analyzer Tracking Generator," *Ham Radio*, April 1978, pages 30–32
2. *MECL Integrated Circuits*, Motorola, Inc., Fourth edition, second printing, 1989, page 6–30. Motorola publication no. 01/89 DL122, Rev. 4.

Phil Salas, *AD5X*
1517 Creekside Drive
Richardson, Texas 75081

AN FT-990/1000 INTERFACE CIRCUIT

Use the band data output to control external devices

Many of today's amateur transceivers come with information on controlling external antenna tuners and amplifiers manufactured by the same vendor. For example, the Yaesu FT-990 and FT-1000 transceivers have a "band data" connector on their rear panels that's used primarily to provide automatic bandswitching data to an FL-7000 linear amplifier when operated with these transceivers. But what do you do if your peripheral equipment isn't made by the same manufacturer? Fortunately, you can build a simple interface that will permit these transceivers to control other pieces of equipment, such as antenna switches, made by other vendors.

Band	A0	A1	A2	A3
160	0	0	0	1
80	0	0	1	0
40	0	0	1	1
30	0	1	0	0
20	0	1	0	1
17	0	1	1	0
15	0	1	1	1
12	1	0	0	0
10	1	0	0	1

Note: A "1" output corresponds to +5 volts, and a "0" corresponds to close to 0 volts.

Table 1. Binary-coded decimal (BCD) output provided by the FT-990 and FT-1000 band data connector.

The interface

The band data connector for the FT-990 and FT-1000 provides a binary coded decimal (BCD) output, as shown in **Table 1**. If you want to control different devices, you must change this information to single output levels for each of the bands. A good way to do this is to use available integrated circuits designed for this task. The 74HC42 1-of-10 decoder is an excellent choice. This device takes a 4-bit BCD input and converts it to ten discreet outputs. These outputs are active low; i.e. the outputs are normally high, and go low with the appropriate BCD input code. This is convenient because these outputs can then be followed with a higher current driver, such as a 74HC4049 hex inverting buffer or a transistor driver.

I wanted to interface my FT-990 with a Ten Tec 253 automatic antenna tuner. The Ten Tec 253 is a full legal limit antenna tuner with four switchable outputs to interface up to four different antennas. It has seven discreet external inputs that may be used to preset the tuner for any antennas connected to the four tuner outputs. Consequently, it can have up to 28 different presets. This external input interface was designed so the Ten Tec 253 would follow band data information from Ten Tec transceivers. When band data information is available, tuning takes place in a fraction of a second.

While the Ten Tec 253 can be used without this band data information, it must start from its last setting and retune whenever you change bands and/or antennas. Unfortunately, the FT-990 puts out BCD, and the Ten Tec 253 takes in discreet inputs.

The Ten Tec 253 requires 10 to 13 volts at up to 3 milliamps of current for the band data inputs. **Figure 1** is the schematic of the circuit I designed to do the job. I built the entire circuit into the Radio Shack 270-283 project box/pc board combo. The FT-990 band data output connector provides +13.8 volts DC at up to 200 mA. Current drain exceeding 200 mA may damage the FT-990, so I placed current limiting

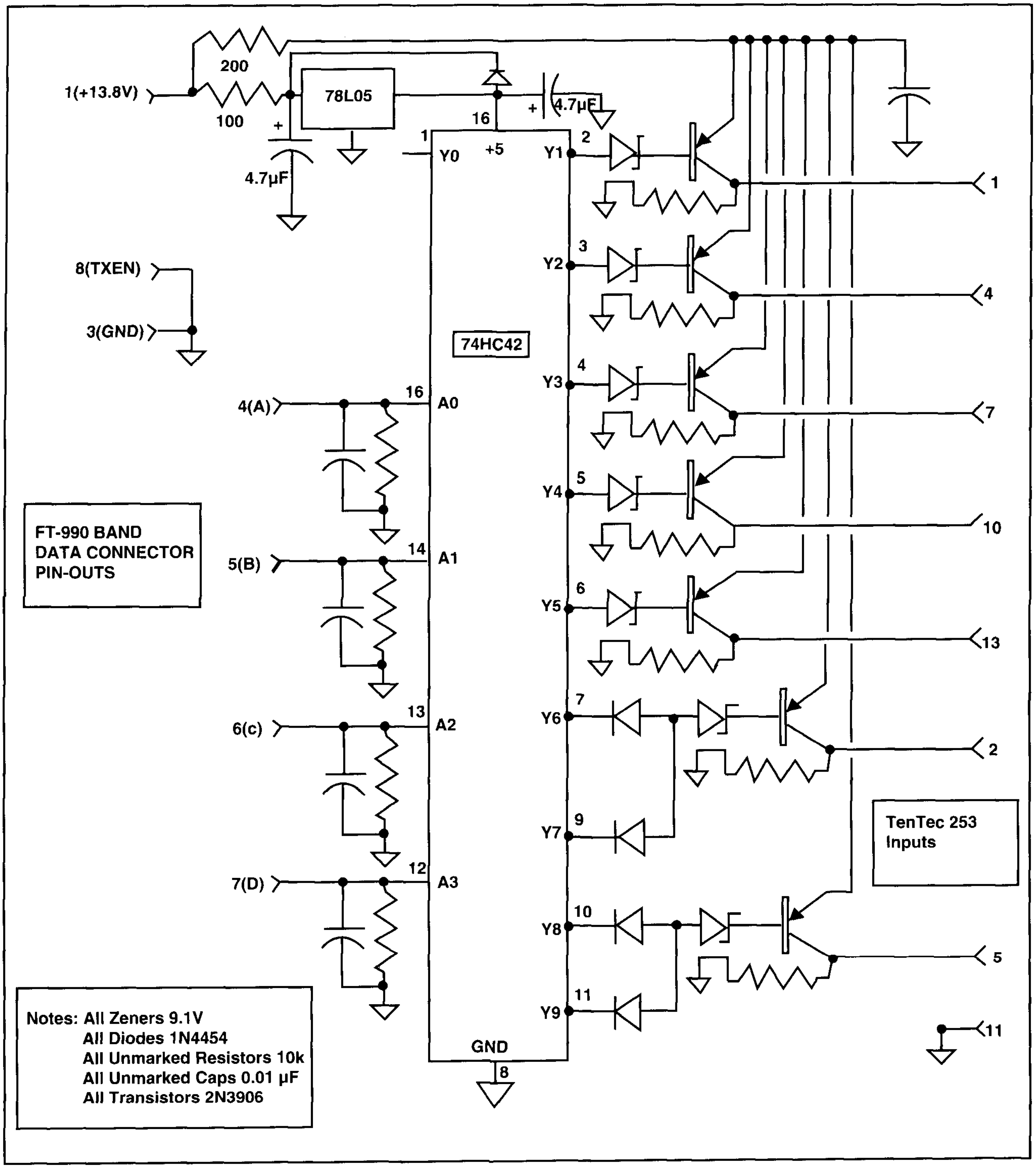

Figure 1. FT-990 to Ten Tec 253 interface.

resistors (100 and 200-ohm resistors shown) in series with the interface circuitry. A 78L05 low-current 5-volt regulator converts the +13.8 volts input to +5 volts for the 74HC42. Seven 2N3906 PNP transistors provide the output drive. If you need higher output current (for driving relays, etc.), use 2N2907 TO-18 metal can transistors and provide the +13.8 volt input from an external power supply.

I diode-"OR'ed" the 6/7 and 8/9 outputs of the 74HC42 together because there are nine ham bands, but the Ten Tec 253 only has seven inputs. Therefore, I combined the 17 and 15-meter band information together, and the 12 and

10-meter band information together. This created no problems because the Ten Tec 253 LC settings for these bands are pretty close together anyway. Note that when an external connector is plugged into the band data connector on the FT-990/1000, pin 8 needs to be connected to ground externally (pin 3) as shown in **Figure 1**. Pin 8 is a transmitter enable input that may be used for QSK operation of the FT-990/1000 with an external amplifier. Pin 8 is normally grounded by a microswitch (normally closed) on the band data connector, or by an external amplifier input telling the FT-990/1000 that the amplifier relays have been enabled. (This switch opens when an external connector is plugged in.) Incidentally, the FT-990 band data connector isn't a standard 8-pin DIN plug. You'll need to order it from Yaesu. It's Yaesu part number P0090160 and it costs less than $2.

Conclusion

Interfacing band data information from many of today's transceivers to external devices isn't a difficult task. I've described a simple band-data interface for the FT-990/1000 transceivers. Simple modifications to this basic design will provide you the flexibility to automatically control a variety of band sensitive devices, such as antenna selection relays or other vendor's antenna tuners. ■

PRODUCT INFORMATION

New Power Products Catalog from Hewlett-Packard

Hewlett-Packard Company's 1996/97 Power Products Catalog is now available. The 61-page catalog offers the latest technical information on altering current sources, direct current power supplies, electronic loads, harmonic/flicker test systems and solar-array simulators for the lab or factory.

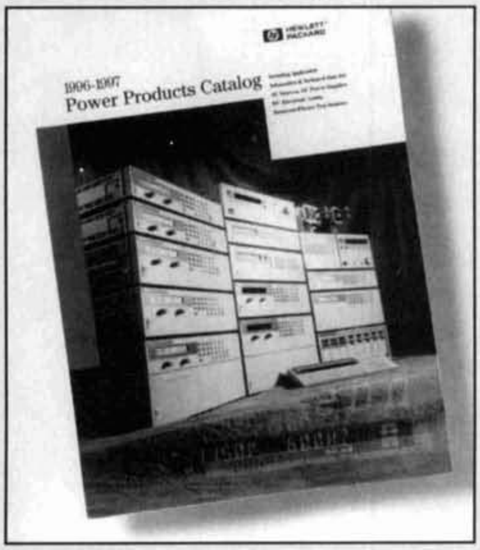

The catalog (Literature 5963-6035) features new products such as the HP 6840 Series Harmonic/Flicker Test Systems for IEC 1000-3/EN 61000-3 compliance testing and the HP 4350A solar-array simulator for aerospace applications. Enhanced 3000VA single-phase and 4500VA three-phase AC power source/analyzers are also new products that Hewlett-Packard has included in their catalog.

Copies of Hewlett-Packard's 1996/96 Power Products Catalog can be obtained in the United States by calling the HP DIRECT support number, 1-800-452-4844. For more information, contact Hewlett-Packard Company, Direct Marketing Organization, P.O. Box 58059, MS51L-SJ, Santa Clara, CA 95051-8059; or e-mail them at http://www.hp.com.

MacRatt™III Shipping Now

Advanced Electronic Applications, Inc. (AEA) is now shipping the new AEA TNC control program MacRattIII. AEA has re-engineered MacRattIII to fully utilize the powerful features of the newer Macintosh operating systems.

This new software provides a multi-functional terminal control program for the AEA TNC. On packet, each station connected will have its own adjustable, split-screen window. Stream switching is automatic and a monitor/unproto window will display incoming packets. Unproto packets may be sent while connected to others. For those TNCs with Pactor, Amtor, RTTY (Baudot & ASCII), Morse, etc. there are convenient interfaces built in. Frequently used commands may be selected from the menus, dialog boxes, and buttons on the windows.

AEA MacRattIII supports VHF Packet (1200 & 9600 bps), HF Packet, Pactor, Amtor, Navtex, RTTY (Baudot & ASCII), Morse, TDM, and AEA's Signal Identification and Acquisition mode (SIAM)™. It does not support Black & White WeFax, QSO logging or SSTV.

MacRattIII requires a Macintosh computer running system 6.05 or newer, 1 MB disk space, 4 MB RAM, a HD floppy drive, and an AEA TNC with August 1991 firmware or better. If the TNC has older firmware, it is possible to purchase a full upgrade by calling AEA's upgrade hotline at 206-774-1722.

For more information, contact AEA at 206-774-5554; or the 24-hour Literature Line at 206-712-8054; fax 206-775-2340; or write to AEA, P.O. Box C2160, Lynnwood, WA 98036.

Because we were unable to obtain reproduction permission from the author, the following article does not appear in the *ARRL Communications Quarterly Collection*...

Antennae Exotica—The Arecibo Dish

By Nathan "Chip" Cohen, N1IR

2 Ledgewood Place
Belmont, MA 02178

Summary: A tour of the Arecibo radio astronomy antenna system in Puerto Rico, the largest of its type in the world. The article includes several photos and an illustration of the antenna design.

Summer 1996 issue, pages 17-24.

Please contact the author for additional information.

PRODUCT INFORMATION

8-Input Audio Mixer-on-a-Chip

Analog Devices has announced their new SSM2163 8-input audio mixer-on-a-chip. It accepts eight audio channels, provides volume control in 63 1dB steps, and can mix individual channels to either the right, left, or both outputs. It replaces other multichip solutions in computer audio systems and improves audio fidelity. The SSM2163 also employs an industry-standard three-wire serial interface and one data output terminal to daisy chain multiple SSM2163s for high-end multi-track audio systems. A single mute pin, when driven by a microprocessor reset signal, will silence all eight audio channels simultaneously. No additional components are needed for fully specified operation. The SM2163 can be powered by a single supply or dual supplies and is available in 28-pin plastic DIP and SOIC packages for $8.00 in 100s with delivery from stock.

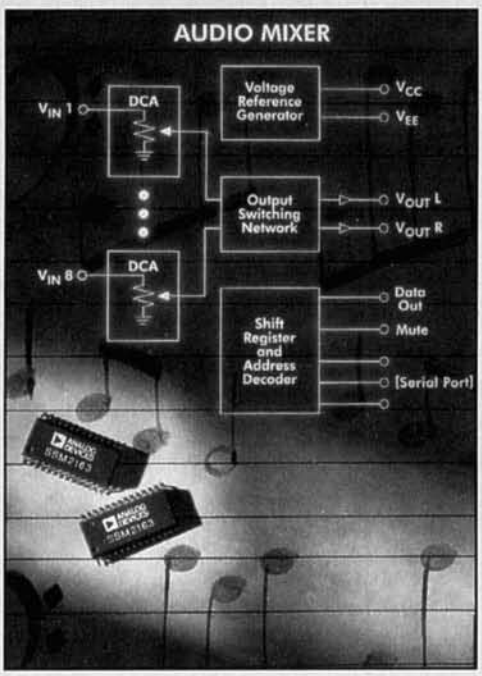

For more information, contact Analog Devices, Inc., Ray Strata Technology Center, 804 Woburn Street, Wilmington, MA 01887; phone 617-937-1428; fax 617-821-4273.

New Software Facilitates the "Mobile Office"

D&L Communications, Inc. has released Wireless for Windows, a new software designed to mobilize the office. Wireless for Windows works on any PC-based system and requires the EDACS® wide-area radio system. Wireless for Windows will eventually be compatible with other radio systems.

Currently, Wireless for Windows is in its first release. Its initial function involves AirMail. Any mail sent to a LAN network base is automatically transmitted to the receiver's vehicle. A screen message informs the receiver of the incoming mail. AirMail can also be sent from the vehicle, and any file type can be attached to the message.

Wireless for Windows can also be customized to fit the specific needs of different businesses, and can be installed on a PC by following simple directions. D&L also provides support.

For further information, contact D&L Communications, Inc., 3512 Cavalier Drive, Fort Wayne, IN 46808; phone 219-484-0466; fax 219-483-5584.

A.E. Popodi, *AA3K/OE2APM*
Moosstrasse 7/6
A-5020 Salzburg, Austria

THE ULTIMATE NOISE BRIDGE

This transformerless bridge provides construction simplicity

The noise bridge is an instrument for measuring impedances, particularly antenna impedances. It's simple in concept, but very difficult to realize as an accurate piece of hardware. The bridge is intended to provide measurements over frequency ranges of 1.8 to 30 MHz and an impedance range of ten to several thousand ohms.

The instrument is configured as a balanced bridge, comparing internal instrument standards against the unknown parameters. An internal noise source in unbalanced form must be coupled to the bridge as a balanced signal. The most critical part of the noise bridge is the transformer required for this function.

Unfortunately, this transformer has been the main contributor to bridge error. Considering that the transformer operates with magnetic coupling, but has capacitive leakage between primary and secondary windings, it is obvious that it's practically impossible to make a transformer that satisfies all requirements.

Many excellent articles have been written covering attempts to improve the accuracy of the noise bridge. Many authors have used ferrite cores for the transformer, others have found that such transformers cause complications. One of the best solutions seems to be a core-free transmission-line type transformer. Twisted quadrifilar windings and a dummy primary winding have been used. In most cases, the transformer must also supply the balanced center tap for the detector connection. There's also the possibility of induced noise in the chassis.

In a letter to the editor of *Communications Quarterly*, Mason A. Logan, K4MT,* suggested a transformerless noise bridge. However, his design produced an excessive error when larger

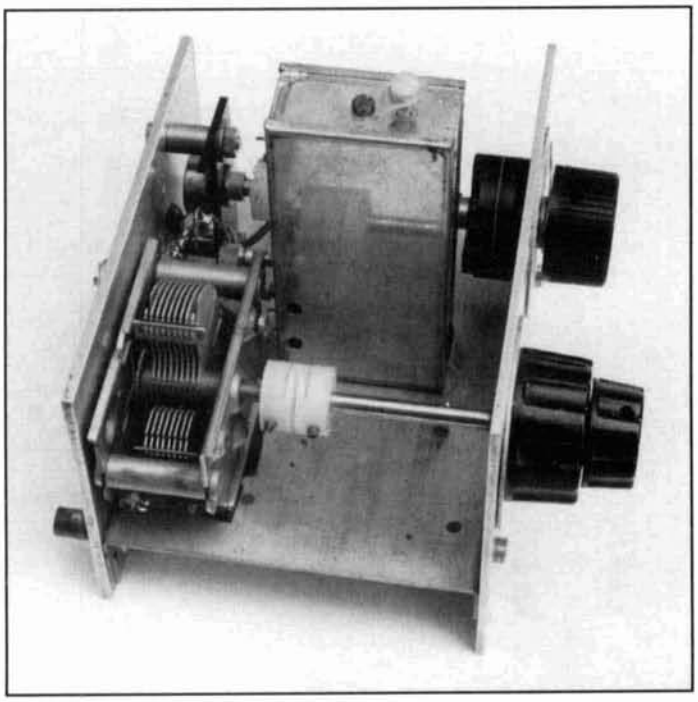

inductances were measured at higher frequencies. Adding a balancing capacitor, C_B, between noise generator and ground, completely balances the circuit and the above-mentioned error disappears.

Bridge design

Figure 1 shows the transformerless noise bridge. It consists of a shielded, small inner box that houses the noise generator, mounted inside, but insulated from, a larger, grounded box. Short, shielded cables connect the noise source to the bridge; matched resistors connect

*K4MT is now a silent key.

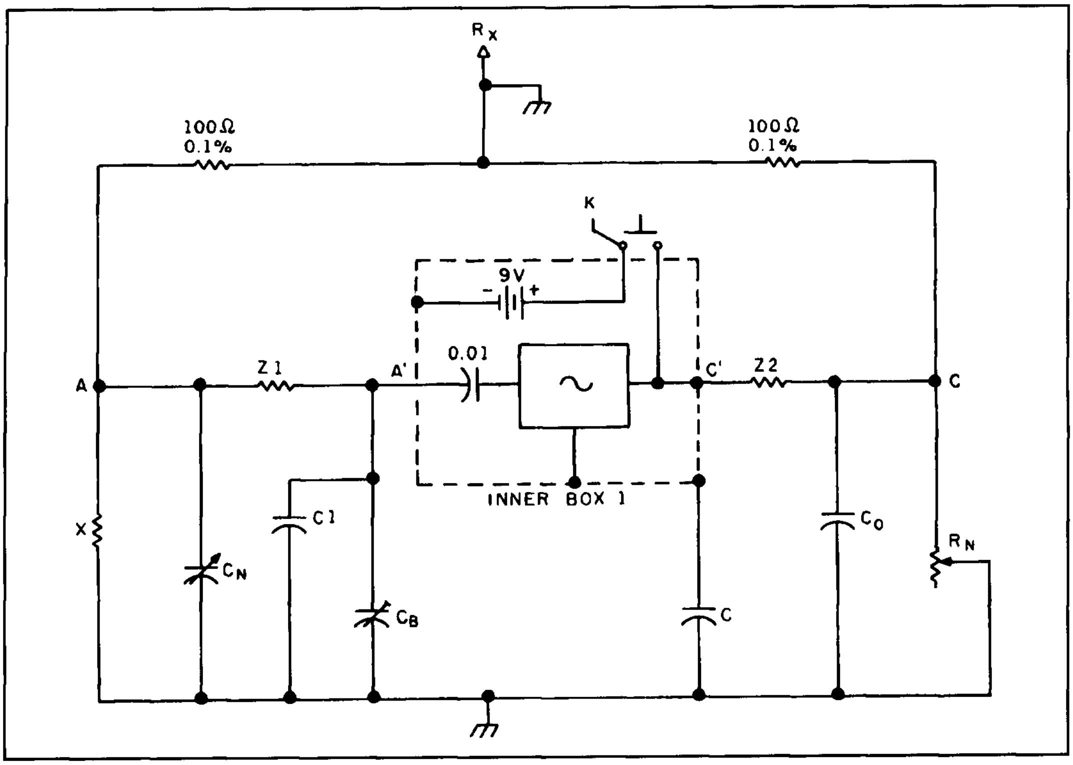

Figure 1. The transformerless noise bridge.

the receiver to the bridge. The inner box also houses a 9-volt rechargeable battery. A miniature, power-on, battery switch is mounted inside the first box and is operated from the outside using a Plexiglas™ rod. This helps reduce the capacitance at point C of the bridge.

The absence of the transformer and any inductance makes the schematic of **Figure 1** easy to read, and the circuit amenable to accurate analysis. Exactly the same noise current

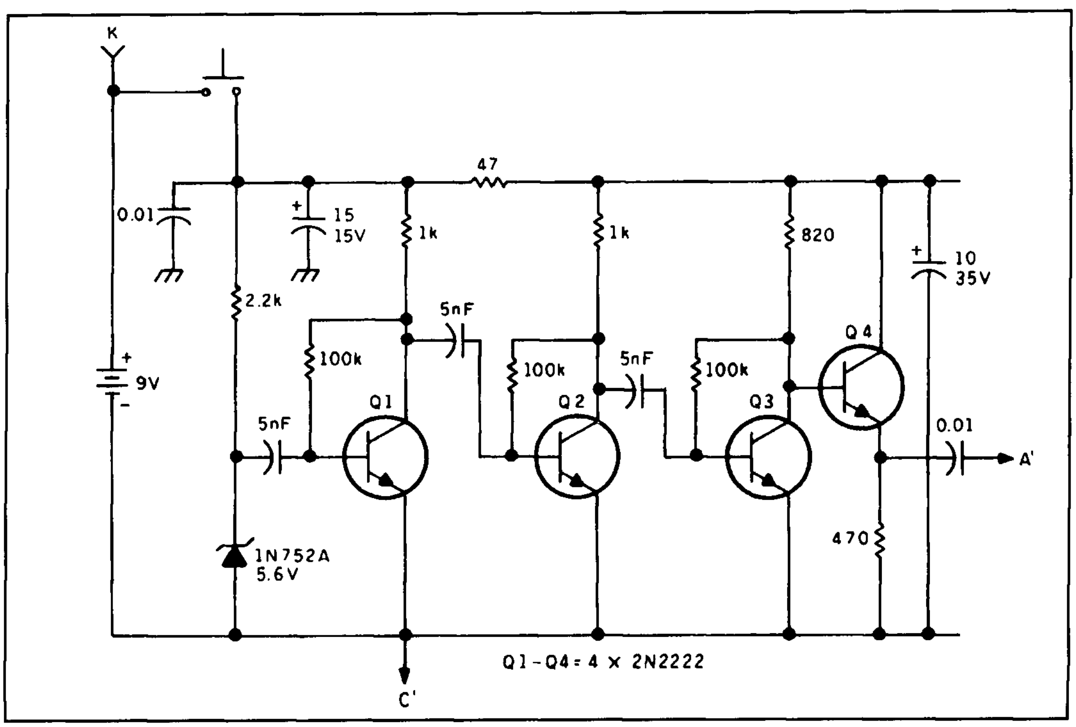

Figure 2. Schematic of the noise generator housed in box 1.

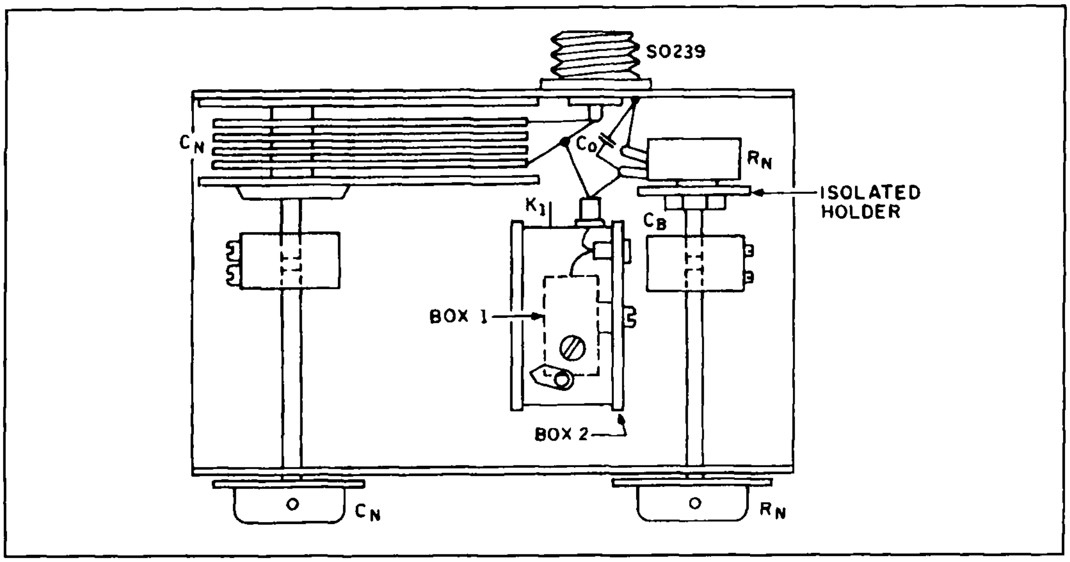

Figure 3. Possible arrangement to reduce long wires in the noise bridge.

flows into points A' and C'. Capacitors C_O,C_N, and resistors X and the variable resistance R_N, are the normal bridge components. Capacitance C lies between the inner and outer box. C_B is the balancing capacitor between noise generator and ground. It must be mounted inside the larger box. Impedances Z1 and Z2 separate bridge points A and C from the inner box.

When the bridge is balanced, the voltages at points A and C are equal in amplitude and phase. Calculations show, and measurements confirm, that for any value of the unknown resistor X, variable resistor R_N is always equal to X. This is true for all frequencies, once capacitors C_B and C_N are determined.

Figure 2 shows the schematic of the noise generator housed in box 1. As can be expected, the transformerless design also applies to the series R-C noise bridge.

After the values for C_B and R_N have been found, the remaining bridge errors are caused by the inductance of variable capacitor C_N and

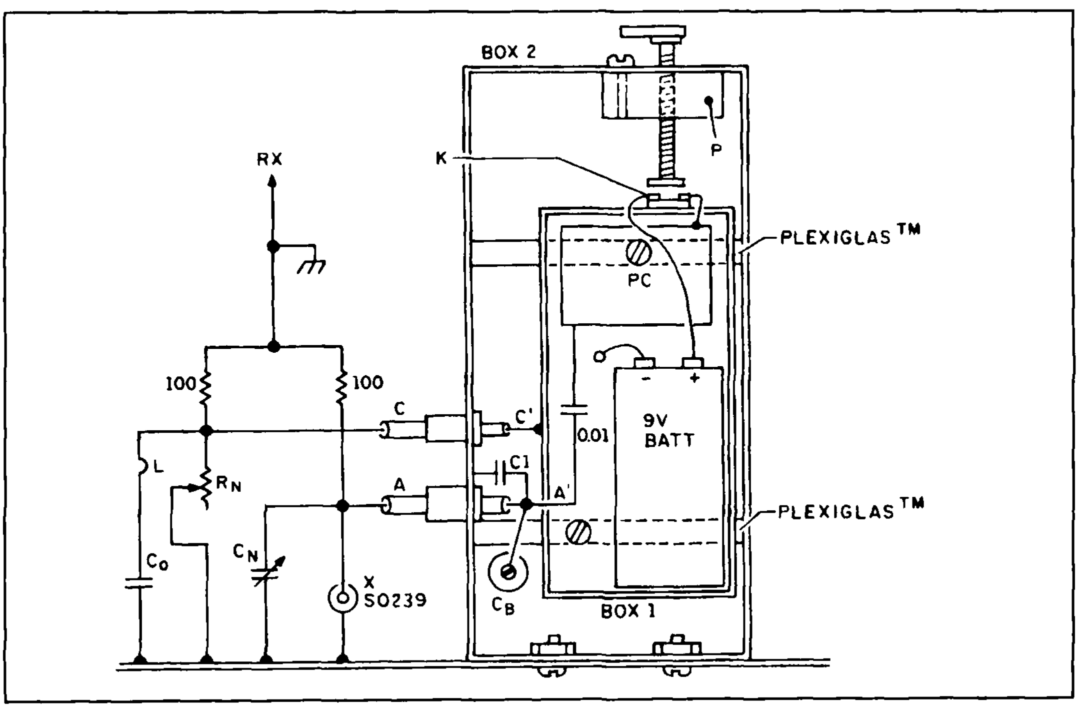

Figure 4. The inside of box 1.

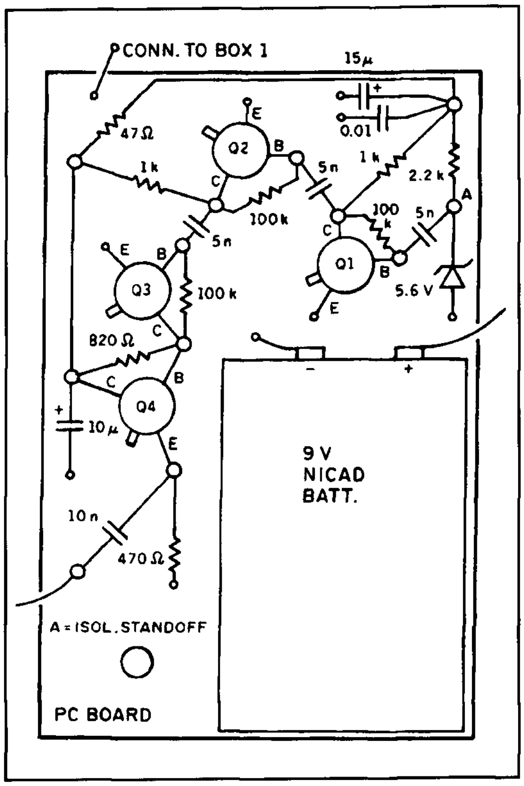

Figure 5. The pc board that houses the noise generator is shown above the 9-volt battery inside box 1.

the small reactive part of variable resistor R_N. The latter is inductive for small resistances and slightly capacitive for larger values. As **Figure 1** indicates, any series inductance of variable capacitor C_N can be compensated by a small inductance in series with C_O in the other bridge leg. This compensation would be perfect if the inductance of variable capacitor C_N was independent of capacitor setting. This, however is not quite true.

To achieve the best possible values, one must build the noise bridge in such a way that no long wires are present. **Figure 3** shows a possible arrangement. Controls for both C_N and R_N have multipliers. The covers are removed from boxes 1 and 2. Box 1 is mounted with two insulated screws directly at box 2, with the two insulating pads in between. **Figure 4** shows the inside of box 1. Above the 9-volt battery lies a pc board that houses the noise generator (see **Figure 5**). Connections A and C are two female and male RF connectors; e.g., type SMD. This allows for clean solder connections and simplifies repair work. C1 is a capacitor, because the trimmer capacitor doesn't have enough capacitance. The power switch is located on the outside of box 1, and is operated by a nonmetallic screw mounted in Plexiglas™ part P. One of the two battery terminals is connected to point K, the charging terminal for the battery. The two 100-ohm feeds for the receiver have equal lead-lengths connected to points A and C. The receiver is connected via shielded coax.

Calibration

After the mechanical layout is finished, one must find the correct values for C_B and C_N. Connect several resistors at terminal X and align the bridge for zero voltage and phase difference at points A and C. The smallest resistor is 22 ohms, the largest is 250 ohms. These resistors should have practically no inductance and very little capacitance. I have used SMD resistors soldered in a 1-millimeter wide piece of pc board material. This is then soldered on a PL259 piece, directly between the center conductor and frame. In most cases, there will be an improvement if a small inductance of less than 1 turn is used in series with the reference capacitor, C_O. This inductance serves to compensate for the inductance of C_N. Capacitance C_N must be measured with a bridge. The C_N dial has its zero point where the null on the audio occurred. To measure C_N, resistor X must be removed and, at point A', the noise source connection opened and the 100-ohm resistor disconnected. The C_B value has been determined before.

Summary

If one builds the noise bridge using the procedure discussed here, he will obtain much higher accuracy than with other such devices. The transformerless bridge eliminates the necessity of building a difficult transformer. High and low frequency operation are very good with this bridge, and the simplicity of construction is apparent. The remaining error is small and depends only on the inductance of C_N and R_N. The C_N error is larger, but can be compensated for with a fixed inductance in series with capacitor C_O. Fortunately, the inductance of R_N is smaller and less significant. Measurements showed that there is an inductive component up to 70 ohms; above 70 ohms, there is a small capacitance. Naturally, these values depend on potentiometer design, and nothing can be done to reduce this small error. The values for Z1 and Z2 should be as small as possible, with Z1 equal to Z2. The fading energy of the noise generator at high frequencies should be no problem at 28 MHz. Practical tests have shown that these errors are, in most cases, smaller than the error caused by gear backlash and the reproducibility of receiver and capacitor settings. In this respect, the transformerless noise bridge outperforms all hitherto existing designs. ■

B.-N. "Bob" Alper, *W4OIW/6*
Product Manager
Svetlana Electron Devices, Inc.
3000 Alpine Road
Portola Valley, California 94028

4CX400A RUSSIAN TUBES FOR THE MLA-2500 AMPLIFIER

Modification allows for economical tube substitution

There are many Dentron MLA-2500s out in the world. Someone may know exactly, but my information is that close to probably 6000 were manufactured. I've performed an MLA-2500 conversion that allows it to run a pair of 4CX400A ceramic tetrodes and will describe the process here.

The MLA-2500 is only five inches high, fourteen inches wide, and fourteen inches deep making it one of the most compact kilowatt amplifiers. The small size allows it to be placed on almost any desk or operating position. The major problem for MLA-2500 owners is that there is no economical source for the 8875 tubes used as the active amplifiers. For under $350 including sockets and tubes, the amplifier can be converted to run two Svetlana Electron Devices, Inc. 4CX400A tetrodes. (The price of a Svetlana 4CX400A is $140.)

The advantages in operating tetrodes are enu-

From Technical Data Sheet

	4CX400[1]	8875[2]
Useful Output RF Power (W)	605	505
Efficiency	60.5	46%
Plate Voltage (V)	2500	2200
Single Tone Plate Current (mA)	400	500
Zero Signal Plate Current (mA)	150*	22
Two-Tone Plate Current (mA)	—	300
Plate Dissipation, Rated (W)	400	300
Screen Voltage (V) Max	400	N/A
Screen Current (mA) Max	20	N/A
Heater Voltage (V)	6.3	6.3
Heater Current (A)	3.2	3.0
DC Grid Voltage (V) Approx.	–35	–8
Cooling Air at Max Plate Dissipation	400W/8 CFM	300W/6 CFM

1 = Grid Driven
2 = Cathode Driven
* = With 6 to 7-ohm cathode resistor installed.

Table 1. A comparison of the published original Eimac 8875 data and the published Svetlana 4CX400 data sheet.

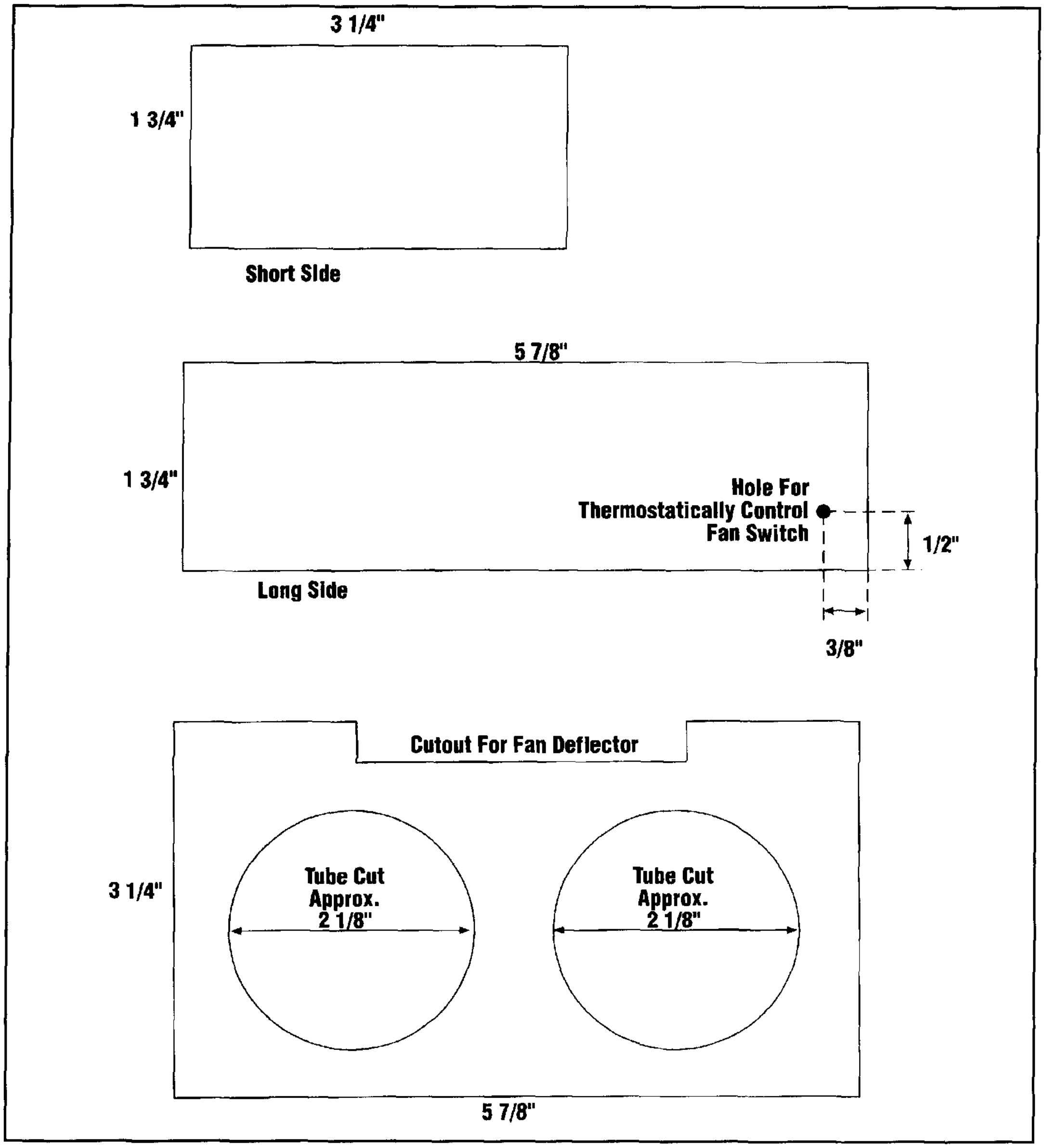

Figure 1. Air plenum parts fabrication.

merated elsewhere, but typically they are easier to drive than triodes, can withstand more abuse (e.g., high reflected power, etc.), provide better linearity, and are easier to adjust for good performance. The Svetlana 4CX400A tetrodes also have gold-plated grids and beam-forming mechanisms for secondary emission reduction and a dual focusing chambered anode feature (U.S. patented) that improves efficiency and linearity over conventional triodes and tetrodes. **Table 1** compares the published original Eimac 8875 data and the published Svetlana 4CX400A data.

Because one of the great advantages of the MLA-2500 is its compact size, one of my goals was to make the conversion with no external chassis or other protrusions from the original cabinet. A review of the 8875 technical data and the MLA-2500 schematic prompted the selection of a pair of the Svetlana 4CX400As because the two Svetlana tubes mount side-by-side in the same mounting holes as the original 8875s. The 4CX400As also operate from the original heater supply. These factors helped me meet my goal of having all components inside the original case.

Overview of tasks

In performing the conversion, five specific needs must be addressed. These are:

- Modification of the final amplifier tube area.
- Adding a screen power supply.

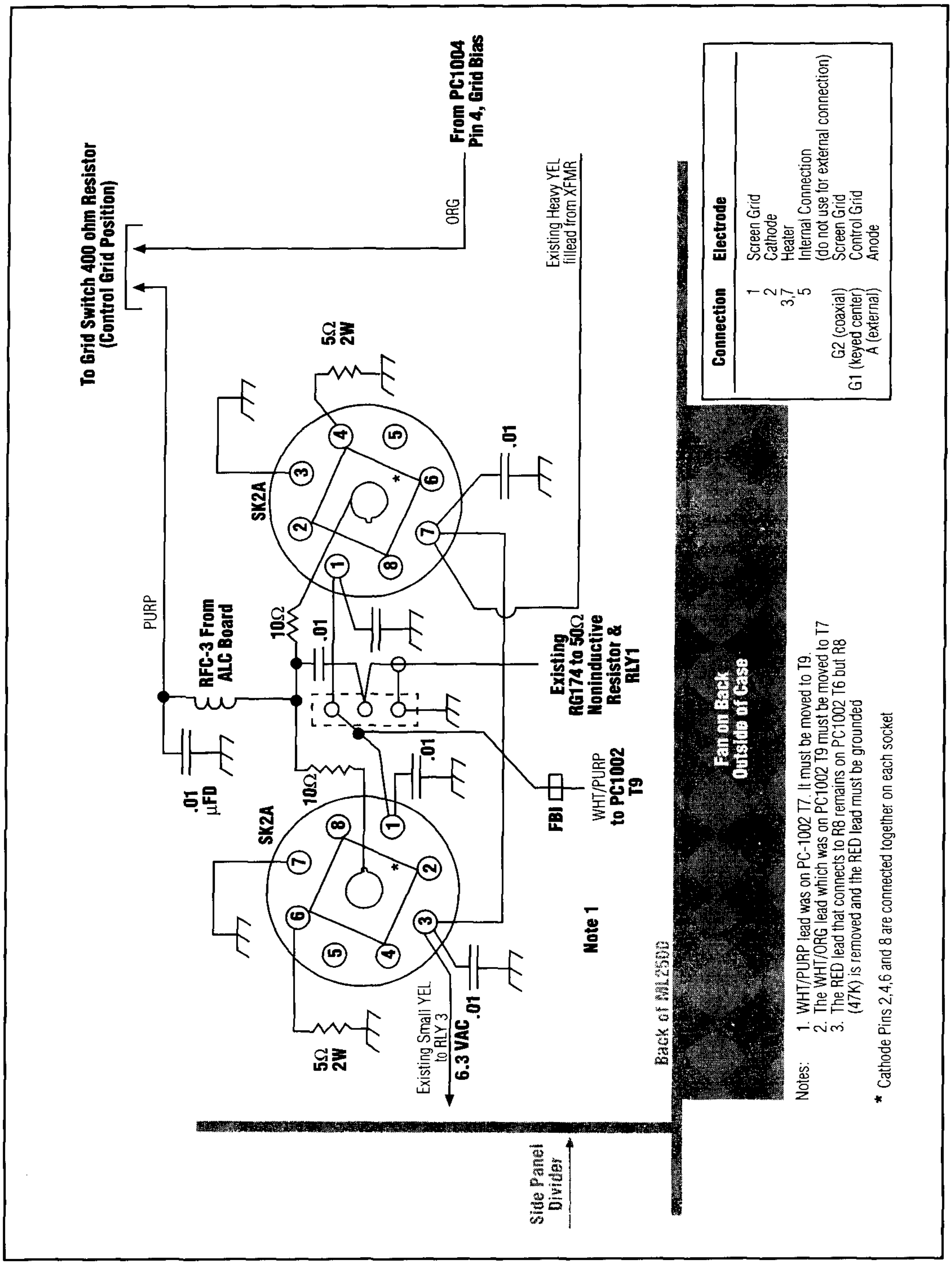

Figure 2. A bottom view of the RCX400A Socket Wiring.

- Meter switching board change.
- Adding a bias power supply.
- Installing the passive input grid circuit.

There are a number of possible solutions to each of these requirements. My desire to maintain the original MLA-2500 package as much as practical, rather than find the best technical solution, may have biased my judgement.

All modifications, with rare exceptions, were performed with light hand tools and available materials. In addition to the usual screwdriver and pliers, I used an electric hand drill, hand saw, two-inch pipe reamer (or hole saw), and tin snips (the saws could have been used instead of tin snips to cut the fiberglass board), and a Dremel® tool. The latter was used to break three traces on the original meter switch-

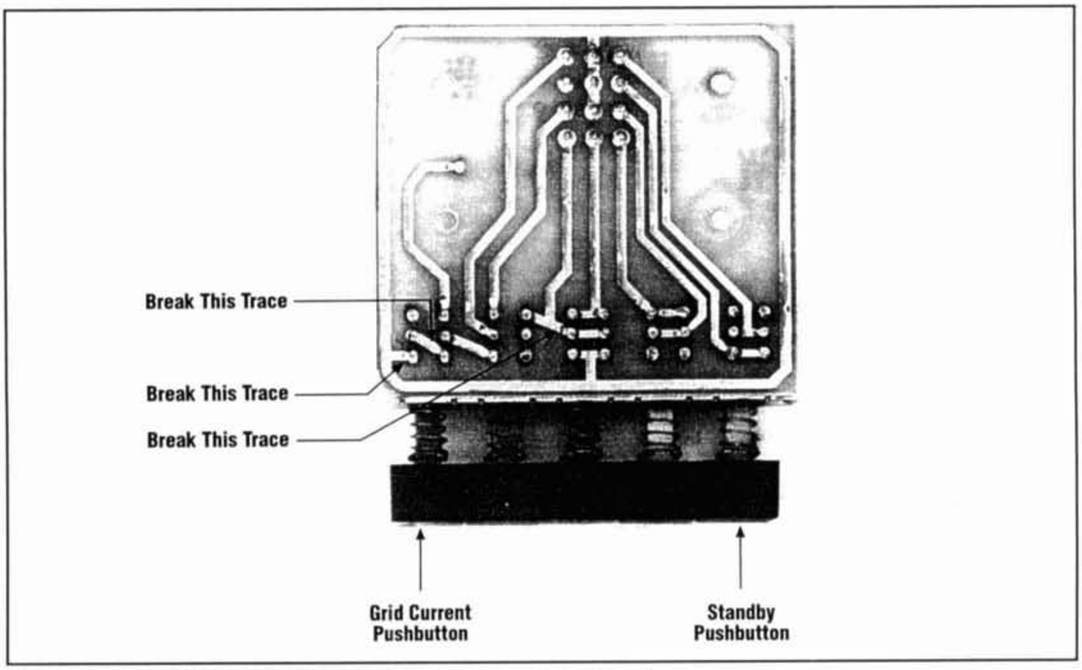

Figure 3A. Unmodified PC-1003 bottom view of meter switching board.

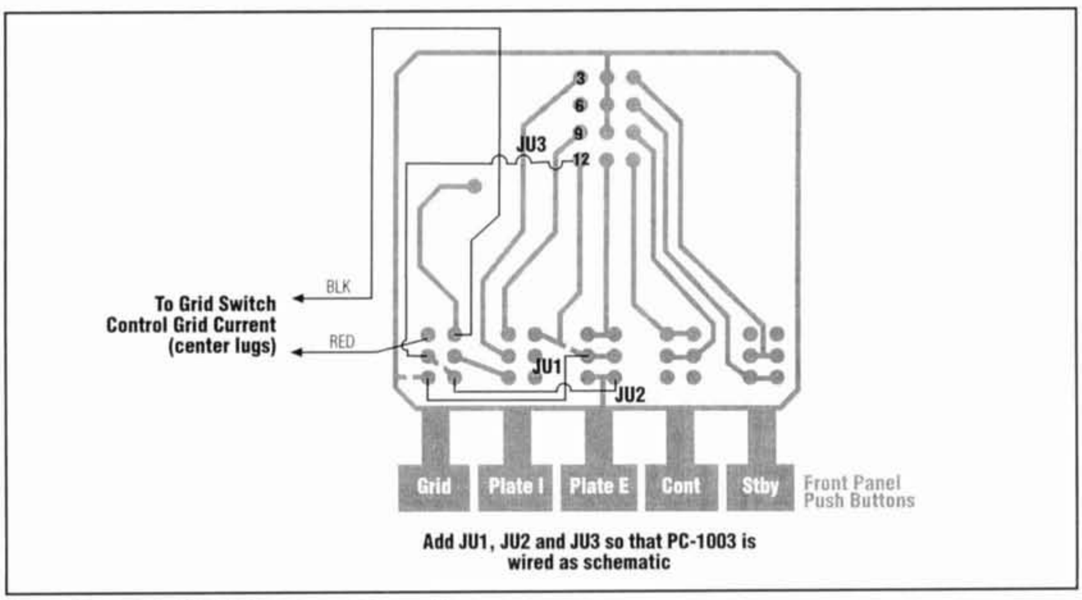

Figure 3B. Modified PC1003 meter switch board.

ing board, PC-1003, ALC board, PC-1004.

Before starting the conversion, test the amplifier so you know its condition. Hopefully, all functions work—even if the tubes are weak and provide only a small amount of additional output over your exciter. Inspect inside for broken wires, damaged or broken components, and so on. Make certain the plate power supply works and will stay on for long periods without arcing. Also, determine if the fan operates on high speed.* To check this, make sure the continuous button on the front panel is activated and relay control is closed to ground. Repairs to place the unit in normal operating condition should be made before your modification begins.

Specifics

Disconnect all power. Remove top and bottom covers. Carefully save and identify all components removed.

Final amplifier tube and cooling air plenum

Remove the tubes, sockets, input terminating resistors (these were not noninductive resistors

*I am advised that the fan operates at a constant speed on the MLA-2500B.

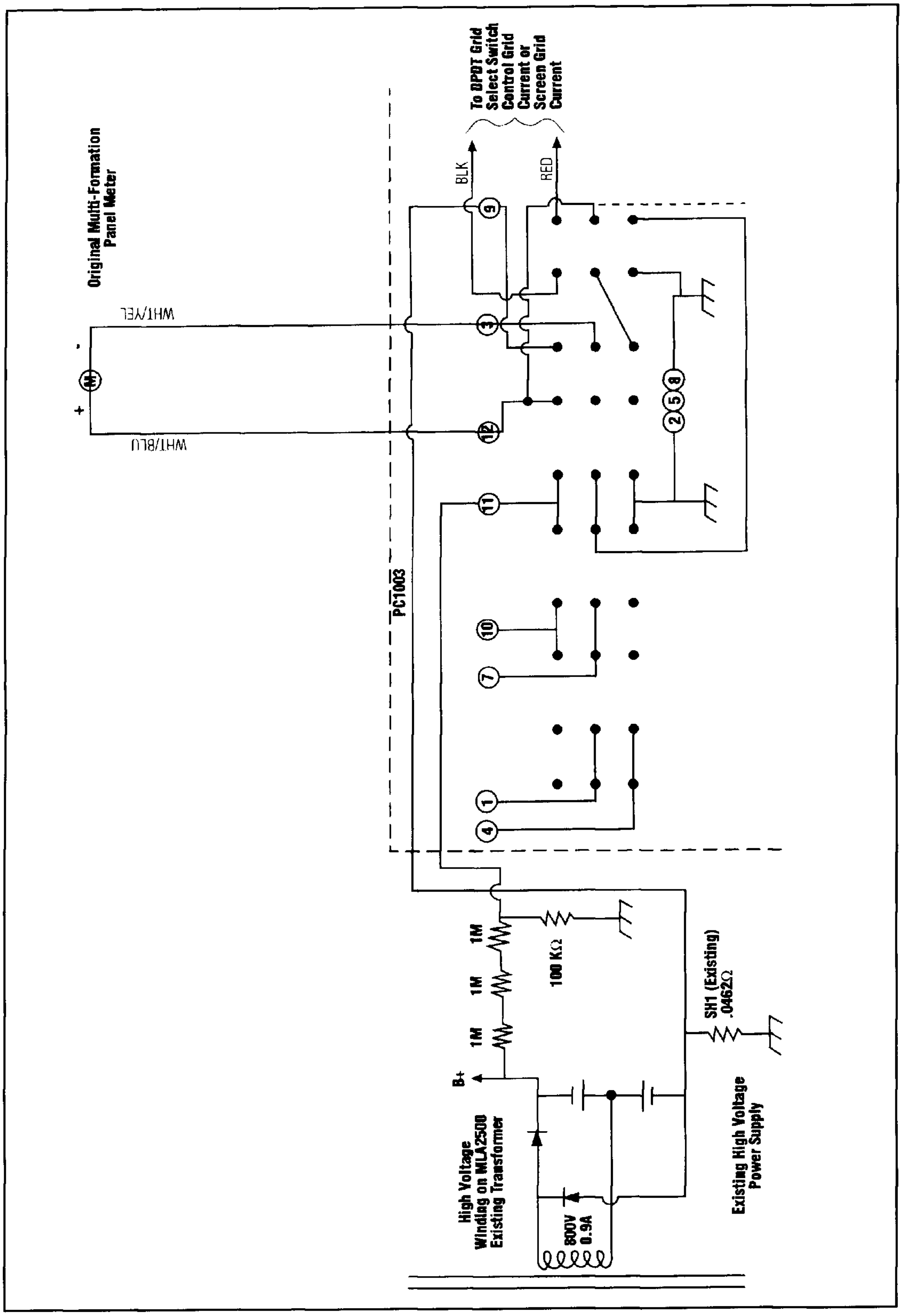

Figure 3C. PC-1003 meter switch board modified electrical wiring.

on my amplifier), bypass capacitors, thermostat switch, the Zener diode and other diodes in the tube cathode circuits, etc. Leave relay RLY1, all cabling, and everything from the plate RF choke to the front panel in place. Clean the chassis and remaining components thoroughly. Seal all holes in the bottom of the tube compartment with duct tape to make a relatively

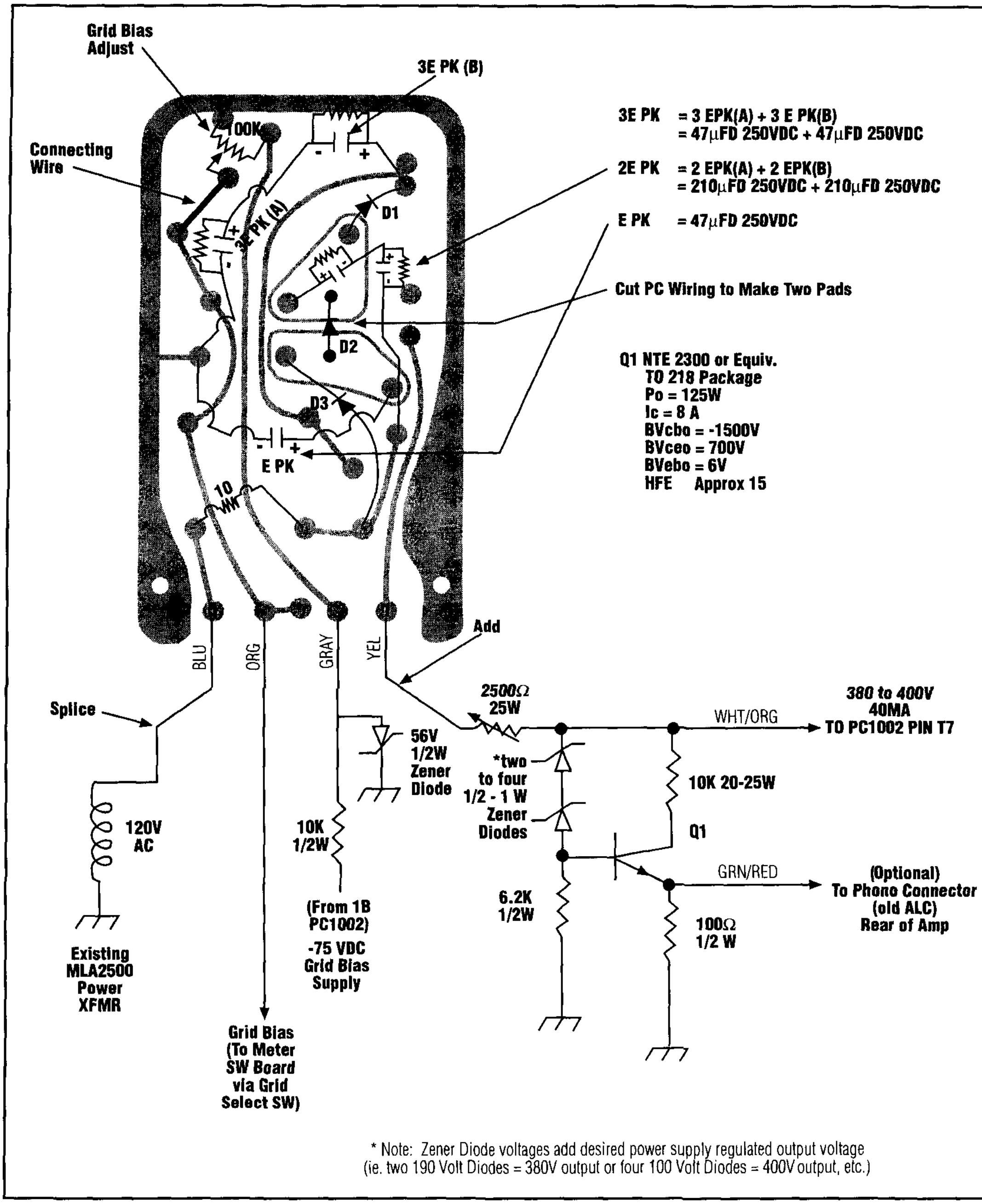

Figure 4A. PC-1004 (Old ALC Board) Screen power supply tripler shunt regulator and wiring.

airtight floor in the area in front of the fan forward to the plate choke.

Mount the new Svetlana SK2A sockets in the original tube socket holes using the original hardware. The keys on the center grid pins should face each other. Using G-19 fiberglass epoxy board or masonite (I used the latter), cut two pieces to the approximate dimensions of **Figure 1**. Leave an extra 1/8 inch in each dimension in order to file them to fit. I used a right-angle mending bracket at the corner between the two side panel pieces and made bottom brackets from soft aluminum strips about 1/2 inch wide. Make certain the height of the side panels plus the planned G-10 top cover are no higher than the top edge of the anode cooler and preferably 1/8 inch lower than the edge of the cooler of the 4CX400A. This is to assure air flow through the 4CX400A coolers. Mount the original fan thermostat on the longer side panel of the plenum. The position selected may be as shown in **Figure 1**. (The thermostat may not exist on some models.)

Cut a piece of G-10 to fit the top of the air

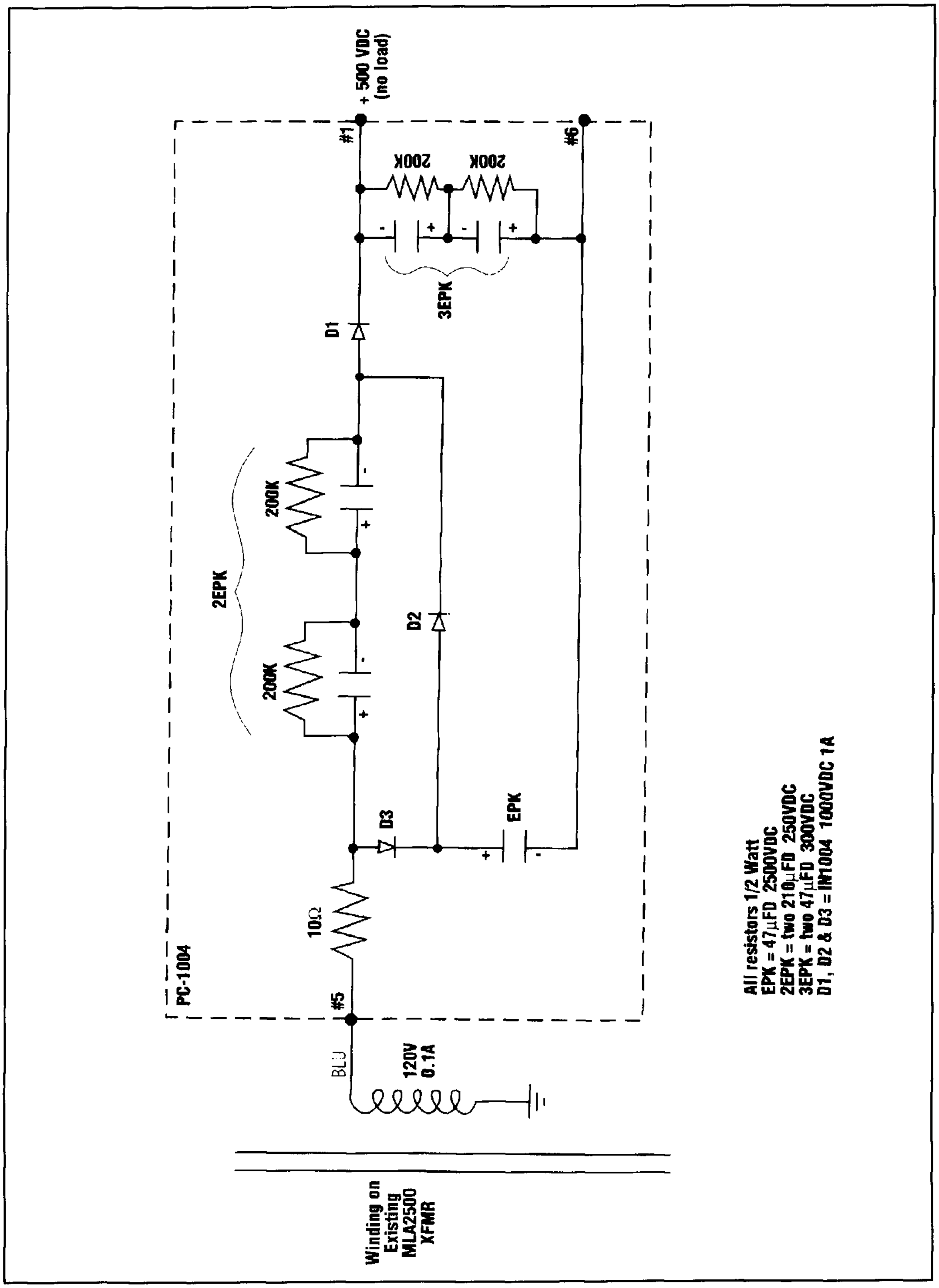

Figure 4B. Screen power supply tripler circuit.

plenum just fabricated (as shown in **Figure 1**). Locate the centers of the tubes and cut two holes in the G-10 to fit the anode cooler of the 4CX400As. Also, cut out a portion of the G-10 in front of the fan to accommodate the MLA-2500 air deflector as shown.

Before sealing the G-10 to the side panels, plug the 4CX400As into the sockets. Attempt to remove them using only a hold on the plate cap and a limited rocking motion no larger than the holes in the G-10. If you can't remove the tubes this way, carefully loosen the tension caused by the SK2A socket. To do so, use an object that's slightly larger than the tube (e.g.,

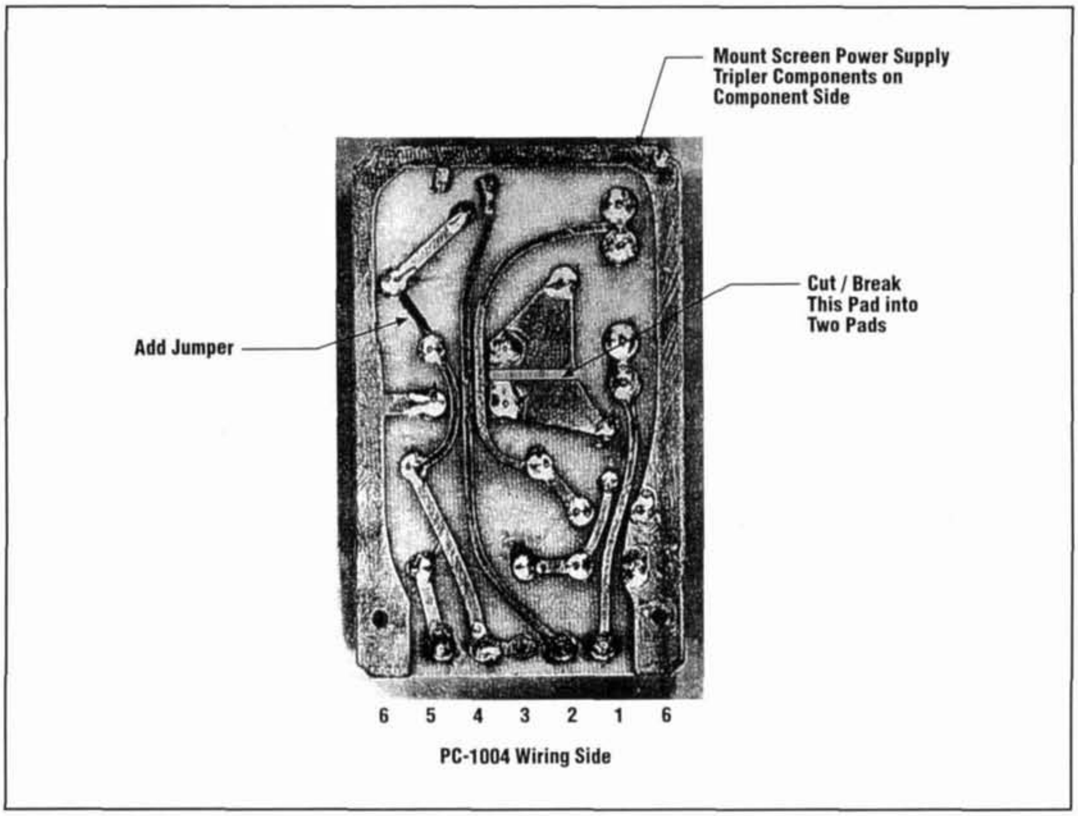

Figure 4C. PC-1004.

finishing nail) to press into the tube pin contacts. Seal the edges of the G-10 top to the side panels using duct tape.

Turn the amplifier over and wire the final amplifier tube sockets in accordance with **Figure 2**. You can use most of the original components removed from the old sockets.

Meter switching board (PC-1003)

Disconnect the white plastic plug on the top of the board and remove the four mounting screws holding it in place. Next, carefully disengage the pushbuttons from the front panel. *Do not* lose the four mounting grommets.

Looking at the wiring side of the pc board (bottom view), break the pc traces at the three points shown in **Figure 3A**. Add the three jumpers shown in **Figure 3B** to the bottom of the board. Remove the old grid shunt metering resistor R19, 510 ohms.

Screen power supply

Remove PC-1004 (the old ALC board) and carefully extract all the components except the fuse clips and the 100-k potentiometer at the top. Now, place the voltage tripler circuit shown in **Figure 4B** on the PC-1004 board. **Figure 4A** shows the cut of the large pc pad and the added jumper.

Detach the blue lead on PC-1002, which comes from the power transformer. Carefully work it out through the transformer lead feed hole on the bottom of the chassis. Now reroute this lead to PC-1004. Add a piece of blue wire to lengthen the transformer lead if necessary. Mount the shunt regulator transistor, NTE 2300, using a single screw and adequate silicon heat transfer compound (see **Figure 5**). Solder it to a newly mounted tie point as shown in the figure. Place the shunt regulator components of **Figure 4A** on the tie point, connecting the transistor to the circuit.

Bias power supply

A small low-voltage transformer is used as the bias power transformer. I chose an 18-volt transformer because I had one; a 12-volt or possibly a 24-volt transformer will be adequate. The bias regulating circuit consisting of the 56-volt, 1/2-watt Zener diode and 10-k, 1/2-watt resistor is based on the use of the 18-volt transformer. Because the MLA-2500 is so tightly packed, I had trouble finding a place for the transformer. I mounted it between the forward foot of PC-1002 and a screw on PC-1003—the

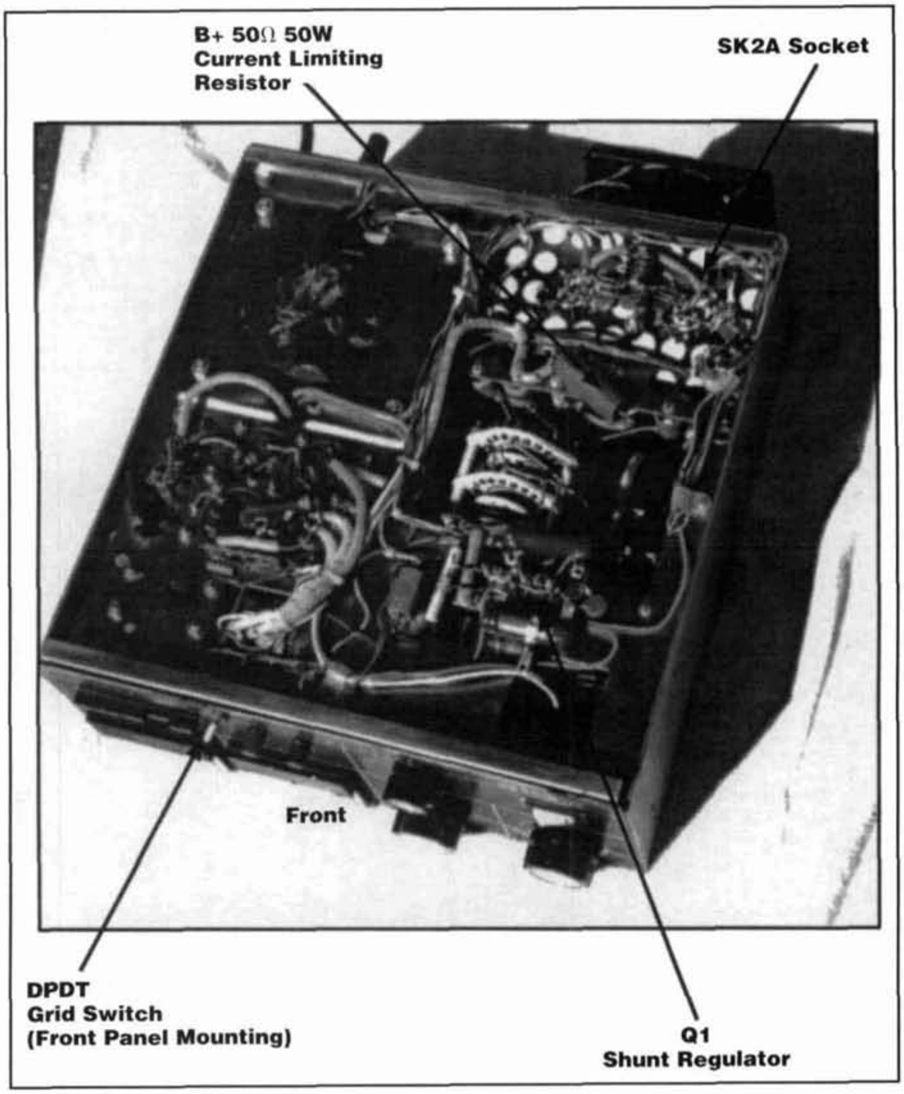

Figure 5. Modified MLA2500 bottom view.

meter switching board. You may find it easier to mount this transformer on the rear apron of the MLA-2500.

Locate diode D16 and capacitor C28 on PC-1002. These are near the edge of the board closest to the front panel. Unsolder and reverse the polarity of D16 and C28 (to provide the negative bias voltage). Wire one side of the 110-volt winding of the low-voltage transformer to PC-1002 terminal B3. Connect the other side of the 110-volt winding and one side of the 12-volt winding to ground. Connect the other side of the 12-volt winding to PC-1002, terminal B2.

Grid input circuit

Mount the 50-ohm, 50-watt noninductive resistor (Caddock model MP850 in TO-220 package) near the antenna changeover relay (RLY1) on the wall of the tube compartment as in **Figure 6**. Remove all original RF input terminating resistors mounted on the chassis wall near RLY1 and connect one end of the 50-ohm noninductive resistor to the center lead of the coax and the other connection to ground.

Miscellaneous

Disconnect R8 (47-k, cathode "standby" bias) resistor and ground the red lead that was connected to this resistor. Find the B+HV lead on the underside of the chassis and remove R2 (approximately 1 ohm). (May not exist on later models.) Connect a 50-ohm, 50-watt resistor in place of R2 (in series with the B+HV) to protect the tube in the event of an internal arc. Mount the DPDT grid current select switch (selects control grid or screen grid) at a convenient location on the front panel. See **Figure 5** for my under the chassis location. Connect the switch as shown in **Figure 3B**.

This wiring provides a selection of control grid current (0 to 1 mA) or screen grid current

CONDITIONS: Primary Power – 117 VAC**
Exciter = ICOM 765
RF Load = 50 ohm antenna
RF Power Meter = Bird 43 1 kW Element

Operating Frequency MHz	28.5	24.9	21.3	18.15*	14.2	10.1	7.2	3.8	1.9
Power Output Watts	750	750	760	750	800	830	840	760	710
Bandswitch	28	21	21	21	14	7	7	3.5	1.8
Drive Power Watts	10	11	11	11	14	15	15	15	15
Efficiency	54	56	57	55	60	65	62	56	53
Plate Voltage**	1820	1820	1820	1820	1820	1850	1820	1875	1875
Plate Current Amps (Single Tone)	0.77	0.73	0.73	0.75	0.73	0.69	0.74	0.72	0.71
Screen Current Amps	0.025	0.028	0.03	0.026	0.023	0.027	0.022	0.022	0.024
Grid Current mA	0.0	0.0	0.0	0.0	0.1	0.15	0.1	0.25	0.1

* My plate choke (which had been damaged) resonated at 18.18 MHz and required adding inductance to move resonance to approximately 16 MHz.

** No Load Plate Voltage = 2250

Table 2. RCX400A/MLA2500 Performance.

(0 to 100 mA) to be read on M2 when the grid pushbutton is depressed.

Energizing the modified amplifier

Resistance checks (primary power disconnected). Place all pushbutton meter switches in the "out" or fully forward position. Remove all tubes, and RLY2 and RLY3, from their plug-in sockets on PC-1002. Using an ohmmeter, check all new wiring; check plate and screen power supplies for shorts. Strap the MLA-2500 primary power strapping for 120 or 240 volts AC operation, as preferred. Depress the plate voltage pushbutton.

Applying AC primary power. Initial operation should be performed with tubes and RLY2 and RLY3 removed.

Check again to make certain the plate caps are clear of all components. Insert a device in the primary line to limit primary power (a variable voltage transformer set at one-half line voltage or a 150 watt lamp as a series resistor). Turn the amplifier AC power switch on, pressing SW1 (top cover interlock) as control. *Danger! High voltage is now present in the amplifier!* If all is okay, the plate voltage should rise to between 1000 and 2000 volts and the screen voltage (measured at the top of the fuse clip PC-1004 with a VOM) should increase to between 200 and 300 volts. There should be no smoke, sparks, etc. in evidence.

Note how long the plate and screen meters take to fall to zero after releasing SW1. There is no bleeder resistor on the plate power supply or the screen supply. Therefore, before working on the MLA-2500, always *discharge* all power supplies to ground using an insulating probe.

Remove the primary power limiting device and reconnect the power plug and again apply power to the amplifier. The plate voltage should be approximately 2200 volts (no load). Screen power supply voltage should be approximately 500 volts (no load).

Turn off and short power supplies DC to ground. During this procedure, make sure to discharge each power supply each time the primary power is removed.

Adjust the 2500-ohm, 25-watt resistor for about 2300 ohms and insert a 0 to 50 mA meter in series with the 100-ohm resistor in the emitter circuit of Q1. The variable 2500-ohm, 25-watt resistor must be set to protect the screens of the 4CX400As. Turn the AC on and read the current drawn by QA and shown on the 0 to 50 mA meter. Turn the AC off and set the Q1 current at 35 mA, limiting screen power to a maximum of 16 watts (8 watts per tube). The voltage on the collector side of the 2500-ohm, 25-watt resistor should measure about 382 volts.

Measure the grid bias voltage at the center grid pin on each tube socket. Turn the 100-k potentiometer at the top of PC-1002 to maximum. This voltage should be –50 volts or more, depending on the bias voltage transformer selected.

Turn off the amplifier and insert the two 4CX400A tubes, time delay relay RLY3, and control relay RLY2. Depress the panel "plate voltage" meter switch to B+. Depress the "continuous" switch so the fan (on most models) runs at full speed when the amplifier is in transmit mode. Connect a dummy load and an RF power meter (if available) to the RF output connector (on the rear panel). Turn the amplifier AC power switch off and mechanically close the top cover interlock using a plastic tie-wrap or other convenient means. Place the MLA-2500 bandswitch in the 28-MHz position.

Apply primary power and observe plate voltage and screen voltage. This should be at/near those previously recorded.

At the base of each tube, carefully remeasure and record:

Heater voltage (should be a nominal 6.3 volts AC ±0.3 volts).

Plate voltage, screen voltage, and grid voltage (should equal the previously recorded voltage). *Danger! High voltage!*

Observe the green "ready" light. For the initial energizing of the tube, it's a good idea to allow additional warm-up time. Ten minutes should be adequate for this class of power tube. After this initial warmup, the RLY3 filament heating delay time of 75 seconds will be conservative (A 30-second warmup is specified for the 4CX400A.)

Depress the plate current switch; there should be no reading.

Close the external relay control line (phono connector on rear) to ground. The red "transmit" light should energize. The fan speed should increase to fast. There should be no plate current indicated.

At the tube socket, measure the screen voltage at each tube. This DC voltage should be as recorded previously. It shouldn't be more than 400 volts DC. Remove the meter test probe.

While observing the plate current, adjust the 100-k potentiometer with an insulated tool (should rotate counterclockwise) to 300 mA. Grid voltage at the 4CX400A grid should now measure –30 to –35 volts DC.

With the "load" control set at "1" (minimum loading), slowly rotate the "tune" control completely through 360 degrees while observing the RF output meter and plate current meter. No RF output or place current variation should be observed. Connect your exciter to the RF input connector and set the MLA-2500 bandswitch and exciter bandswitch for 28 MHz, and CW or RTTY operation. Turn both the exciter RF output control and the mic gain

PARTS LIST

4CX400A CONVERSION FOR MLA-2500

The following are the only parts needed for the 4CX400A/MLA2500

RESISTORS

1	50 ohm non-inductive 50 watt; Caddock MP850, Caddock Electronics, Inc., 1717 Chicago Ave., Riverside, CA 92507-2364
1	400 ohm 1/2 watt
1	10,000 ohm 1/2 watt
2	5 ohm 2 watt
1	10,000 ohm 25 watt
1	100 ohm 1/2 watt
1	6,200 ohm 1/2 watt
3	10 ohm 1/2 watt
1	47,000 ohm 1/2 watt
4	200,000 ohm 1/2 watt
1	2500 ohm adjustable, 25 watt
1	50 ohm 50 watt wire wound

CAPACITORS

6	.01 MFD 1000 VDC
2	210 MFD 250 VDC
3	47 MFD 250 VDC

DIODES & TRANSISTORS

1	IN4762 82 VDC 1W Zener Diode
3	IN4764 100 VDC 1W Zener Diode
3	IN4001 1000 VDC 1A
1	IN4758 56 VDC 1/2 W
1	NTE 2300 (Po = 125 W; Ic = 8A; BVcbo = 1500 VDC; BVceo = 700 VDC; BVebo = 6 VDC

MISCELLANEOUS

1	12 VAC – 120 VAC transformer
1	Tube of heat conducting silicon grease
1	Ferrite bead (existing)
1	Fuse 0.1A
2	Svetlana SK2A tube sockets
1	DPDT bat handle switch

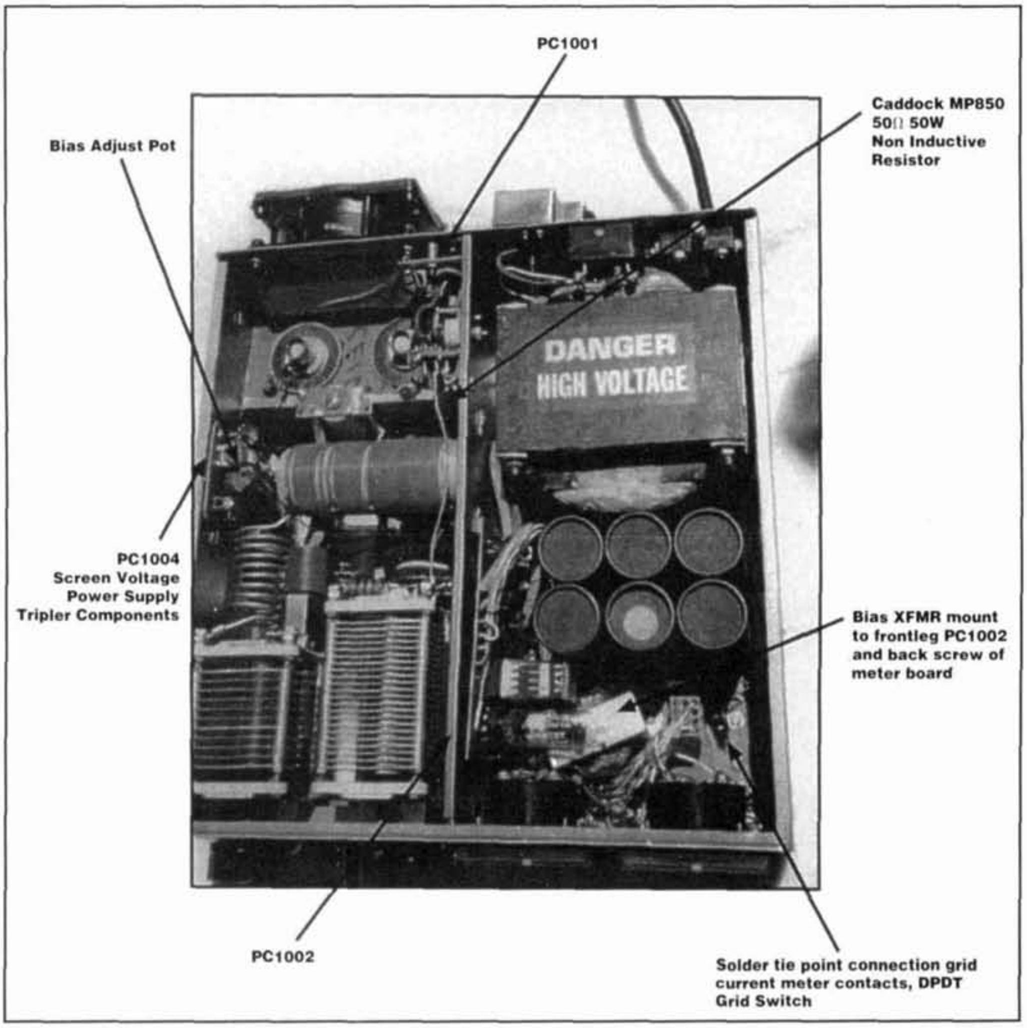

Figure 6. Top view of modified MLA2500.

to zero. It may be necessary to construct a resistive pad to be placed between the exciter and the MLA-2500. (Refer to any of the popular *Radio Handbooks*.) Many exciters have a variable RF output control but the output, even in the minimum position, may be 5 to 10 watts.

Energize the amplifier with a few watts of exciter RF output, and quickly adjust the "tune" for maximum RF output from the MLA-2500. Note: Maximum transmit time during initial adjustment steps in this portion should be limited to 10 seconds of keydown operation.

Alternately adjust the "load" and "tune" control for maximum RF output as indicated on the panel meter. Next, increase the exciter output until you observe an increase in the MLA-2500 plate current to at least 400 mA. Once again, adjust the "tune" and "load" controls for maximum RF output.

Check the screen current (grid pushbutton depressed and DPDT panel switch in screen grid position). Observe the screen current; it should *never exceed 40 mA*. Slowly increase the RF drive and again alternately optimize the "tune" and "load" controls for maximum RF output. Slowly increase RF drive until RF output won't increase further. The grid current on my MLA-2500 ran from 0 to 0.25 mA.

Increase loading under loaded conditions until not more than 800 mA of plate current is indicated. Again, make certain the screen current is less than 40 mA.

If a calibrated external RF wattmeter is available, adjust "wattmeter calibrate" R11 on PC-1001 for the same reading as the external wattmeter using an insulated tool. The old MLA-2500 manual suggests 20 meters for this calibration. It may be necessary to adjust C14 of PC-1001 and compromise the error difference of the front panel meter readings and the external wattmeter between lower and higher frequency bands, as the MLA-2500 wattmeter circuit probably won't track the external wattmeter from band to band.

If operation is from a 120 volt AC primary power source, the plate voltage can be expected

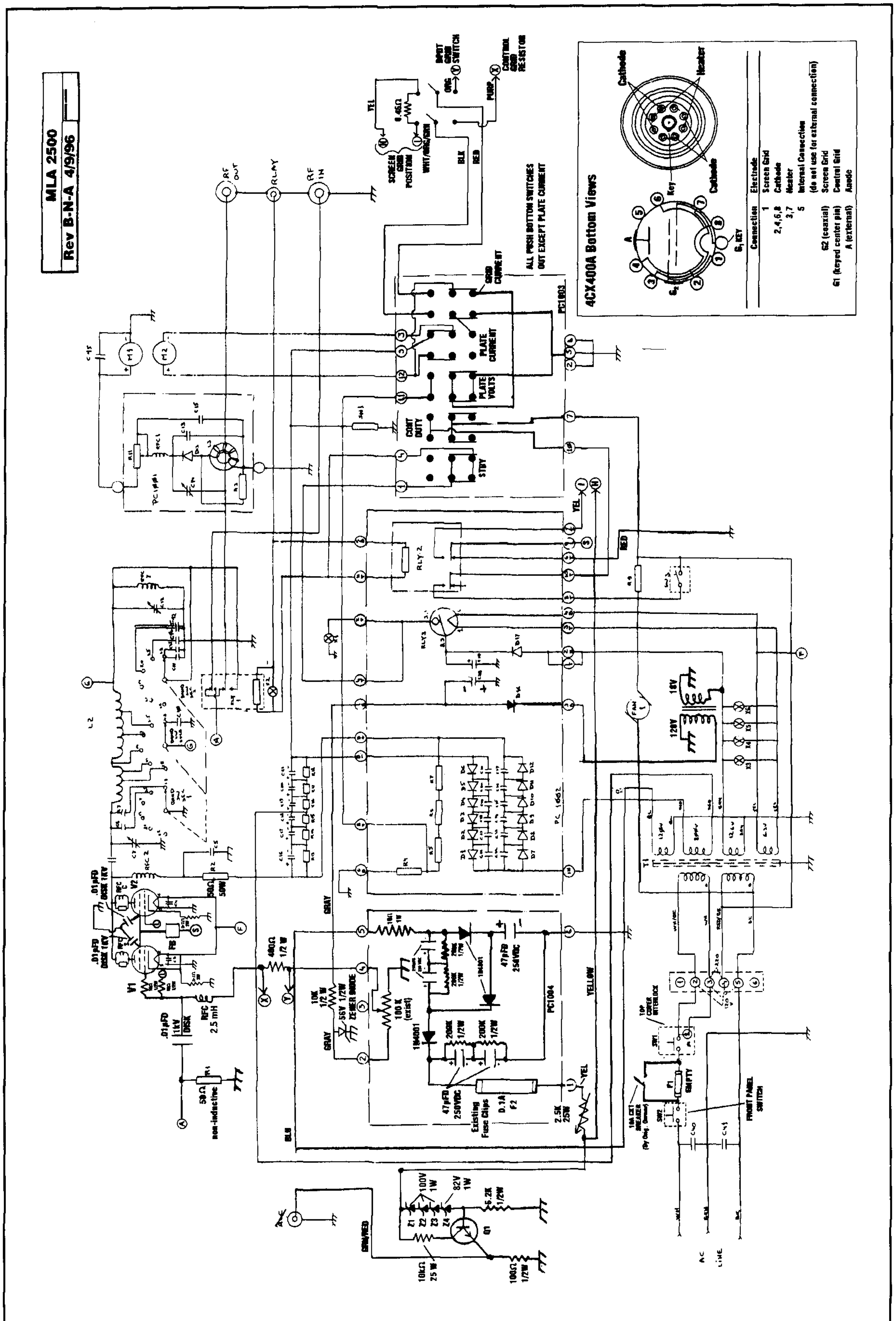

Figure 7. The schematic of the modified 4CX400A MLA-2500.

to sag to 1800 to 1900 volts and the screen voltage to 370 to 380 volts.

Table 2 summarizes modified (4CX400A) MLA-2500 operation into a dummy load for all amateur HF bands. I recommend that you make a PA tune and load chart for each band. A helpful addition to **Table 2** is the approximate RF output level control setting or exciter driving power. While the 4CX400As are very rugged and will accept much abuse (I know this from personal experience gained while developing this modification), longevity will be increased if tune up is accomplished rapidly. A complete, revised schematic of the modified MLA-2500 is shown in **Figure 7**.

SSB adjustments

Although the adjustment method described here provided adequate results, the best way to set up an exciter-power amplifier combination is to use the techniques described in *The ARRL Handbook*. Grid bias may be adjusted for minimum distortion while not exceeding the zero-signal plane current that results in not more than 800 watts plate dissipation.

Operational notes and summary

On the air testing was performed with local stations and other stations at 1200 to 1500 miles under strong signal (9+20 dB) conditions. Signal bandwidth reported was 3 to 3.3 kHz under the adjustments described.

Anomalies and unusual observations

1. Depending on the test configuration it's possible to observe a high VSWR on the exciter VSWR meter. This didn't shut down my IC-765 exciter/transceiver which was operating at relatively low RF outputs (under 50 watts) forward power.

2. The linear amplifier conversion is very stable. No instabilities were observed for any of the tuning settings. The RF drive power required at 10 meters is less than that required at 40 meters. This indicates a regenerative effect (or possibly a reduction in degeneration), but amplifier instabilities were not observed.

Acknowledgements

George Badger, W6TC, provided the principal encouragement for this article and also offered may good ideas and suggestions. Others influencing the article include: Bill Orr, W6SAI, George Daughters, AB6YL, David King, KK6WQ, and Don Priebe, K4QKR. ■

PRODUCT INFORMATION

New Line of 2-Meter VHF Amplifiers

Tucker Electronics has introduced a new line of 2-meter VHF amplifiers including the Tucker V-35W and the Tucker V-100W. Both amplifiers are designed to be used with 2-meter handheld transceivers and low-wattage 2-meter desktop transceivers, such as the Icom IC-706.

The Tucker V-35W will accept 0.5–8 watts input power and produces up to 35 watts of output power. It features a built-in 15dB pre-amplifier and a DC Monitor Meter feature that provides a constant reading of the DC input voltage. Also included in the V-35W is a built-in RF power meter. The V-35W operates on both FM and SSB/CW.

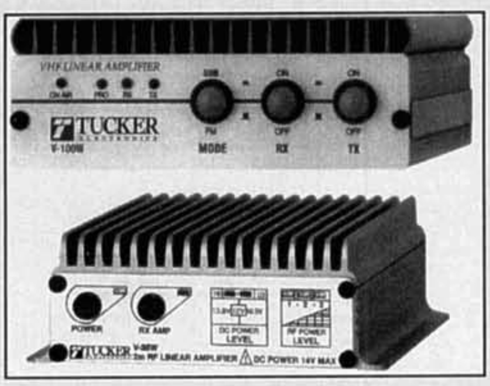

The Tucker V-100 watts will accept 0.5–8 watts input power and produces up to 100 watts of output power. An input power signal of 0.5 watt is required to produce 50 watts of output power, and 3–8 watts will drive the V-100 watts to full power output of 100 watts. It also features a built-in 15dB pre-amplifier and a built-in RF power meter. The V-100W operates on both FM and SSB/CW.

Both amplifiers are covered by Tucker Electronics' 1-year warranty and 30-day "Satisfaction Plus" No-Questions Asked Return Privilege.

For more information, contact Tucker Electronics at 800-559-7388; or fax 214-340-5460.

Robert R. Brown, *NM7M*
504 Channel View Drive
Anacortes, Washington 98221

DATA ON LONG-PATH PROPAGATION

At low latitudes and solar minimum

Most of the world's population resides in the Northern Hemisphere, and major concentrations of people are found in North America and Europe. As a result, short-path contacts between North America and Europe are made across the North Atlantic Ocean, with paths to Western Europe at mid-to-high-latitudes and paths to Eastern Europe going across the polar cap. For long-path communication, routes to Europe go into the South Pacific and Indian Oceans and some go across the Antarctic Continent.

Successful communication on paths that go more than half way around the world involves conditions in which ionospheric absorption is minimal, with little, if any, illumination on the

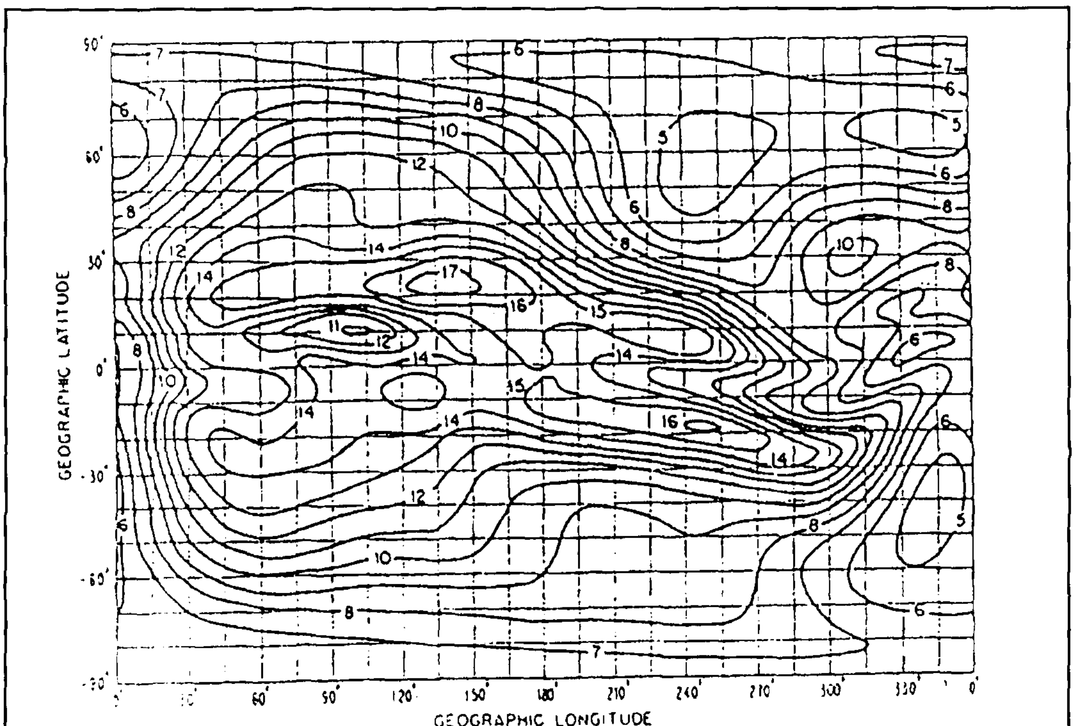

Figure 1. Contour map (in MHz) of the global representation of the median value of foF2 for March 1979 (SSN=137) at 0600 UTC.

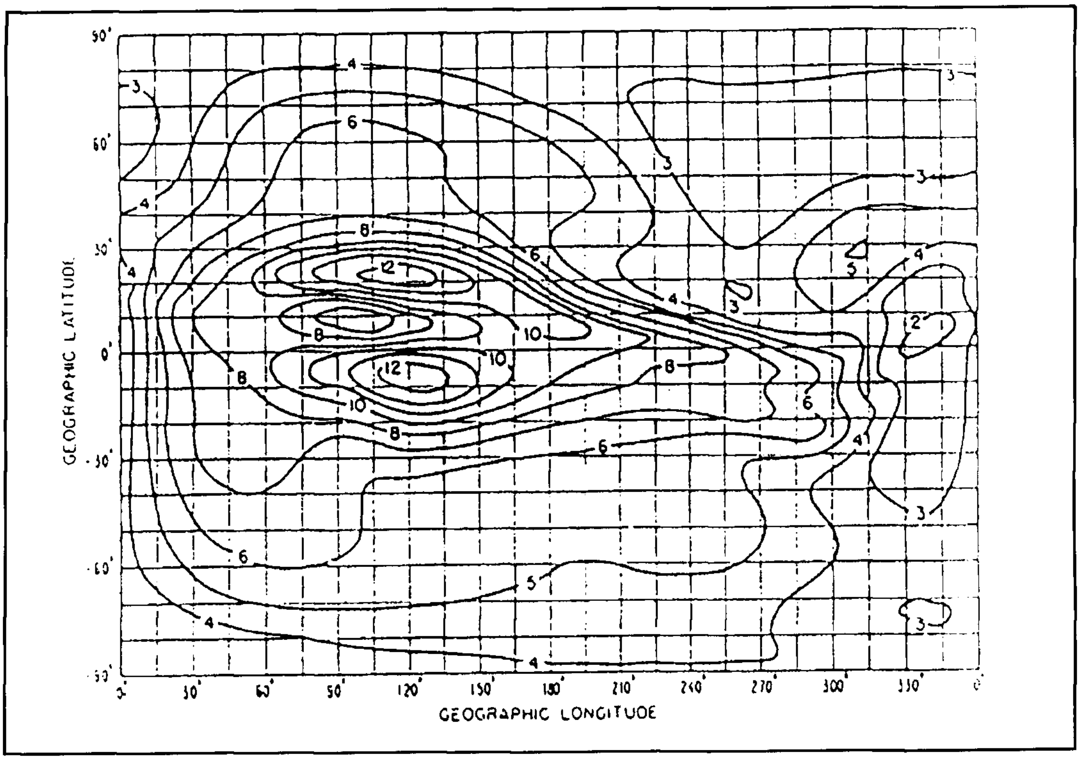

Figure 2. Contour map (in MHz) of the global representation of the median value of foF2 for March 1976 (SSN=12) at 0600 UTC.

path. Typically, termini of the paths are close to sunrise and/or sunset. In addition, long-paths having a terminus in the Northern Hemisphere frequently go to high southern latitudes—reaching beyond the central region of the ionosphere. In any event, ionization along the paths must still be at a level that will support propagation on the frequency in use.

The circumstances for a path at a given date and time may be examined by superimposing it on the corresponding ionospheric map. The basic or standard map of the ionosphere for a given sunspot number is one that shows the isofrequency contours of the F-region critical frequency, foF2, at an equinox. Two such examples are shown in **Figures 1** and **2**, one for the solar maximum (SSN=137) in March 1979 and the other for the previous solar minimum (SSN=12) in March 1976. Those maps are for 0600 UTC; the sub-solar point is at 90 degrees East longitude, with sunlight extending to 180 degrees East longitude, and darkness eastward of that longitude.

For other times of the year, ionospheric maps are shifted up or down with displacements of the sub-solar point, and solar illumination goes beyond one pole or the other. The results are seen in Mercator projections with foF2 contours extending over more than 180 degrees of longitude in the E–W direction at high latitudes. In any event, the major part of the ionization is found in the illuminated region that lies within the bounds of the solar terminator on the ionospheric map.

Successful long-path contacts occur when paths fall within regions that contain sufficient ionization to support propagation on the operating frequency. At dawn in the summer, such paths from northwest Washington head off to the southeast toward India, Sri Lanka, and the Indian Ocean area, passing close to the part of the gray line that goes below the main region of ionization. In winter, the paths at dawn go off to the southwest to reach Europe and Africa and travel close to the part of the gray line that lies west of the main region of ionization.

Long-path propagation at high latitudes

Just after the peak of Cycle 22, I carried out a propagation study from April 1, 1991 to March 21, 1992. I was looking for long-path contacts in the early morning hours during 339 of the 355 days; on the remaining 16 days, long-path contacts were not pursued because of major contests in progress. In the course of the study, a total of 1,689 long-path contacts were made and then analyzed with respect to path, season, solar, and magnetic conditions in progress at the time. A summary of the study was published privately[1] and a condensation of the study appeared in the fall and winter issues of

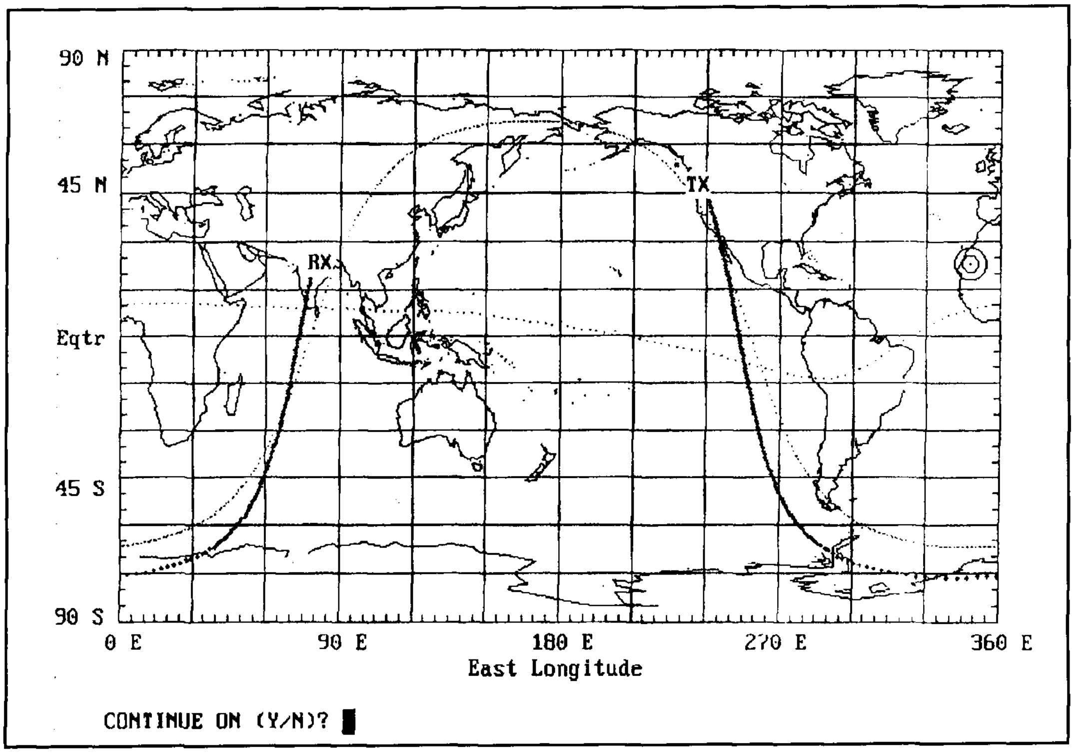

Figure 3. Great-circle path from Guemes Island, Washington to India at 1249 UTC on June 6, 1991.

the 1992 *Communications Quarterly*.[2]

The long-path contacts made during that study ranged in distance from just over 20,000 km (to Crozet Island) to 33,368 km (on the north coast of Norway). Because of my location here in the northwest corner of Washington, the paths went mostly through the southern auroral zone or across the southern polar cap, toward Africa, the Indian Ocean area, and into Europe. The only sub-auroral

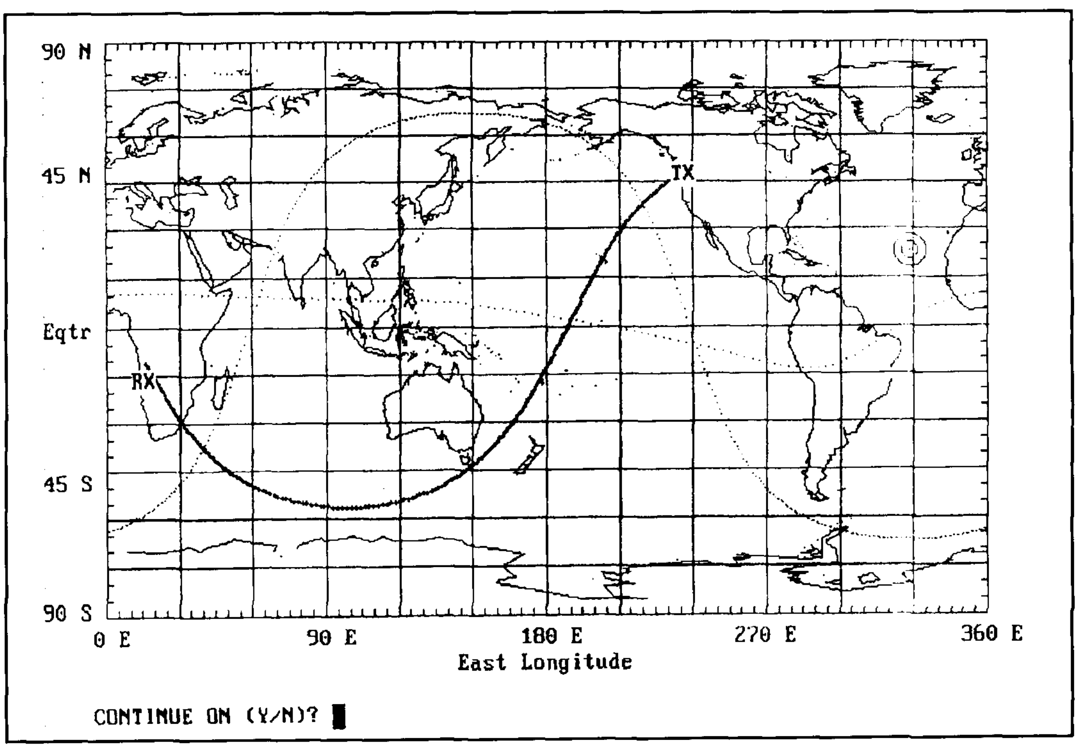

Figure 4. Great-circle path from Guemes Island, Washington to Angola at 1407 UTC on June 6, 1991.

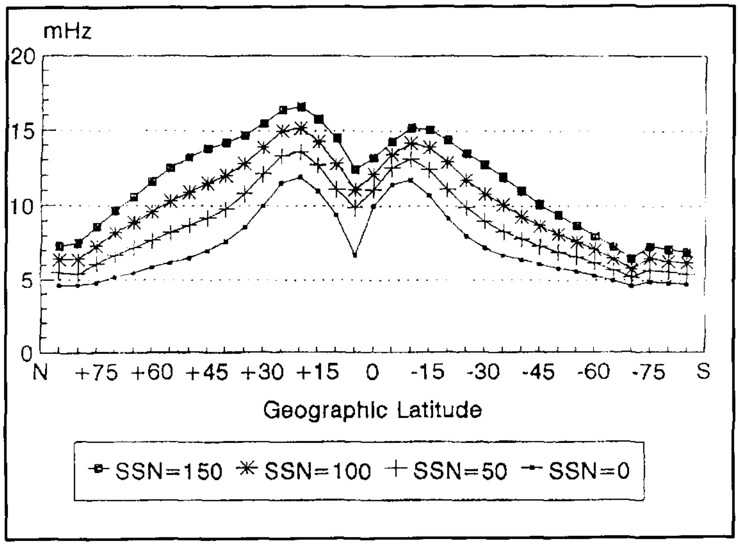

Figure 5. foF2 at the spring equinox at 0600 UTC at 120 East Long.

path was to Capetown, South Africa. As a result, the study dealt mainly with high-latitude paths and the solar-terrestrial processes that affect them.

Given the high latitudes of those paths, a significant number of the contacts were made when the paths were close to the gray line, with Europe in our winter and India and Sri Lanka in the summer. Thus, in the report giving the results of the study,[1] there was discussion of gray line propagation and how it involved D-region considerations, as well as the increase in critical frequencies in the F-region with sunrise on the path. The last point was discussed with the aid of paths to Switzerland and India and was included in the condensation,[2] while the

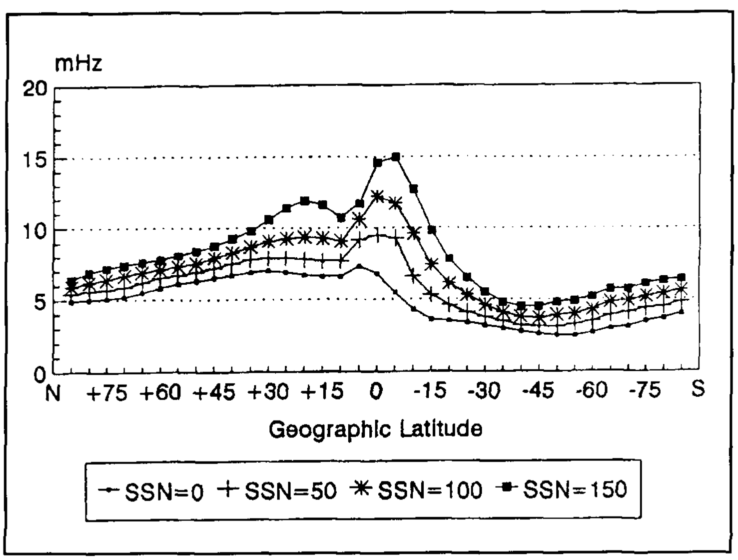

Figure 6. foF2 at the summer solstice at 1400 UTC at 100 East Long.

effect of the current decline in solar activity on the F-region sunrise variation was examined in a recent publication.[3]

While the gray line has an important role in propagation, it was pointed out in the results of the LP study that propagation is still quite possible for paths which go off almost perpendicular to the gray line. For example, a case was cited where a gray line contact with a VU in India in June of 1991 (shown in **Figure 3**) was followed shortly by a contact with a D2 in Angola for which the path started on a direction not far from perpendicular to the gray line, shown in **Figure 4**. As such, that contact indicated that levels of ionization comparable to those along successful gray line paths existed on the path to Angola, right across the dark ionosphere. That result was reinforced by more than 200 contacts made with stations on the African continent with beam headings 60 to 80 degrees away from the gray line.

Those paths across the dark ionosphere to the west were at high latitudes, the example to Angola involving one that reached almost 57 degrees south geographic latitude. That contact, as well as the others cited in the study, showed that close to solar maximum, the level of ionization in the dark ionosphere, even at high latitudes, did not decay away in the hours after sunset to levels below those required for propagation on 14 MHz. Unfortunately, the discussion of contacts on darkened paths was not included in the condensation of the study.[2]

Long-path propagation at lower latitudes

The long-path study explored features of that mode of propagation and how it is affected by solar-terrestrial disturbances, most often in the form of magnetic storms. In this regard, the data obtained from the northwest corner of Washington was mainly for paths that went through the auroral zone or beyond, over the polar cap. However, it was possible to extend the study to sub-auroral latitudes in the same time period of 1991 by using long-path data for contacts with South Africa provided by operators in the Los Angeles-San Diego area. The results were not unexpected and showed in a quantitative manner that sub-auroral paths, starting 15 degrees more equatorward and only reaching 47 degrees south magnetic latitude, were less susceptible to disruption than those into the auroral zone and the polar cap.

In the time since the original study in '91–'92, additional LP operations were carried out on 14 MHz during the winter months of '93–'94 and '94–'95—making contacts largely

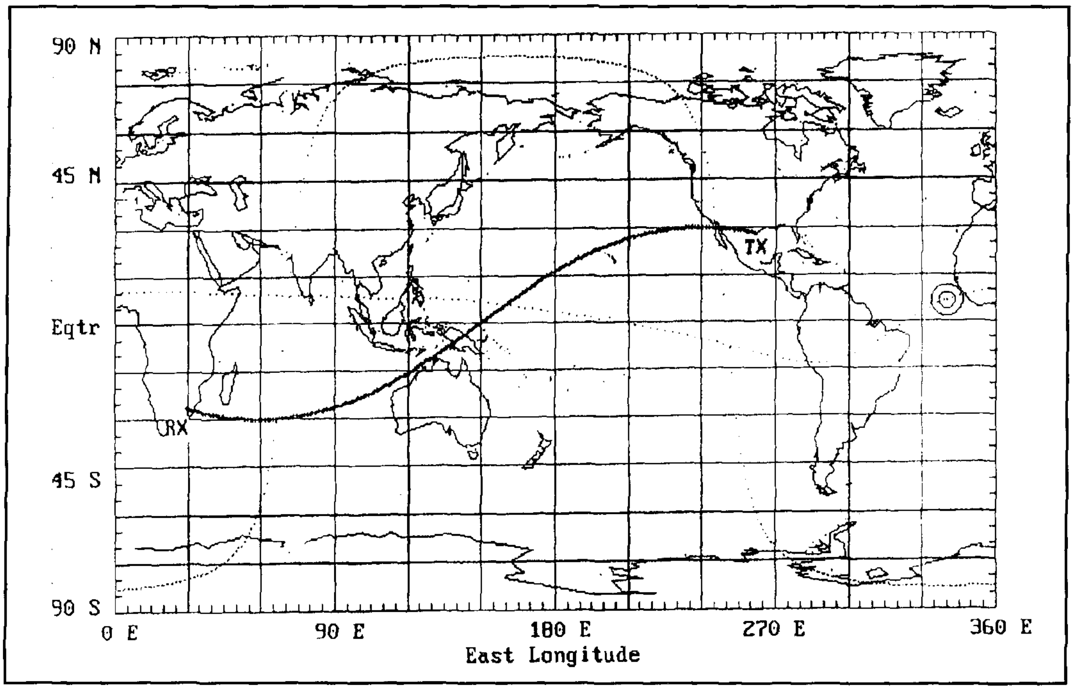

Figure 7. Great-circle path from Portland, Texas to Boksburg, South Africa at 1320 UTC on September 4, 1995.

via high latitude paths with European stations. Those contacts were made in a less structured manner than before and without any detailed analysis, but some features are of interest. For example, toward Europe, in '94, the last LP contact of the season was with 4Z5AF at 1530 UTC on March 5; and in '95, the last LP contact was with HA9UU at 1554 UTC on February 24. During the study in '91–'92, no such early closures of the paths were evident.

In the summers of '92 and '93, there were gray line contacts with stations in India and Sri Lanka, as well as with African stations across the dark ionosphere (**Figure 3**), but the last summer contact of that type was with ZS6ME at 1342 UTC on August 22, 1993. No signals were heard from South Africa in the summers of '94 and '95, and one must conclude the ionization on darkened paths reaching 56 degrees south geographic latitude has declined, along with solar activity, and is now unable to support propagation on 14 MHz.

Those remarks deal with consequences of the decline in solar activity in Cycle 22, essentially from the "downsizing" of the ionosphere. Another view of the "downsizing" is obtained by comparing the features of an ionospheric map for a solar maximum with one for a solar minimum, say using **Figures 1** and **2**. Such a comparison[4] shows a lowering of critical frequencies over the globe as solar activity declined and a contraction of the outer reaches of the ionosphere toward the central region under solar illumination.

Another view of the "downsizing" is shown in **Figure 5**, obtained by plotting how the critical frequency varies with solar activity along N-S traces across the most robust portions of foF2 maps. That figure is for the spring equinox, similar to the map in **Figure 1**, but at 120 degrees east longitude. As such, it shows that as the SSN goes from 150, a value comparable to the maximum in Cycle 22, to zero, the ultimate solar minimum. The critical frequencies drop by about 50 to 60 percent at middle and high latitudes, but only 30 percent at lower latitudes, where ionization is most intense.

With those results in mind, one can understand why the dark auroral paths to Africa began to fail on 14 MHz after the summer months of '93. For one thing, there was the overall decrease in critical frequencies that followed the decline in solar activity—also the summer ionosphere contracted northward, further decreasing the magnitudes of the critical frequencies at high southern latitudes. Thus, a similar figure for June at 1400 UTC, the time of the contact with Angola, is shown in **Figure 6** and the N-S cut is at 100 east longitude—the most southerly excursion of the path.

The figure illustrates that the critical frequency at 56 S latitude drops by 50 percent, from 4.9 to 2.5 MHz, in going from an SSN close to that for the solar maximum in Cycle 22 to the present level near solar minimum. For oblique propagation to be supported, a median foF2

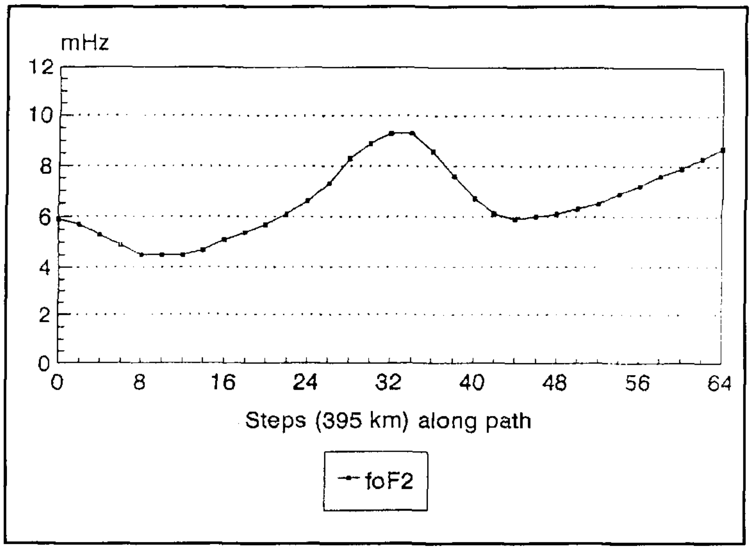

Figure 8. foF2 variation along the path to Boksburg, South Africa at 1320 UTC on September 4, 1995.

value of about 4.5 MHz is needed (approximately one-third of the 14-MHz operating frequency) and the 50 percent decrease in foF2 with declining solar activity easily explains the lack of propagation across the dark ionosphere to Africa in the summer months of '94 and '95.

In spite of the discouraging results for long-path propagation across high latitudes that follow from the fall-off of foF2 values with declining solar activity, an encouraging result is seen in **Figure 5** and should be noted: foF2 values at low latitudes are more than enough to support propagation on 14 MHz, even at low levels of solar activity. This has been borne out by recent long-path contacts with Africa and the Indian Ocean area by Michael Mauldin, K5NU.

Long-path propagation near solar minimum

Beginning in early August 1995, K5NU had a series of long-path contacts on 14 MHz with stations in South Africa, Zimbabwe, Kenya, Mauritius, and Reunion Island, all on paths that go across the dark ionosphere to the west of his QTH in Portland, Texas. The great-circle path for one contact, with ZS6AVM in Boksburg at 1320 UTC on September 4, is given in **Figure 7**. This shows that about 75 percent of the 25,400 km path was in darkness after sunrise in Texas and as sunset approached in Africa. Note that the path covers 234 degrees in longitude and is nearly symmetrical, starting from 27.9N, ending at 26.2S, and reaching about 30 degrees latitude on each side of the equator.

In **Figure 8**, one sees the variation of critical frequency along the length of the path at 1320 UTC. The median foF2 values are low at the Texas end of the path, rise to a peak over 9 MHz south of the equator, fall again on the western part of the path, and finally rise again on approaching South Africa. Those values show that propagation on 14 MHz was supported toward South Africa.

A more complete view of the situation in early September is shown in **Figure 9,** where the MUF is plotted as a function of time and losses are shown for signals from both ends of the path. Here, the path is not open before 1300 UTC, and the signal losses from the west end of the path represent the losses in the illuminated region just west of Boksburg, South Africa. Losses for signals from the eastern end of the path began after 1300 UTC, when the path opened at sunrise. Both loss calculations included reflection off the ocean and D-region absorption; no effort was made to include polarization coupling loss or excess system losses discussed by Davies.[5]

It is clear from **Figure 9** that the long-path contact was made when the total signal loss from the two ends of the path was at a minimum. A more complete view of the signal propagation on that path may be seen in **Figure 10** where the MUF has been calculated, with the aid of the IONCAP program, for smoothed sunspot counts from zero to 150. Those results show that long-path propagation on 14 MHz is feasible even at the ultimate solar minimum, with no spots on the sun. Beyond that result, it is clear that for the same level of solar activity, the path will open earlier in summer and later in winter, just from the change in shape of the terminator with seasons.

It should be noted that the MUFs are median (50 percent) values and that the critical frequencies of the ionosphere along a path show daily variations, as described by their lower (90 percent) and upper (10 percent) decile values. In a dark ionosphere, as was the case just west of the Texas terminus, the spread of the daily variation is 20 to 25 percent either side of the median. As a result, the availability of long-path connections at low levels of solar activity for the path in **Figure 8** is about 50 percent. This is set largely by the variability of foF2 values around steps 8 to 12; i.e., at distances of 3,500 to 5,300 km from the eastern terminus.

Discussion

It is interesting to compare the circumstances of the two examples of long-path propagation across a dark ionosphere—that cited earlier to Angola and the present one to Boksburg, South Africa. The dates and paths have already been given, close to a solstice on one hand and the fall equinox on the other, as well as after the solar maximum and just before the solar minimum of Cycle 22, respectively. More important, however, are differences in the sources of the ionization along the paths and how well ionization is retained or controlled by the earth's magnetic field.

The ionization on the two types of paths has its origin in photo-ionization processes from the incidence of solar ultraviolet radiation on the atmosphere. Ionospheric electrons are released on geomagnetic field lines, but the altitudes of origin are strikingly different in those two cases and the ionization is located on field lines of quite different radial extent. Thus, ionospheric electrons on the path to Angola were released at F-region altitudes on high-latitude field lines that reach out more than 6 earth-radii; but at that distance, their retention in the F-region could be affected by magnetic activity resulting from the impact of the solar wind on the magnetosphere.

On the other hand, electrons on the path to South Africa were released on low-latitude field lines that reach out only 1.5 earth-radii or so. However, their origin may have been partly at E-region altitudes as well as in the F-region. That is the case, as the low-latitude F-region has part of its origin in the "fountain effect."

There, because of solar heating, electrons and ions formed in the E-region are carried in E-W directions by atmospheric motions. With that, the magnetic forces brought into play by their motion across the horizontal geomagnetic field serve to redistribute the ionization, electrons around the equator rising and spilling over to form peaks in ionization at low latitudes on both sides of the equator. Those peaks are called the equatorial anomaly,[6] and are well developed by late afternoon and early evening—as may be seen from the foF2 iso-frequency contours around 180 degrees east longitude in **Figures 1** and **2**. The critical frequencies in those regions are among the highest in the ionosphere, even exceeding 10 MHz at solar minimum.

At the equinox, inspection of those two figures shows F-region ionization persists after sunset; i.e., beyond 180 degrees longitude. But those figures show that for both solar maximum and minimum, critical frequencies at high latitudes decay after sunset while significant amounts of ionization continue to be present at low latitudes, extending well into the evening and decaying at a much slower rate. Beyond noting those two extremes, it is instructive to compare the loss of ionization on the two paths crossing a dark ionosphere with the decline in solar activity between 1991 and 1995.

For that purpose, model calculations were made to determine the lowest foF2 value along each path at the time in question, and comparisons were made between the two levels of solar activity. Also considered was how the lower levels compared with the median foF2 value (4.5 MHz) needed to support propagation on 14 MHz. For the path from northwest Washington to Angola in June, the lowest foF2 value on the path fell from 5.2 MHz in 1991 to 3.0 MHz for current conditions, down to only 58 percent of the value in 1991. And for the path from Texas to South Africa in September, the lowest foF2 value for the path dropped from 6.2 MHz in 1991 to 4.5 MHz for 1995—73 percent of the earlier value. From the first result, one sees that long-path propagation to Angola around dawn would not be supported presently, while the other result shows propagation from Texas to South Africa is quite possible, as confirmed in the 1995 observations.

In addition to the results for the foF2 variation along the path from Portland, Texas to Boksburg, RSA shown in **Figure 8**, values of the lowest critical frequency foF2 around dawn were determined throughout a year and for three levels of solar activity, all higher than at present. They are shown in **Figure 11**.

Relation to earlier work

Recent long-path contacts to South Africa, around dawn and near solar minimum, were possible due to the high levels of ionization that still remain at low latitudes after the sun has set on the equatorial anomaly. To some extent,

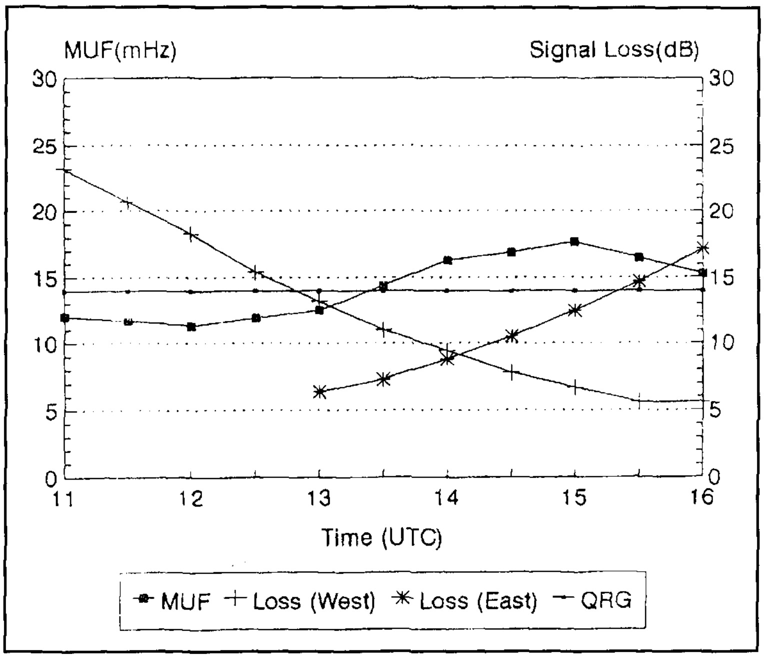

Figure 9. MUF and signals loss variations on the path to Boksburg, South Africa on September 4, 1995.

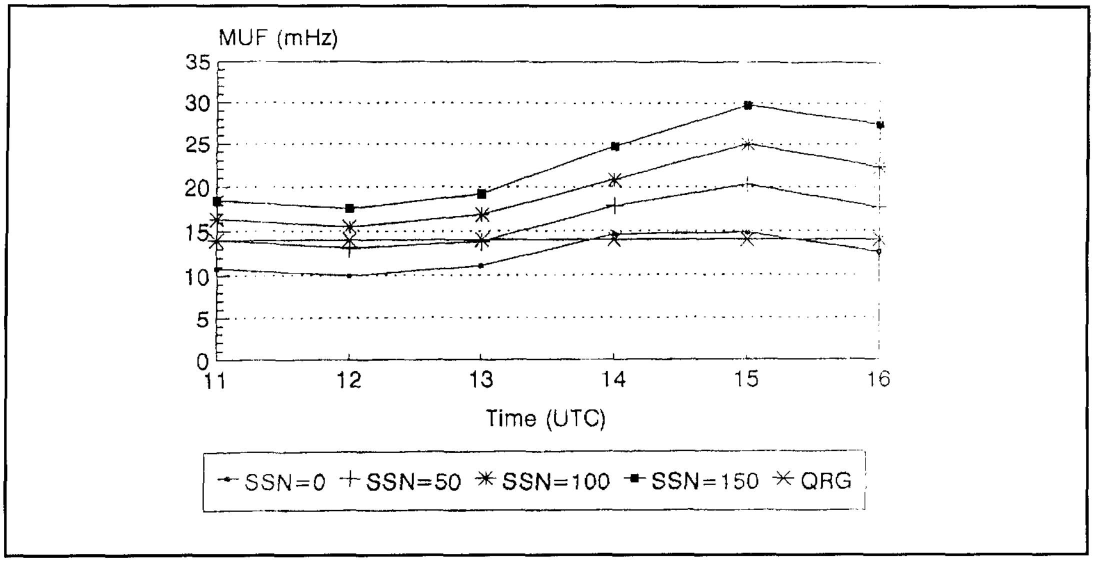

Figure 10. MUF variation with solar activity for the path to Boksburg, South Africa.

those observations bear a relationship to earlier work by R.B. Fenwick, K6GX, and O.G. Villard, W6QYT, on Around-the-World (RTW) propagation in 1963.[7] In that study, the possibility of RTW propagation was explored during February 1963 by sending signals, in the range from 12.2 to 21.7 MHz, westward from Okinawa and listening for their arrival at Guam.

On Okinawa, transmitter powers ranged from 600 to 770 watts output, and the transmitting antennas were terminated rhombics with gains of 17-18 dBi; at Guam, 2,250 km to the southeast, the receiving antenna was a small, terminated rhombic directed to receive incoming RTW signals. With both sites in the northern hemisphere and differing in latitude and longitude by 12.5 and 14.8 degrees, respectively, the great-circle path between the two points was rather inclined—reaching 50 degrees north at 60 degrees east longitude and 50 degrees south at 120 west longitude. Solar conditions at the time were those at about two years before the end of Cycle 19 and with a sunspot number of 30, comparable to conditions in March 1994.

For the Texas-South Africa contacts, the transmitter in Texas ran 1 kW into stacked 4-element Yagis at 43 feet and 105 feet. In South Africa, the transmitting systems ranged from 80 watts into a mobile whip to 100 watts into slopers, dipoles, inverted Vees, and a 3-element Yagi. As noted earlier, the paths covered about

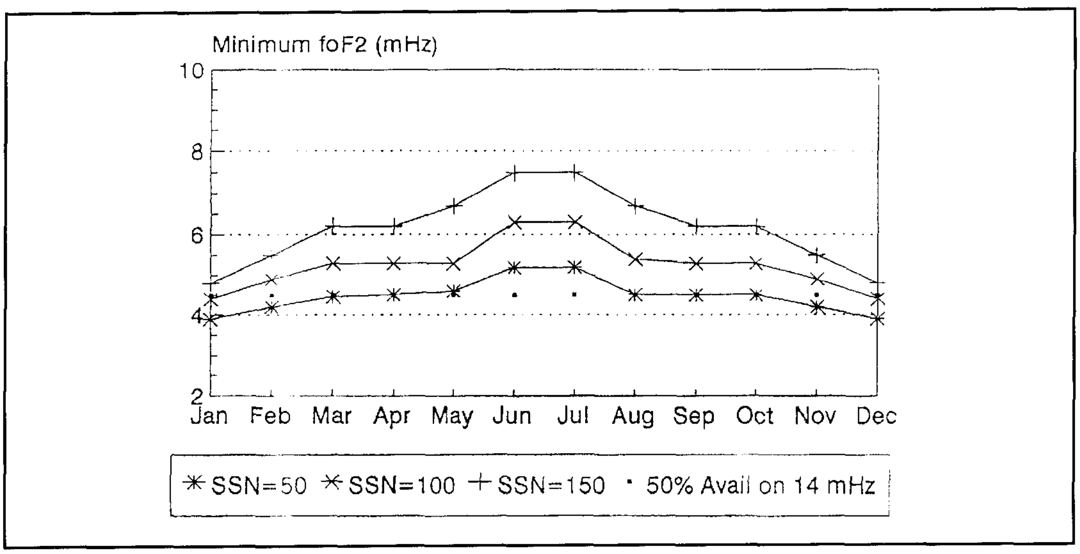

Figure 11. Monthly values of the minimum foF2 on the path to South Africa at dawn and for different sunspot numbers.

234 degrees in longitude and from one terminus to the other. They were nearly symmetrical with respect to the equator and reached 30 degrees north and south latitude, as shown in **Figure 7**. Solar conditions, of course, were those in August to September 1995, just before the minimum of Cycle 22 (the date of which is yet to be determined).

The RTW study aimed at exploring tilt-supported modes of propagation expected from longitudinal gradients in the ionization in the F-region. Such modes result in what are commonly called "chordal hops", ionosphere-ionosphere reflections without any intermediate ground reflections. In the study, receivers were located in Salonika, Greece and Malta, and the lack of signals there at times of RTW transmissions to Guam was taken as evidence to support the idea of tilt-mode propagation from longitudinal gradients in the F-region.

One case discussed by Fenwick and Villard occurred at 0200 UTC in mid-February, with the path shown superimposed on an ionospheric map. In that instance, gradients were evident to the west of Okinawa. The map of the region showing foF2 declined from 9.6 MHz to about 7.2 MHz in the first 2,500 km along the path toward dawn. Numerically, the longitudinal ionization gradient would be expressed by the change in the number of electrons in unit volume per unit distance along a path.

Because data on critical frequencies are more readily available, and electron density is proportional to the square of the critical frequency, a measure of the ionization gradient may be expressed by the differences in squares of foF2 per unit distance along a path, using units of MHz-squared per km. Thus, at 0200 UTC, the longitudinal gradient just to the northwest of Okinawa would be 0.016 MHz-sq/km, or -16E-3 (MHz-sq)/km, and the critical frequency continued its decline along the path to Malta. The fact that signals from Okinawa were not heard at those times in Salonika or Malta was attributed to a reduction in downward ionospheric refraction of signals due to the decrease in electron density; i.e., a negative gradient along the path before those locations.

It is natural to ask if similar effects were present during the long-path contacts around dawn on the path from Portland, Texas to South Africa. It would seem unlikely, at least in that magnitude, as the effective sunspot number was lower than during the RTW study. That proved to be correct as similar calculations show that the electron density gradient along the path just to the west of Portland averaged -5E-3 (MHz-sq)/km, essentially a factor of 3 lower than in the RTW study. Given the difference in magnitudes, the role of tilt-supported propagation seems less important in the long-path case than was apparent for the RTW study—but it cannot be ruled out completely. Thus, ionospheric gradients might increase the duration of openings at somewhat higher levels of solar activity, because of the higher MUFs possible from the lowering of angles by refraction in the gradient region. But the gain would be from path geometry rather than due to any reduction in losses from ground reflection or D-region traversals, as the path is largely over sea water and in the dark.

Beyond the different levels of solar activity, the numerical values for the two cases reflect that the transmissions from Okinawa were four hours after sunrise and into a well-developed ionosphere to the west, while transmissions from Texas were about an hour after ground sunrise and just after the path opened. In a rough way, the circumstances in local time for those two situations may be seen by looking back at **Figure 2**. A comparable situation to the Okinawa path would be a great-circle path heading to the northwest from 26N, 60E and for the path from Texas; it would a great-circle path heading essentially west from 28N, 15E. The foF2 values would be somewhat higher in the first instance, making the differences in longitudinal gradients more striking than in **Figure 2**.

In the case of long-path contacts on 14 MHz, the opening shown in **Figure 9** appears to be rather brief, the MUF going through a maximum about the same time the absorption is increasing. With sunrise on one end and sunset on the other, at a low level of solar activity as now, propagation on the path begins with the rise in critical frequency at the sunrise terminus, or control point. The path most likely fails because of the increase in absorption in that same region. At higher levels of solar activity, the rise in MUF would open the path somewhat earlier on 14 MHz and it would be available over a greater portion of the year, as shown in **Figure 11**.

At some point, MUF values would no longer be the limiting factor for long-path propagation through the low-latitude ionization remaining from the equatorial anomaly. Instead, at higher levels of solar activity, the path would become absorption-limited on 14 MHz—as is the case when frequencies are below 14 MHz—for openings on the familiar long-path circuits that pass through latitudes largely outside the reach of ionization from the equatorial anomaly.

Conclusions

After the maximum of a solar cycle, the decline in solar activity which follows takes F-region critical frequencies at each location through progressively lower values and the iso-frequency contours on ionospheric maps move equatorward, toward the kernel of the ionosphere around the sub-solar point. For long-path propagation, that means high-latitude paths along the gray line between fixed terminii begin deteriorating in reliability and finally fail at the time when one or more regions on the path no longer support propagation on the operating frequency, say 14 MHz in the present discussion.

Long-path propagation across dark portions of the ionosphere also becomes less reliable and viable paths that go through high latitudes are fewer in number as they fail progressively with the "downsizing" of the ionosphere. Ultimately, the paths that still remain and offer long-path propagation are those which go across low-latitudes, within about 30 degrees either side of the equator.

While the gradual reduction in the number of long paths at high latitudes involves the decline of ionization processes at F-region altitudes, long paths remain effective at low latitudes around solar minimum because of E-region processes. In particular, their basis is in the photo-ionization at E-region altitudes, which goes to form the equatorial anomaly and then remains in significant amounts in the F-region in the hours after sunset at those latitudes.

Because the terminator is so far removed from dark paths at low latitudes, the conventional ideas regarding path directions relative to the gray-line have little, if any, bearing on long-path propagation across those latitudes. And considering that F-region ionization at low latitudes is held on field lines deep within the magnetosphere, paths that travel through those regions are much less vulnerable than high-latitude paths to the effects of any decline of solar activity, or to any disruption by magnetic storminess.

Acknowledgements

I am indebted to Michael Mauldin, K5NU, for calling my attention to these interesting long-path openings and for sharing his log data. In addition, I want to thank Jacky Mandary, 3B8CF, Jack Snyman, ZS1OU, Frank Franklin, Z21FN, and Ron Faulkner, W6TUR, for their comments on long-path propagation—particularly on the loss of high-latitude paths on 14 MHz with the decline in solar activity in Cycle 22. ■

REFERENCES

1. Robert R. Brown, NM7M, "A Study of Long-Path Propagation in Solar Cycle 22," Anacortes, Washington, March 1992.
2. Robert R. Brown, NM7M, "Long-Path Propagation," condensed for publication by Ward Silver, N0AX, *Communications Quarterly*, Fall and Winter, 1992.
3. Bob Brown, NM7M, "The Last Hop," *The DX Magazine*, May/June 1995.
4. Bob Brown, NM7M, "On the Down-Sizing of the Ionosphere," *The DX Magazine*, July/August 1994.
5. Kenneth Davies, *Ionspheric Radio*, Peter Peregrinus, Ltd., 1990.
6. Leo F. McNamara, *Radio Amateurs Guide to the Ionosphere*, Krieger Publishing Co., 1994.
7. R.B. Fenwick and O.G. Villiard, "A Test of the Importance of Ionosphere-Ionosphere Reflections in Long Distance and Around-the-World High-Frequency Propagation," J. Geophys. Res. Vol. 68, p. 5659, 1963.

PRODUCT INFORMATION

Digital I/O Extender Module Models 232IOEXT and 422IOEXT

B&B Electronics Manufacturing Company has two I/O Extender modules that allow you to turn on a device or sense a contact closure from a remote location. When the state of an input changes at one I/O Extender, this change is converted to serial data and is transmitted out its serial port to the other I/O Extender. The data is then converted back and the corresponding digital output changes state. Each I/O Extender has 8 digital inputs and 8 digital outputs that are brought out on a DB-25 female connector. All digital inputs and outputs are 0 to +5 V CMOS/TTL compatible.

Two models are available: an RS-232 serial port Model 232IOEXT, and an RS-422 serial port Model 422IOEXT. The serial ports signals are brought to a DB-25 male connector. The RS-232 model can be used to extend I/Os up to 50 feet or can be used over a leased telephone line system. The RS-422 model can be used to extend I/Os up to 4,000 feet. The 232IOEXT serial port requires 3 lines: TD, RD, and SG. The 422IOEXT serial port requires 5 lines: TD(A), TD(B), RD(A), RD(B), and SG.

For further information, contact B&B Electronics Manufacturing Co., 7078 Dayton Rd., P.O. Box 1040, Ottawa, IL 61350; phone 815-433-5100 (8 am to 4:30 PM Central); 24-hr. fax 815-434-7094; 24-hr. BBS 815-434-2927 (home page http://www.bb-elec.com); or e-mail catrqst@bb-elec.com.

Because we were unable to obtain reproduction permission from the author, the following article does not appear in the *ARRL Communications Quarterly Collection*...

Fractal Antennas Part 2

By Nathan "Chip" Cohen, N1IR

2 Ledgewood Place
Belmont, MA 02178

Summary: A discussion of the qualities of fractal antenna design. In particular, the text focuses on resonance, gain and bandwidth properties.

Summer 1996 issue, pages 53-66.

Please contact the author for additional information.

PRODUCT INFORMATION

New RF/IF Product from Analog Devices

Analog Devices has announced its newest RF/IF product, the AD6432 3-V transceiver. This device includes all the building blocks needed for modulation and demodulation of signals for digital wireless systems, and replaces a dozen or more discrete components. It can be used by itself for low-power systems up to 300 MHz RF carrier frequencies or with RF up- and down-converters for higher carrier frequencies. The I/Q modulation and demodulation method enables the chip to be used with the modulation formats most commonly used in digital wireless systems, including GMSK, QPSK, DQPSK, and spread-spectrum systems.

The receive section accepts input signals up to 300 MHz, down-converts to a user-selected IF between 10 and 30 MHz, provides gain from –20 to +60 dB, and provides baseband I and Q output signals with up to 8 MHz bandwidth. The gain is controlled by an analog control voltage with linear-in-dB voltage control. Input 1 dB compression point is –15 dBm, and the minimum input signal level is –90 dBm for 3 dB S/N at the output. The quadrature demodulator provides ±1.5 degree phase accuracy.

The transmit section includes I/Q modulators and summing amplifier, accepting modulation bandwidths up to 1 MHz and modulating a carrier frequency up to 300 MHz. The output level is nominally –15 dBm and can drive an up-converter to a higher carrier frequency or a power amplifier. The AD6432 also includes a PA-control amplifier, useful in systems where output power control is needed. This amplifier accepts inputs from a power setpoint and a power sensor and delivers a PA control voltage to set the power amplifier's operating point to the desired level.

The AD6432 operates on a single power supply voltage of 2.7 to 5.5 volts, and includes provision for independent sleep modes for the transmit and receive sections. Both the receive and transmit sections consume 8 mA in active

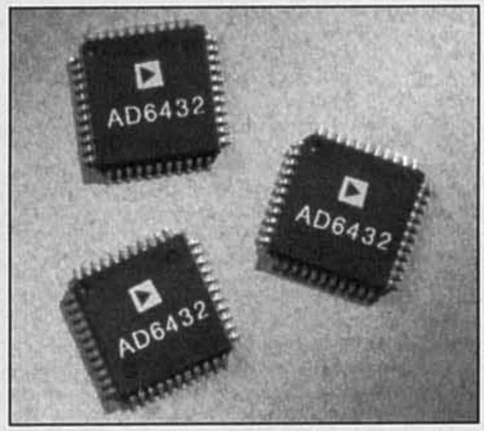

mode and less than 100 microamps in sleep mode. The unit can be used with the Analog Devices AD20msp410 GSM baseband chipset to implement a GSM handset. The AD6432 can also be used in other digital, cellular and PCS systems such as the North American IS-136 TDMA and IS-95 CDMA standards.

The AD6432 comes in a 44-pin plastic TQFP package and is rated for operation over the –40° to +85°C temperature range. It is priced at $7.25 in lots of 10,000. For details, contact Analog Devices, Inc., Ray Stata Technology Center, 804 Woburn Street, Wilmington, MA 01887; phone 617-937-1428; fax 617-821-4273.

New Ultra Low Noise Synthesizer

RF Prototype Systems has introduced an ultra low noise synthesizer that can be used for low noise applications. The phase noise is better than <–102dBc/Hz at 1kHz offset and <–110dBc at 10kHz offsets. It has its own internal reference oscillator and will accept an external reference as well.

For more information, contact RF Prototype Systems, 9400 Activity Rd., Ste. J, San Diego, CA 92126; phone 619-689-9715; fax 619-689-9733; or toll-free outside of California 800-874-8037.

Yardley Beers, *WØJF*
740 Willowbrook Road
Boulder, Colorado 80302

ANAPOLES

A different view on radiation from toroidal inductors

The article on practical toroidal antennas by Roger Jennison, G2AJV[1] surprised me on first reading. For some time, I've had an interest in radiation from toroidal inductors and included a discussion of it in a paper I gave at a meeting of physics teachers.[2] I've recognized that toroids can radiate but, under most circumstances, very weakly. I didn't think anyone would use them for practical antennas. On my second reading of Jennison's article, I realized that his are larger than the ones of interest to me, and may be considered as continuously loaded loop antennas.

The mechanism that is my primary interest is the magnetic analog or "dual" of a small circular loop of wire carrying an electric current, which produces a magnetic field along the axis. According to a principle I discuss below, the alternating current magnetic field inside a toroidal inductor acts as an alternating current of magnetic poles and produces an electric field along the axis. The field inside the toroid is the magnetic analog of displacement current on which Jennison places much attention. It can be called "magnetic displacement current," but I think it more properly should be called "induction current." For reasons discussed in Appendix 1, I call the type of radiation emitted by toroids "anapole radiation."

Modern circuit board technology usually uses toroidal inductors because of their assumed small external fields. Therefore, there's little or no use in shielding, as required with older technologies. Any student taking a second college course in electromagnetic theory learns that the external field of a circular toroidal inductor carrying a DC current is identically zero, under idealized conditions. In practice, these conditions aren't fulfilled. A toroid has external fields for a variety of reasons, which from the present point of view, I consider "spurious."

The idealized conditions assumed in the textbooks are that the situation of the toroid is perfectly symmetric, which among other things, implies that the voltage everywhere is the same. In principle, this could be realized only if the winding had only one turn made of a sheet of metal so broad that it covered the entire toroid—a very impractical assumption. In practice there are many turns, resulting in an unbalanced magnetic field of the current as it proceeds around the circumference of the toroid—what I call a "one-turn effect." It's possible to effect an approximate compensation for this by including a "back turn," where at the end of the winding the wire turns around and loops around to the beginning of the winding. In practice, the wire has a finite resistance, and there are voltage differences along the winding. As a result, there's an electric field outside the toroid. At high frequencies, the voltage is greater for the same current because of the EMF generated by the inductance of the toroid. Also, there may be contributions to external fields from non-uniformity in the winding and from fringing between the turns. Jennison's toroids are large. These non-idealized features are accentuated, so his toroids are self-resonant loop antennas.

The Equivalence Principle

The phenomenon of anapole radiation is explained by Schelkunoff's "Equivalence Principle,"[3,4,5] which is a special case of a more general principle, the principle of "duals." Electromagnetic situations usually occur in pairs such that the same equations apply to both—sometimes approximately and sometimes exactly—provided that one interchanges symbols in accordance with a prescribed plan. With circuits, voltages and currents are interchanged. With fields, electric and magnetic fields are interchanged, although sometimes (as in the present case) it's necessary to reverse signs. Because of this sign reversal, there's justification for the statement that the laws of electromagnetism are "antisymmetric" (rather than "symmetric") with respect to the interchange of electric and magnetic fields.

The most elementary example of duals consists of (1) two resistors in series and (2) two conductances in parallel. (Conductance is the reciprocal of resistance.) The statement "the current in the two resistors is the same," as applied to the first circuit, has its dual "the voltage across the two conductances is the same" as applied to the second circuit. The reader can easily formulate other dual pairs of statements for these two circuits.

The original purpose of the equivalence principle was to deal with problems of radiation from the ends of open-circuited transmission lines, waveguides, and horns. Consider a horn, for example. Suppose you covered the mouth of a horn with a perfectly conducting sheet of metal. The fields inside the horn would cause electric currents to flow on the sheet, so that the field outside the horn completely cancels the original external field. Also, the currents greatly modify the field inside the horn and in the waveguide that feeds it. With an open horn, Schelkunoff deduced that, if magnetic poles existed, a proper arrangement of currents of poles could leave the fields inside unchanged while canceling the fields outside. In other words, this current acts as a "sink" for the internal fields. At the same time, he recognized that a system of currents flowing in opposite directions but otherwise identical can generate the fields outside the horn. In other words, these currents act as a "source." Taken together, the two systems of currents cancel each other and do not have to exist physically.

Schelkunoff rewrote Maxwell's equations to include the presence of free poles. In examining them, he saw justification for interpreting the well-known term in the time rate of decrease of the magnetic induction ($-\delta \mathbf{B}/\delta t$) as a current density for the magnetic equivalent of displacement current, as expressed in certain units, which I don't specify. This might be called "magnetic displacement current" density; it should be more properly called "induction current" density.

Inside a toroid carrying a high-frequency current, there is such an induction current. In my paper,[2] I used the principles outlined in the previous paragraph to calculate the radiation resistance. I summarize the results.

Textbooks[6,7] give the derivation of the radiation resistance of a circular loop of radius "a" carrying an electric current.

$$R = \frac{\pi Z}{6} (ka)^4 \qquad (1)$$

where:

$$Z = \sqrt{\frac{\mu_o}{E_o}} = 120\pi \text{ ohms}$$

(intrinsic impedance of empty space)

$$k = \frac{2\pi}{\lambda} = \frac{2\pi f}{c}$$

$\lambda =$ wavelength (m)
$c =$ speed of light (m/sec)
$f =$ frequency (Hz)

I apply the principle to this assuming the toroid to be "thin"; that the inner and outer radii are nearly equal and can be represented by an average value "a" with the result:

$$R = \frac{k^2 c^2 L^2}{6ZN^2} (ka)^4 \qquad (2)$$

where:

L = inductance, and
N = number of turns

Many textbooks give the following approximate formula for the inductance of a thin circular toroidal inductance:

$$L = \mu \frac{N^2 A}{2\pi a} \qquad (3)$$

where:

A = the area of cross section (sq. m), and
μ = the permeability of the core material (4 x 10^{-7} henry/m for air and plastic)
$= \mu_r \mu_o$

When **Equation 3** is substituted into **Equation 2**:

$$R = \frac{Z\mu_r^2 N^2 k^6 a^2 A^2}{24\pi} \qquad (4)$$

where:
$\mu_r \equiv$ relative permeability.

Equation 4 was the principle result of my paper. Derivation is provided in Appendix II.

Experiments

Anapole radiation has its electric vector parallel to the axis of the toroid, while all of the spurious types of radiation mentioned above have electric fields with components in the median plane of the toroid. Therefore, experimental verification of the existence of anapole radiation requires the demonstration that the observed radiation has the electric field parallel to the axis.

In any valid experiment, the toroid and receiving antenna must be separated by at least a few wavelengths because there's a longitudinal component of the field in the near-field region that might alter the results. Also, the toroid and antenna should be at least a wavelength or two above ground.

Because of the limitations of the facilities available to me, I've carried out experiments at 144 MHz. There are two types. In one set, I have directly observed the radiation with a shielded receiver operated from internal batteries (Yaesu FT-290R transceiver) connected to a 3-element Yagi antenna about 50 feet from the toroid. The toroid is driven by a 144-MHz 1.5-watt transceiver in a shielded box. In the other experiments, I've taken this transceiver into the fringe area of a repeater and tried to find with which polarization I can turn on the repeater more easily. Both have ambiguous results as far as polarization is concerned, but both demonstrate that toroidal inductors have observable external fields. I have been able to turn on a repeater at distances comparable to a half mile, even though I've taken precautions to minimize spurious radiation. Designers of circuits using toroidal inductors should beware! Details of the apparatus follow.

In turn, I have used four toroids wound on plastic forms with average radii from 0.4 to 0.8 centimeters and with inductances of about 0.22 μH. A representative inductor has seven turns and a radius of 0.5 centimeters. According to **Equation 3**, the anapole resistance is about 2×10^{-5} ohms. (If there had been no compensation for the one-turn effect, its radiation resistance, according to **Equation 1**, would have been one half this large.) These toroids are mounted on RCA coaxial plugs. Each inductor has a back turn and electrostatic shield composed of strips of copper foil grounded at one point.

The transceiver is housed in a 3 x 5 x 13-inch metal box. A RCA jack for the toroid is mounted on one 2 x 5-inch side. Connected between the jack and the center conductor of the transceiver is a 50-ohm dummy resistor and a trimmer capacitor in series to resonate the reactance of the inductor. This is adjusted by the aid of a temporary insertion of an SWR bridge between the transceiver and its load. The system is grounded only at the jack. There should be a minimum of ground currents on the surface of the box.

Because the resistance of the coil is small compared to 50 ohms, the load impedance is essentially 50 ohms, and the radiated power is the radiation resistance multiplied by the square of the current through 50 ohms for an output power of 1.5 watts. The calculated radiated power is 0.6 μW. If this were used in a line-of-sight system where both antennas have the directivity of dipoles, the noise figure and the bandwidth of the receiver would be, respectively, 4 dB and 3.5 kHz—the calculated distance for which signal = noise is about 21 miles. Therefore, it's reasonable that I have been able to start up a repeater from a point about half a mile away.

In the experiment with a 3-element Yagi receiving antenna, the signal is too weak to be detectable with the crystal detector, DC amplifier, and meter that I have on hand. I've had to use the S-meter of the Yaesu transceiver to observe the signal strength. Probably, this has a logarithmic response and is insensitive to small changes in signal strength. As a result, I have been unable to tell unambiguously which polarization is more favorable.

I hope someone with better facilities will repeat these experiments. Because the factors in **Equations 2** and **4** are interdependent, I haven't been able to deduce how to choose the parameters to optimize the experiment. I'm under the impression that 144 MHz isn't the optimum frequency. The presence of a back turn and an electrostatic shield increased the distributed capacitance, which probably has a large effect at this frequency. I believe the experiment should be repeated at lower frequencies; however, the toroid and pick up antenna must be further apart and higher off the ground, as measured in meters. Ideally, the experiments should be performed on towers or on the roofs of high buildings. Undoubtedly, there are also better DC amplifiers and meters than the ones I used. At any rate, I've shown that small toroidal inductors can radiate!

Appendix I: Anapoles

My concern with radiation from toroidal inductors did not originate from my interest in antennas, but from an interest in theoretical physics. A few years ago, during an informal discussion on radiation problems, Professor David Bartlett of the University of Colorado Physics Department happened to mention that a Russian physicist[8] had suggested that certain experimental results might be explained if within the body of electrons there were toroidal currents. He gave the name "anapole" to this effect. I saw that this hypothesis had the macroscopic analog in the radiation from a toroidal inductor. This observation led to my present work.

The anapole hypothesis has been used in calculations involving other particles beside the electron and has extended to whole atoms, as well. Any reader desiring more information *should send me an S.A.S.E., and I shall send a* list of some references. ■

REFERENCES

1. Roger C. Jennison, G2AJV, "The G2AJV Antenna and Maxwell's Displacement Current," *Communications Quarterly* Summer 1995, page 23.
2. Yardley Beers, "Dipoles, Quadrupoles, and Anapoles," *Journal of Colorado-Wyoming Academy of Science XXV*, 1993, page 13. Title listed in *Announcer* (American Association of Physics Teachers) **23**, No. 2, page 20 (1993).
3. S.A. Schelkunoff, "Some Equivalence Theorems of Electromagnetics and Their Applications to Radiation Problems," *Bell System Technical Journal 15*, 1936, page 92.
4. R.S. Elliot *Antenna Theory and Design*, Prentice Hall, Englewood Cliffs, New Jersey, 1981, Sec. 1,12.
5. A.B. Bronwell and R.E. Beam, *Theory and Application of Microwaves*, McGraw-Hill, New York, 1947, Sec. 21.07.
6. Reference 5, page 418–420.
7. J.C. Slater, *Microwave Transmission*, McGraw-Hill, New York, 1942, pages 232–234.
8. Ia. B. Zel'dovich, "Electromagnetic Interaction With Parity Violation," *Soviet Physics JETP*, 6, 1958, page 1184 (English translation of Russian paper.)

BIBLIOGRAPHY

1. N.J. Carron, "On the Fields of a Torous and the Role of the Vector Potential," Am. J. Physics, 63, No. 8, page 717, 1995.

Appendix II: Derivation of Anapole Radiation Resistance

Maxwell curl equations with term for current density of magnetic poles. All six terms have units of ampere/meter:[2]

$$\frac{1}{\mu}\nabla \times \underline{B} = \underline{J} + \epsilon_0 \frac{\delta \underline{E}}{\delta t}$$

$$\frac{1}{Z}\nabla \times \underline{E} = -\frac{\underline{M}}{Z} - \frac{1}{Z}\left(\frac{\delta \underline{B}}{\delta t}\right)$$

$$Z \equiv \sqrt{\frac{\mu_0}{\epsilon_0}} \doteq 120\pi\Omega = 377\Omega$$

Magnetic induction current (analog of displacement current).

$$I_m \equiv -\frac{1}{Z}\int \frac{\delta \underline{B}}{\delta t} \bullet \delta \underline{A} = -\frac{1}{Z}\left(\frac{\delta \emptyset}{\delta t}\right) = -\frac{1}{ZN} L \frac{\delta Ie}{\delta t} = \frac{1}{ZN} V$$

$N \equiv$ number of turns on toroidal inductor.
For current varying harmonically in time with angular frequency ω:

$$I_m = -\frac{i\omega}{ZN} LI_e = -\frac{ikc}{ZN} LI_e$$

where:

$I_e \equiv$ electric current in winding, and

$$k = \frac{2\pi}{\lambda} = \frac{\omega}{c}$$

The radiation resistance of a one-turn loop of radius "a" carrying electric current[6,7] is:

$$R = \frac{\pi Z}{6} (ka)^4$$

By Schelkunoff's Principle, this applies both with respect to a one-turn loop carrying an electric current, or a toroid carrying a magnetic current I_m.
The radiated power:

$$P = \frac{R_m I_m^2}{2} \equiv \frac{R_e I_e^2}{2} \qquad (5)$$

This equation defines R_e. R_m is given by the previous equation.

$$R_e = \frac{R_m I_m^2}{I_e^2} = \frac{\pi k^2 c^2 L^2}{6Z N^2} (ka)^4 \quad \textbf{(6)}$$

According to many textbooks, the self-inductance of a "thin" circular toroidal coil is:

$$L \doteq \frac{\mu N^2 A}{2\pi a} \quad \textbf{(7)}$$

where:

$N \equiv$ number of turns
$A \equiv$ area of cross section
N = permeability of medium = $\mu_r \mu_o$

$$Z = \sqrt{\frac{\mu_o}{\epsilon_o}}, \quad c = \frac{1}{\sqrt{\mu_o \epsilon_o}}, \quad \mu_o = \frac{Z}{c}, \quad \mu = \mu_r \frac{(Z_o)}{c}$$

When these equations are combined:

$$R_e = \frac{Z \mu_r^2 k^6 a^2 A^2}{24\pi} \quad \textbf{(8)}$$

PRODUCT INFORMATION

1996 Measurement Products Catalog from Tektronix

The 1996 Measurement Products Catalog is now available from Tektronics, Inc. The 600-page, soft-cover catalog includes a full-color new product section that presents a synopsis of Tektronix' business focus and features their new form-factor measurement solutions. Nearly 100 new products are highlighted.

The catalog provides detailed product descriptions that are backed by an on-demand fax service, available via a toll-free 800 number, offering application and technical notes; comprehensive indexes that lists products by name and by function; and a list of all Tektronix worldwide sales offices, distributors, and representatives.

For more information about the 1996 Tektronix Full-Line Measurement Business Catalog, write on company letterhead to Tektronix Measurement Business Division, Literature Distribution Center, P.O. Box 1520, Pittsfield, MA 01202; or call 1-800-426-2200 (when prompted, press 3 and ask for program 499). You can also order the catalog directly via the World Wide Web using the following address: http://www.tek.com/mbd/w499.

New Information Technology Standards Book

Digital Press has published *Information Technology Standards: The Quest for the Common Byte* by Martin Libicki. The book examines information technology standards and discusses what they are, what they do, how they originate, and how they evolve.

Some of the topics covered in this new book are: Unix; Open Systems Interconnection; Front-line Manufacturing; Computer-aided Acquisition and Logistic Support; The Ada Programming Language; and ISDN: Narrow and Broad.

Information Technology Standards: The Quest for the Common Byte is a 432 page paperback and is available for $59.95 from Digital Press, Sales and Marketing Department, 313 Washington Street, Newton, MA 02158-1626; phone 617-928-2500; fax 617-928-2620.

Rick Littlefield, *K1BQT*
109A McDaniel Shore Drive
Barrington, New Hampshire 03825

QUARTERLY DEVICES

The Wiltron Site Master

Antenna designers depend heavily upon the services of a good return-loss bridge or network analyzer to serve as their eyes and ears while working in the RF domain. Unfortunately, lab-grade analyzers seem only to come in two sizes these days—very old or very expensive. For the advanced hobbyist, competitive manufacturer, service shop owner, or inventor-entrepreneur, neither choice may represent a satisfactory solution. Indeed, a third alternative may provide a better option. In this installment of "Quarterly Devices," I'll look at an innovative new piece of RF test equipment from Anritsu Wiltron: the Wiltron Site Master.

The Wiltron Site Master

The Wiltron Site Master is a precision-quality handheld tester for measuring return loss and distance-to-fault (DTF) in antenna systems, transmission lines, and other RF components. Although designed primarily for on-site field maintenance, it also provides many of the functions required for a wide range of lab and manufacturing tasks. Indeed, the Site Master represents a new breed of electronic test equipment entering the high-tech marketplace. On one hand, it's a small battery-powered package you can take anywhere. On the other hand, it's far more sophisticated than its simple exterior suggests. When paired with a personal computer and the "Site Master Software Tools" package provided by Wiltron, the Site Master becomes a powerful virtual instrument with excellent data resolution and many interesting features.

The Site Master presently comes in six models. One chooses the appropriate model based upon the frequency coverage and operating features needed. Complete specifications for all models are provided in **Table 1**.

Site Master's list of standard features is well documented in Wiltron literature. Rather than recounting all of them here, I'll devote the col-

Specifications—Site Master III

Model	Sweep Range	Accuracy	Resolution	RF Immunity	DTF*	RF/Po
S110	600-1200 MHz	75 ppm	100 kHz	+10 dBm	N	N
S111	300-1200 MHz	75 ppm	100 kHz	+10 dBm	Y	N
S112	5-1000 MHz	75 ppm	10 kHz	+10 dBm	N	opt
S113	5-1200 MHz	75 ppm	10 kHz	+10 dBm	Y	opt
S330	700-3300 MHz	75 ppm	100 kHz	-15 dBm	N	N
S331	25-3300 MHz	75 ppm	100 kHz	-15 dBm	Y	N

All models measure Return Loss, VSWR, and Cable Insertion Loss.
*Models without built-in DTF display can plot DTF via Site Master Tool software.

Return Loss: Range = 0.00 to 54.00 dB, Resolution = 0.01 dB
VSWR: Range = 1:1 to 65:1, Resolution 0.01 units
RF Po: Display = 10 pW to 100 kW, Detector = -50 to +20 dBm, Offset = 0 to +60 dB
Cable Insertion Loss: Range = 0 to 20 dB, Resolution = .01 dB
Maximum Input: N(f) Test Port = +22 dBm, RF Po Detector = 20 dBm @ 50-Ohms
RS232: 9-pin D-sub, 3-wire serial. **Operating Temp:** 0 to +50 degrees C
Weight: 2.2 lbs. **Size:** 8 x 7 x 2.25 inches

Table 1.

umn to a walk-through of what it was actually like to use a Site Master for the first time.

Documentation

Every introduction to a new piece of test equipment begins with a look at the operating manual. Personally, I hate wading through thick volumes of documentation, so I was especially pleased to find only a pocket-sized 24-page "Users Guide" packed in with my demo unit. Opening the guide, I found much of the content consisted of handy reference charts and diagrams—a digest of items you'd need to look up from time-to-time to refresh your memory while operating the unit. Most of the Site Master's features and functions are demonstrated in an instructional video, rather than tediously spelled out in print. This "show-me" approach was refreshing and easy to follow. In fact, the Site Master is a user-friendly piece of equipment, and volumes of documentation aren't really needed to support most of its functions.

Setup and operation

After turning the unit on, one of the first steps is to establish a useful sweep range. Normally, there's no benefit in using more frequency span than you need for a return-loss or VSWR plots unless you are profiling for multiple resonances. Wide sweeps, on the other hand, improve DTF resolution (detailed information for setting optimal DTF sweep range are provided in the unit's documentation). Sweep range is set by entering start and end frequencies via the keypad. Two movable frequency markers are also available, and these are turned on and set via the keypad as well.

As with most RL bridges, a simple initial procedure is required to normalize the unit for anomalies introduced by test cables, connectors, etc. Calibration involves sweeping the unit into its test cable and sequentially presenting three conditions at the far end (an open, a short, and a 50-ohm load). The unit's microprocessor then compiles the data from each sweep and calibrates the instrument for you. N-connector components needed to perform this operation come with the unit, and the entire procedure takes about a minute.

The screen prompts and key functions are outlined in the instruction manual. For the most part, these are clear and intuitive. The unit's LCD screen is divided into a display and message area. I found the display easy to read, even in direct sunlight (if you've worked with CRTs outside, you'll really appreciate this feature). Backlighting is available for darker locations.

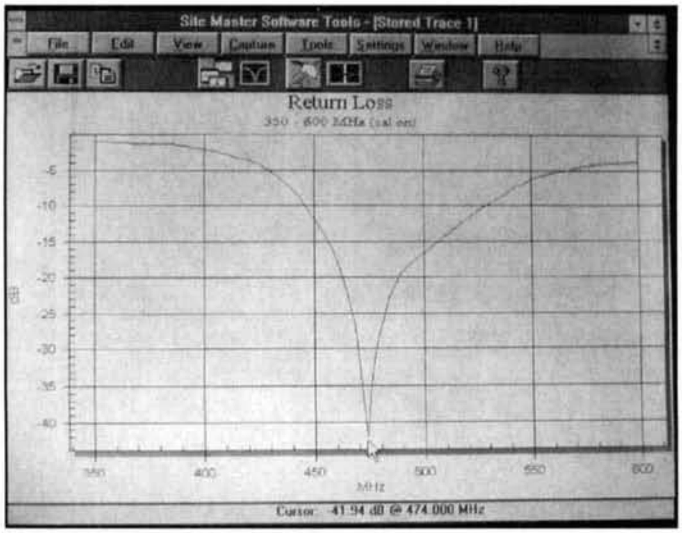

Photo A. Return-loss chart as it appears on computer screen.

Each analyzer sweep pass takes about two and a half seconds to complete, and the LCD display continually updates itself as the sweep cursor moves across the screen. A sample-and-hold function allows you to stop the sweep and capture a single frame for prolonged inspection.

An "alarm" function can be turned on and set to provide an audible signal whenever a particular screen parameter is exceeded. Also, autoscaling may be turned on to reproportion the amplitude range of the screen to match the characteristics of your trace. Return loss, VSWR, cable loss, and (in specified units) distance-to-fault displays can be viewed on-screen with the proper setup. An RF power meter option is available on some models as well.

In one sense, the Site Master is a real-time instrument, with continuous screen updates and complete portability. In another sense, it's a sophisticated data gatherer and recorder, where traces can be committed to the unit's memory for later analysis or printout using the PC interface and memory locations for storing screens. Entering a screen into memory is simple: you simply assign the screen a location number, then push the "enter" button. In addition to screen memory, nine nonvolatile memory locations are provided for storing commonly used setups. When the system is turned off and then repowered, the last operating setup used is automatically restored.

To test a "real-world" antenna on my S111 demo unit, I hastily constructed a 450-MHz Discpole (see "Tech Notes" in this issue for a description of that antenna design). I then attached it to the Site Master's test cable through a short hank of RG-58 and a BNC adapter. Despite this sloppy bit of methodology, the antenna resonated near its intended fre-

Photo B. Site Master's built-in display.

quency, and the unit's LCD screen gave me an on-the-spot indication of return-loss performance. Finding the antenna's exact Fr (frequency of resonance) took a little more work—sweep start and end points are defined on screen, but no detailed frequency scale is provided in between. To determine Fr, I set a marker at the bottom of the RL plot (S111 markers have 100-kHz resolution, and their frequencies are displayed numerically on the screen). After determining Fr, I entered the plot into memory for later analysis and turned off the unit.

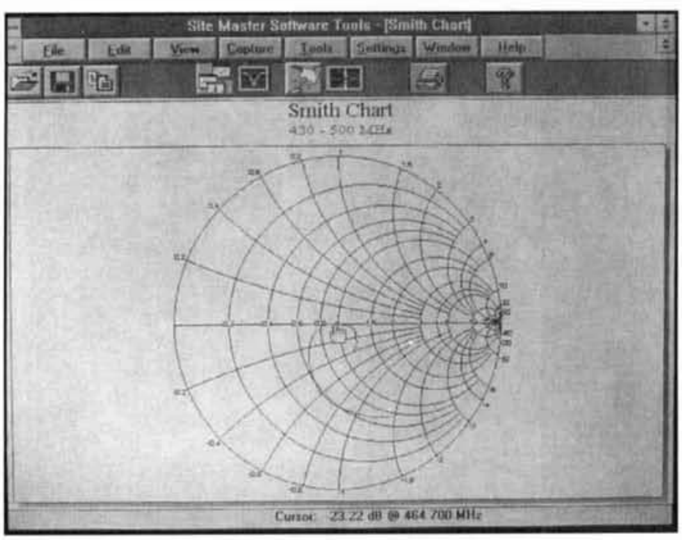

Photo C. The Smith Chart function provides a comprehensive picture of the antenna under test.

Computer software and interface

Having committed my Discpole data to the Site Master's memory, I was eager to load the software package and review it through my computer. "Site Master Software Tools for Windows" comes on a single 3-1/2 inch disk and is self-installing through Program Manager. It loaded into my IBM 425C notebook without a hitch. Any first-time apprehensions over using the Site Master Tools program vanished as soon as I brought it up on the screen. In minutes, the Site Master unit was plugged into my computer's serial port and dumping data. On-screen prompts were clear and the process couldn't have been simpler!

The first graphic I brought up for examination was a return-loss curve (**Photo A**). The high resolution multicolor image appearing on my screen was a stunning improvement over the monochrome LCD image rendered by Site Master's built-in display (**Photo B**). Both axes of the chart were clearly marked and finely calibrated. As I moved my cursor along the frequency scale, the corresponding data values for that position displayed numerically at the bottom of the screen. In truth, the display looked more like a readout from a $65,000 network analyzer than the readout from a $5,000 test set! I clicked on the print icon and waited while the (color) chart in **Figure 1A** took shape inside my HP-660C printer. (Plotter printouts are reformatted from the horizontal aspect ratio used for monitor display to a vertical aspect ratio more suitable for print media.)

Next, I accessed the program's Smith Chart function to obtain a vector plot for my antenna. Once again, a highly detailed and beautifully rendered display appeared on the screen, revealing a comprehensive picture of what my antenna was doing (**Photo C**). Detailed plot data for any point on the Smith Chart trace could be retrieved by simply setting the cursor on the desired spot and clicking. When this is done, a sidebar appears midscreen that numerically displays frequency, Rho, phase, r, x, return loss, and VSWR for that point (**Photo D**). The print version of the Smith Chart, vertically reformatted, appears in **Figure 1B**.

In addition to the major display functions provided by the software, there are other useful RL tools provided in the software tool kit. For example, there's a measurement calculator that crunches equivalent numbers for any value of return loss, VSWR, reflection coefficient, or percent of transmitted power you enter. Also, any plot may be named, saved as a graphics file (through the clipboard function), and later imported as a drawing into word-processor text. Data may also be transferred into a spreadsheet file for analysis or long-term cataloging. Other features permit the PC to take control of the Site Master and operate it as a PC-driven virtual instrument. You can even bring up traces and overlay them—one on top of the other—to compare plots visually for subtle differences. This is especially useful for the DTF function.

Distance-to-fault

Speaking of DTF, I've tended to focus on return loss and VSWR functions, mostly because of the RF-design slant of this column. But the Site Master is also a powerful maintenance tool for ferreting out 50-ohm transmission problems.

Most of us are familiar with the concept of using a narrow DC pulse in conjunction with an oscilloscope to locate shorts, opens, and prominent impedance humps in transmission lines. This technique is called time-domain reflectrometry (TDR). The Site Master uses a somewhat newer and more sophisticated approach for line-fault detection, called frequency-domain reflectrometry (FDR). Without getting overly technical, FDR uses the Site Master's return-loss capability—along with some unique signal processing—to assess the cable's characteristic impedance at every point along its length. With the help of Software Tools, DTF plots can be saved over time, overlaid, and visually compared for changes. This technique allows site operators to spot subtle and slowly developing cable faults very early on.

For example, a leaking connector may admit moisture for some time before the resultant corrosion and contamination becomes severe enough to badly deteriorate reception or knock a transmitter off the air. Once that occurs, however, the entire line will probably need to be replaced. Clearly, it's much cheaper to change the seals in a connector than it is to remove and replace 300 feet of hardline. This level of fault-detection and preventive maintenance is only possible using DTF analysis.

Conclusion

There's little doubt that the face of today's lab and field instrumentation is changing for the better. Thanks to innovations in microprocessing, LSI, DSP, and automated surface-mount manufacturing, today's bench anchors are becoming tomorrow's handhelds. In addition, with PC interface and software enhancement, even small, easily affordable units can achieve more accuracy and perform more com-

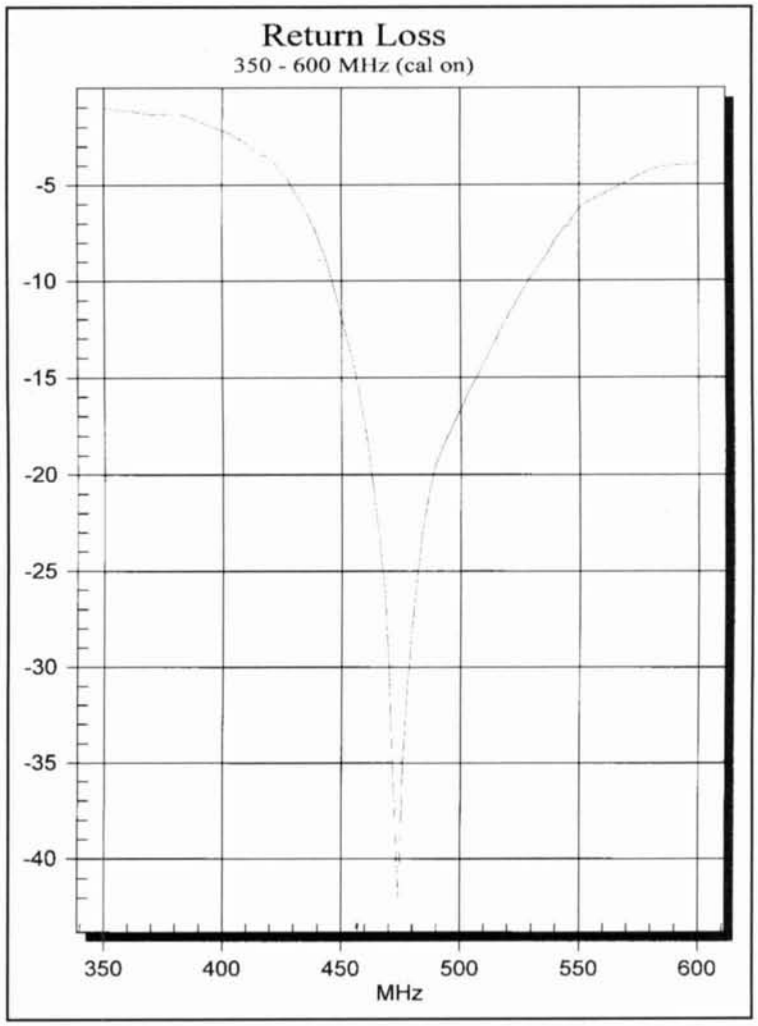

Figure 1A. Return-loss chart generated by "Site Master Software Tools for Windows."

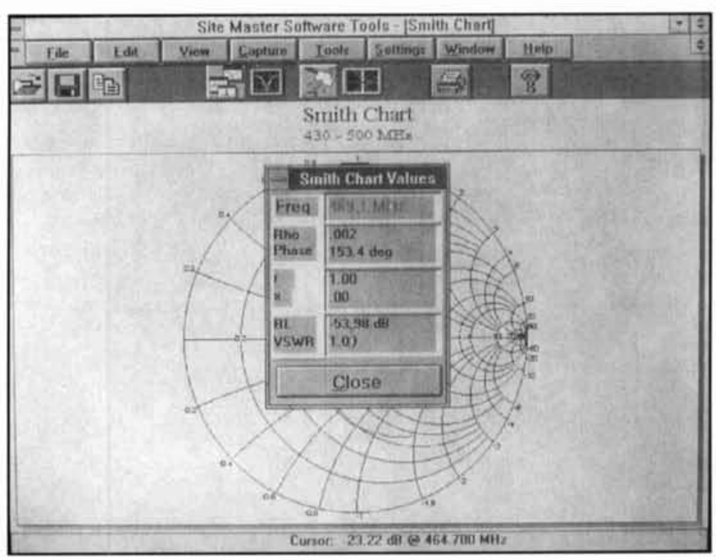

Photo D. Detailed plot data for any point on the Smith Chart can be retrieved by setting the cursor on the desired spot and clicking.

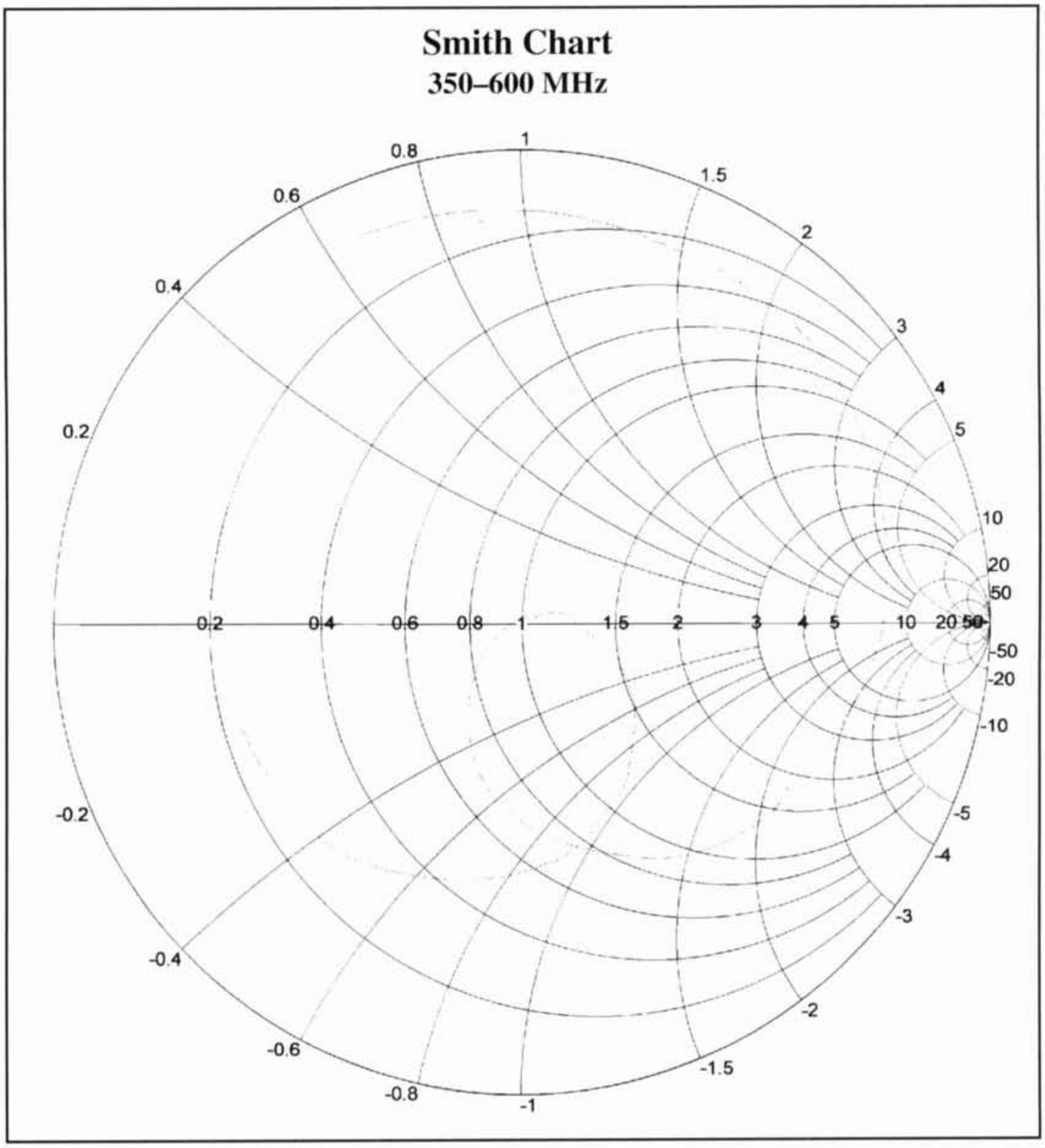

Figure 1B. Print version of the Smith Chart, vertically reformatted.

plex tasks than ever before. The Wiltron Site Master is one example of the direction this revolution is taking.

In my opinion, the Site Master's usefulness extends considerably beyond its maintenance functions. In many cases, it could be directly substituted for expensive and less portable network analyzers for design, development, and production testing.

Site Master models range in price from $4,900 to around $7,900, depending upon frequency coverage and features. All models are presently available for delivery. For more information, contact your local Wiltron sales representative, or call (408) 778-2000. For assistance with technical application questions, contact the Anritsu Wiltron Technical Hotline at (201) 227-8999. ■

PRODUCT INFORMATION

New Catalog of Small Surface Mount Trimmer Capacitors

Voltronics International Corporation has a catalog of its miniature 1/2 turn surface mount trimmer capacitors. Two new 40 pF parts have been added, and the high frequency charts of Q and self-resonant frequencies have been amplified.

For more information, contact Voltronics International Corporation, 100-10 Ford Rd., Denville, NJ 07834; phone 201-586-8585; fax 201-586-3404; or e-mail @styx.ios.com.

Compiled by Peter Bertini, K1ZJH
Senior Technical Editor

The 2-Meter Discpole Antenna

Here's a great little performer for 2-meter voice or packet operation.

Rick Littlefield, K1BQT

Just when it seems like there's nothing new under the sun, here's a compact VHF antenna that can give your 2-meter voice or data radio a lift. Tests indicate the Discpole performs on a par with a vertical 1/2-wave dipole or a four-radial groundplane—yet, it occupies only half the space (see **Photo A**). Here's a rundown of the Discpole's main characteristics:

1. The antenna is vertically polarized.
2. A feedpoint is provided at the antenna's base.
3. The radiating element is shortened by 50 percent without using inductive loading.
4. Current distribution is symmetrical, with I-max occurring at the element midpoint.
5. 1.5:1 VSWR bandwidth is 7.5 percent.
6. Lateral footprint is 15 percent that of a vertical using 1/4-wave radials.
7. The vertical element is fully isolated, preventing feedline or chassis radiation.
8. No external matching is required for 50-ohm operation.
9. Capture sensitivity (gain) is roughly equal that of a full-size 1/2-wave dipole.

If this seems a bit too good to be true, I assure you there's really no magic. The Discpole is simply designed for minimal losses and optimal current distribution.

Photo A. Discpole antenna mounted for service on a metal mast. Note that PVC mast isolates antenna from the conductive support pipe.

Theory of operation

The Discpole began as part of a comparative experiment to assess the merits of various loading structures (fractals, radials, and discs) on a small VHF antenna. The original Discpole prototype used a single disc at its base, as shown in **Figure 1**. This design worked well on-air and exhibited some other promising characteristics not covered here. I then carried the Discpole experiment one step further, adding a second disc to the top end of the element. This proved to be a significant modification (see **Figure 2**).

Adding a second disc and re-optimizing the antenna for 50 ohms produced some interesting changes. For one thing, disc radius decreased from 0.047 to 0.036 wavelength, making the antenna's footprint smaller. Also, as anticipated, radiator length decreased—from 0.33 to 0.24 wavelength. In addition, current distribution along the vertical element showed marked improvement. On the single-disc version, the point of maximum current occurred approximately 3-1/2 inches above the feedpoint. On the double-disc prototype, the current loop moved to 9-1/2 inches above the feedpoint—to the exact midpoint of the element. Because most of a Discpole's radiated energy is concentrated in the middle half of its current-distribution curve, this condition is optimal. Even though radiation resistance was lowered by shortening element length, there are no significant sources of resistive loss in the element—except the tubing itself—to detract from efficiency. Thus, the Discpole's performance was, if anything, improved by adding the second disc and making the antenna smaller.

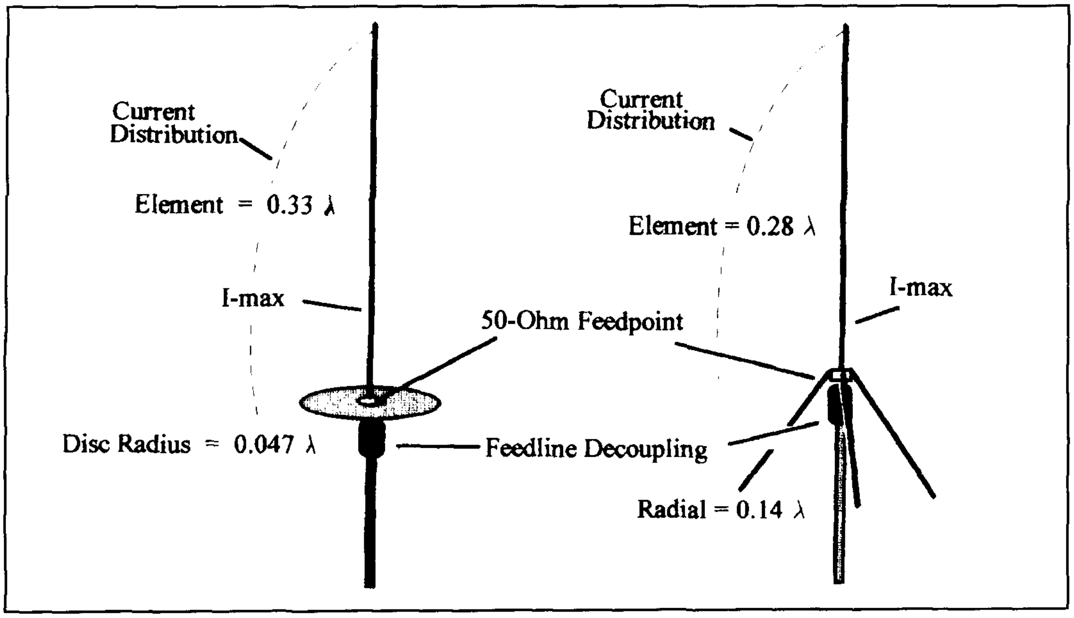

Figure 1. Single-disc version of Discpole Antenna, as compared with a 2-meter off-center-fed vertical using decoupling radials.

Although physically unwieldy for many HF applications, end-loading discs provide several advantages in VHF and UHF applications. First, discs preserve bandwidth as the antenna is shortened by increasing the element's apparent diameter. Second, unlike inductive loading methods, capacitive end discs contribute little resistive loss to the element structure. Finally, end discs do not radiate significantly or skew the pattern.

On the down side, feedline decoupling through a disc may prove more difficult

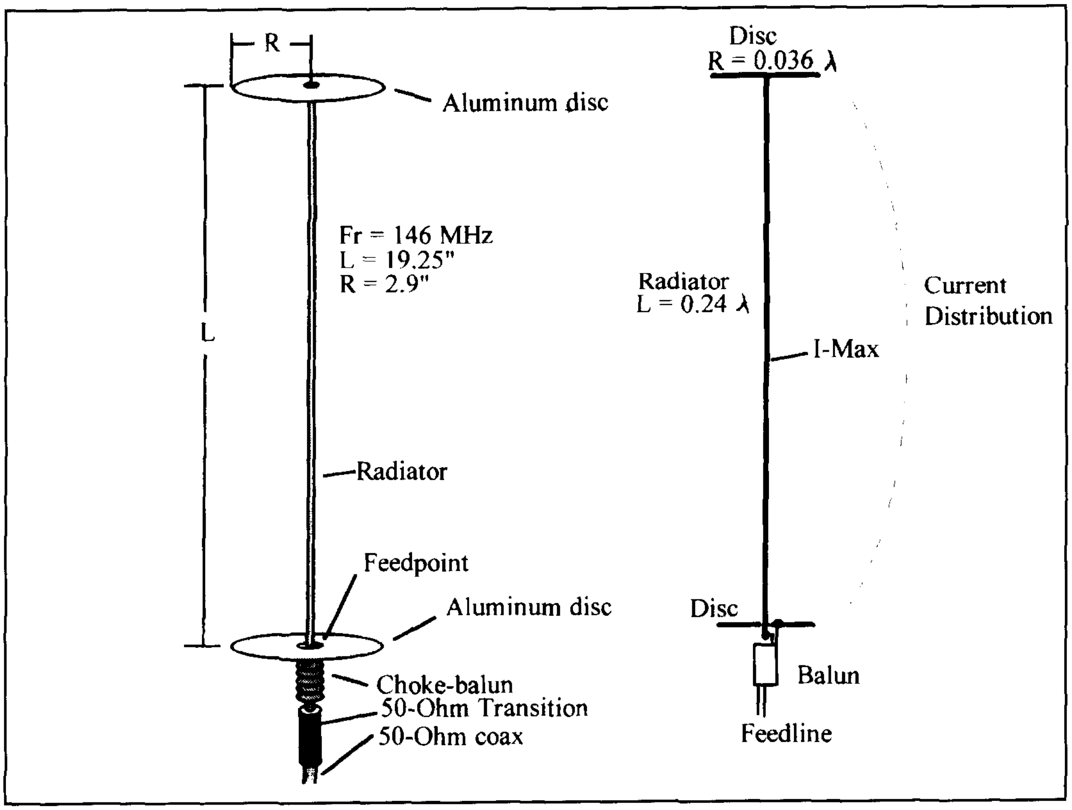

Figure 2. Discpole Antenna with second disc installed, as constructed for the 2-meter amateur band.

because of the voltage gradient that appears on the disc's distal surface (this doesn't happen with decoupling radials, where E-max is drawn away from the feedpoint to the radial tips). Because the outside surface of the disc is "hot," careful decoupling is needed to prevent parasitic end loading and feedline radiation. Ferrite beads are insufficient for this purpose. Instead, I used a high-Q wound coaxial choke made from 50-ohm Teflon™ mini-coax. At 2 meters, a minimum inductance of 1 µH was required to effectively isolate the line. With the coax choke installed, handling the feedline produced no visible shift in VSWR, and current distribution was symmetrical along the radiating element.

Matching

For a 1/2-wave wire or rod-type element, terminating impedance normally increases as the feedpoint is shifted away from the antenna's center. With a Discpole, it's more useful to think of this dynamic in terms of the relationship between disc radius and element length. For example, a large disc with a small radiator will have a relatively low impedance feedpoint, and a small disc with a large radiator will exhibit a higher impedance.

To build a "real-world" Discpole with a 50-ohm feedpoint, it was first necessary to determine the correct relationship between these two components. I did this by experimentation—beginning with equal-size discs mounted on an adjustable element. Using an MFJ-259 Analyzer and manipulating the element length, I searched out the frequency where a 1:1 match would occur. My initial prototype optimized well outside the 2-meter band, but yielded the baseline data I needed to write transposition formulas (see **Table 1**). I then built a rescaled version to formula. This antenna resonated in the middle of the 2-meter band on the first try.

The scaling formulas provided in **Table 1** should apply to the Discpole over a wide range of frequencies, as long as similar construction practices are followed. However, changing variables such as element diameter, dielectric constant of the base insulator, or reactance provided by the feedline choke may introduce some error into your result. Undefined parasitic variables such as these may also yield some degree of error in NEC-based predictions of Discpole performance.

Construction

In some respects, it's easier to build a Discpole than to describe how one works. Construction is quite simple, as shown in **Figure 3**. With the exception of Teflon mini-coax, you should find the materials you need at a well-stocked hardware store and a RadioShack. A list of materials is provided in **Table 2**.

$$\text{Disc diameter in inches} = \frac{854}{\text{Freq. in MHz}}$$

$$\text{Element length in inches} = \frac{2810}{\text{Freq. in MHz}}$$

Table 1. Formulas for calculating disc diameter and element length for 50-ohm feed.

Prototype discs were made from aluminum flashing, mostly because this is a particularly easy method. I used a large drafting compass to draw out two 5-15/16 inch diameter circles and tin shears to cut the flashing to shape. I then cut a 5/8-inch hole in the center of one using a circle punch, and drilled a 1/4-inch hole in the center of the other. If you anticipate using the antenna for rough outdoor service, you may want to use heavier-gauge aluminum discs. Thicker disc stock shouldn't alter the antenna's tuning or performance.

To prepare the lower disc for mounting, drill three no. 6 clearance holes in a tight triangular pattern around the 5/8-inch hole. Using the disc as a template, transfer this pattern to the center of the PVC cap and drill (this ensures that your mounting holes will line up). Also, drill a 1/4-inch hole at the center of the PVC cap to pass the element-mounting stud. To prepare the vertical element, cut a 19-inch length of 5/16-inch thin-wall aluminum stock and run a 1/4-inch tap about 1-1/2 inches into each end. Cut a 24-

1	24 x 1-3/8" OD PVC thin-wall pressure pipe
1	PVC end cap for 1" ID Schedule-40 pipe
1	1-3/4 x 1/2" ID (5/8" OD) PVC Schedule-40 pipe
2	5-5/16" diameter disc, cut from aluminum flashing or sheet stock
1	1/4 x 1-1/2" machine screw, stainless or aluminum
1	1/4 x 3/4" machine screw, stainless or aluminum
1	1/4" nut, stainless or aluminum
3	6-32 x 1/2" stainless steel screw
3	6-32 stainless steel nut
2	6-32 x 1" nylon screw
2	6-32 nylon nut
1	no. 6 solder lug
1	1/4" ID solder lug
1	19 x 5/16" OD thin-wall aluminum tubing
1	28" length of 50-ohm Teflon mini coax cable, RG-316 or equivalent
1	Small pc-board transition (see text)

Note: To check PVC end caps for dielectric contamination, place one in a microwave and cook it on high for one minute (include a glass of water to serve as an RF load for the oven). If the PVC doesn't heat, it's OK to use (*QST*, June 1996).

Table 2. Parts list.

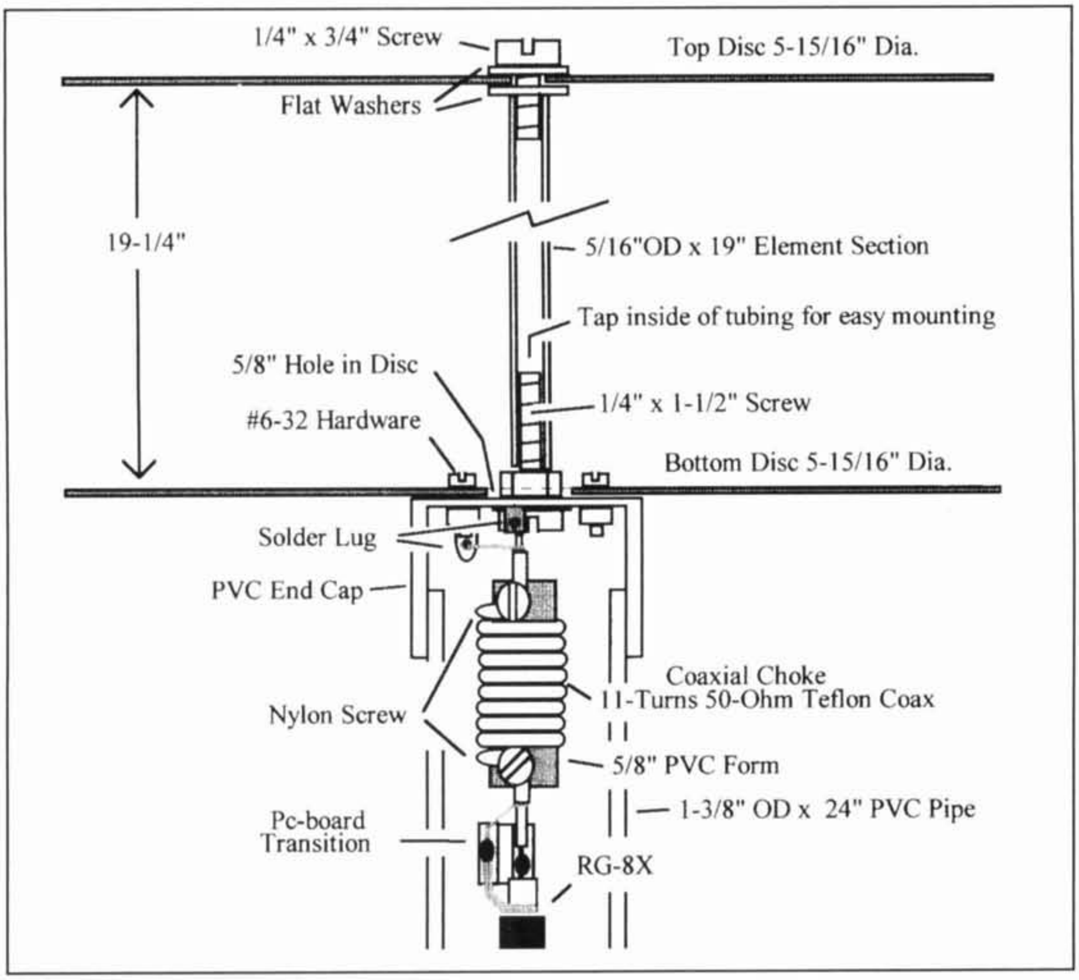

Figure 3. Construction details for the 2-meter Discpole Antenna.

inch piece of 1-3/8-inch OD PVC thin-wall pressure-pipe (SDR-23) for an insulated mounting mast.

I made my feedline choke from 28 inches of 0.1-inch diameter 50-ohm Teflon mini-coax (RG-316). Avoid using RG-174 for this application, especially if you plan to run more than a few watts into the antenna. I wound my choke onto a short length of 1/2-inch ID PVC pipe (5/8-inch OD) and used nylon screws to immobilize the windings at both ends. Eleven turns were required to make up a 1.0-μH choke. I then attached two solder lugs—a large one for the center conductor and a small one for the braid—at one end and prepared pigtails at the other end (see **Photo B**). To complete the assembly, I ran RG-8X feedline up through the 24-inch length of plastic PVC pipe and connected it to the pigtail ends of the coil. A small pc-board transition was used here to provide stress-relief and add mechanical strength.

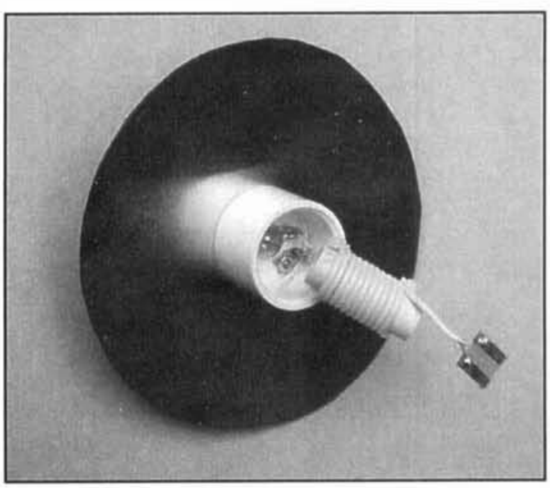

Photo B. Feedpoint assembly shows 1-μH coaxial choke and pc-board transition used in antenna decoupling circuit.

To begin final assembly, mount the lower disc onto the top surface of the PVC end-cap with no. 6-32 stainless hardware. Use one of the disc mounting screws to connect the shield side of the feedline choke to the disc. Install the 1/4 x 1-1/2-inch machine screw through the large choke lug and push through the mounting hole in the PVC end cap. Install a 1/4-inch nut on the topside and secure in place. Install the element on the screw. To install the top disc, place a 1/4-inch flat washer on either side of the mounting hole, then bolt this assembly to the topside of the element with a 1/4 x 3/4-inch screw. To complete assembly, friction-fit the PVC end-cap over the length of PVC pipe. You shouldn't need Genova™ pipe cement or mounting screws to hold the cap in place.

As an alternative to mast-mounting, you can configure your antenna to hang from a nylon line, to sit on an insulated window-bracket, or to mount directly onto a PL-238 connector. Simply make a short PVC base enclosure to encase the feedline choke, as shown in **Photo C**.

Set-up and testing

When mounting the Discpole, be sure to provide at least five or six inches of clearance between the discs and other metallic surfaces. Otherwise, unwanted end-loading may detune the antenna and degrade its performance. Also, whenever possible, mount VHF antennas as high and in-the-clear as possible. For mast-mounting the PVC tubing, I recommend using 2-1/2-inch hose clamps rather than TV-style mast clamps. Finally, to prevent feedline breakage at the transition, immobilize the coax by taping it securely to the mast.

Before placing your antenna in service, check VSWR to make sure it's tuned and working properly. If you have a low-power VSWR analyzer, like an MFJ-259 return-loss bridge, or network analyzer, you can observe current distribution by running a finger along the vertical radiator (don't try this with a transmitter connected). Minimum VSWR should occur as your finger passes the center-portion of the element, indicating the zone of maximum radiation—and the lowest impedance point along the radiator. To observe the voltage gradient present on the loading discs, touch the disc's distal surface—VSWR should deflect sharply upward (remember to mount the antenna out of reach of humans or pets). Finally, check feedline decoupling by gripping the feedline two or three feet below the antenna and moving your hand down the coax. VSWR should change by no more than 0.1 unit—but, preferably, not at all.

Conclusion

Normally, I expect physically shortened antennas to exhibit a narrow bandwidth and/or lowered radiating efficiency. However, "real-world" tests seem to indicate that the Discpole suffers little from either malady. The prototype exhibited a VSWR of 1:1 at Fr, while providing a 1.5:1 VSWR bandwidth of 10.6 MHz (7.5 percent). When compared to a drooping-radial groundplane reference antenna, the Discpole delivered virtually identical capture sensitivity on distant repeater signals, as monitored on a sensitive field-strength meter calibrated in dBm. On-air checks using a low-power HT confirmed similar performance characteristics. Every repeater workable on the reference antenna was also workable on the Discpole. Because of its compact size and uncompromising performance, this design should play well against other low-cost omnidirectional antennas, such as the traditional groundplane, 5/8-wave over radials, 1/2-wave "stick," and J-pole. So if you're looking for an unobtrusive-yet-efficient antenna for voice and data applications at VHF or UHF, the Discpole might be just the ticket!

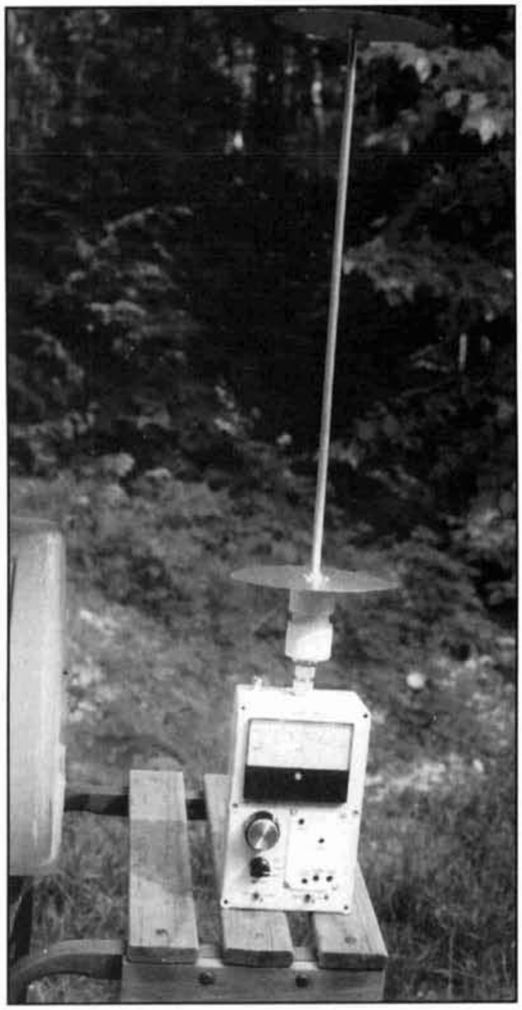

Photo C. Discpole using alternative base assembly. In this configuration, the antenna may be suspended by a nylon line or sill-mounted (like a bird-feeder) using an insulated bracket.

Finally, there are many ways to skin a cat—and more than one way to shrink or enhance an antenna. The Discpole is one solution that appears to work well. The investigation that led me to design and build this antenna, however, was initially inspired by Nathan "Chip" Cohen, N1IR's article on fractal structures which will appear in an upcoming issue. Beyond that, Chip contributed valuable support and encouragement, for which I owe him my thanks.

Variable High-Power Biasing

Here's a handy circuit that decreases voltage shift and provides a variable bias voltage for your power amplifier.

Marv Gonsior, W6FR

Zener diode biasing is usually associated with high-power grounded-grid triode amplifiers. While they're easy to use and relatively inexpensive, Zener diodes have two inherent problems: they are available only in discrete voltage increments, and they have a pronounced positive voltage shift characteristic with increasing current. Here's a way to decrease this shift and provide a variable bias voltage for your power amplifier.

The quest

Besides finding a mechanism to overcome the Zener problems, I also wanted to be able to set the bias for optimum quiescent current for any applied anode voltage and class of operation. A thorough search through the available literature and responses from a number of queries yielded nothing. Most published power amplifier designs seem to favor using a Zener diode, and a few others use a pass transistor with a Zener reference.

Unfortunately, tests showed the Zener diode-pass transistor combination is less effective than using a Zener alone! Knowing that a silicon power diode has a forward drop of about 0.7 volts, a string of forward-biased silicon diodes to develop the bias voltage was investigated. The results were even worse than the Zener-pass transistor scheme. More on this later.

Observing other bias schemes

I obtained some interesting and valuable data when using a bias module constructed to create 4.5 volts. It used a 4.5-volt, 1-watt Zener to stabilize a TO-3 packaged 2N3055 NPN silicon power transistor. With a quiescent anode current of 180 mA, the initial bias voltage was 4.6 volts—but this rose to 8 volts at 635 mA of anode current! Based on the operating parameters of that particular kW amplifier, the quiescent anode current would have dropped to approximately 50 mA! Consequently, while under full load, the resulting bias increase would have reduced the anode current by approximately 130 mA—not exactly conducive to the best output or linearity for a triode.

In another test, forward-biased 1N5062 silicon diodes were configured in series for 3.3 volts. Using the same operating conditions as above, the bias rose an average of 2.3 volts—

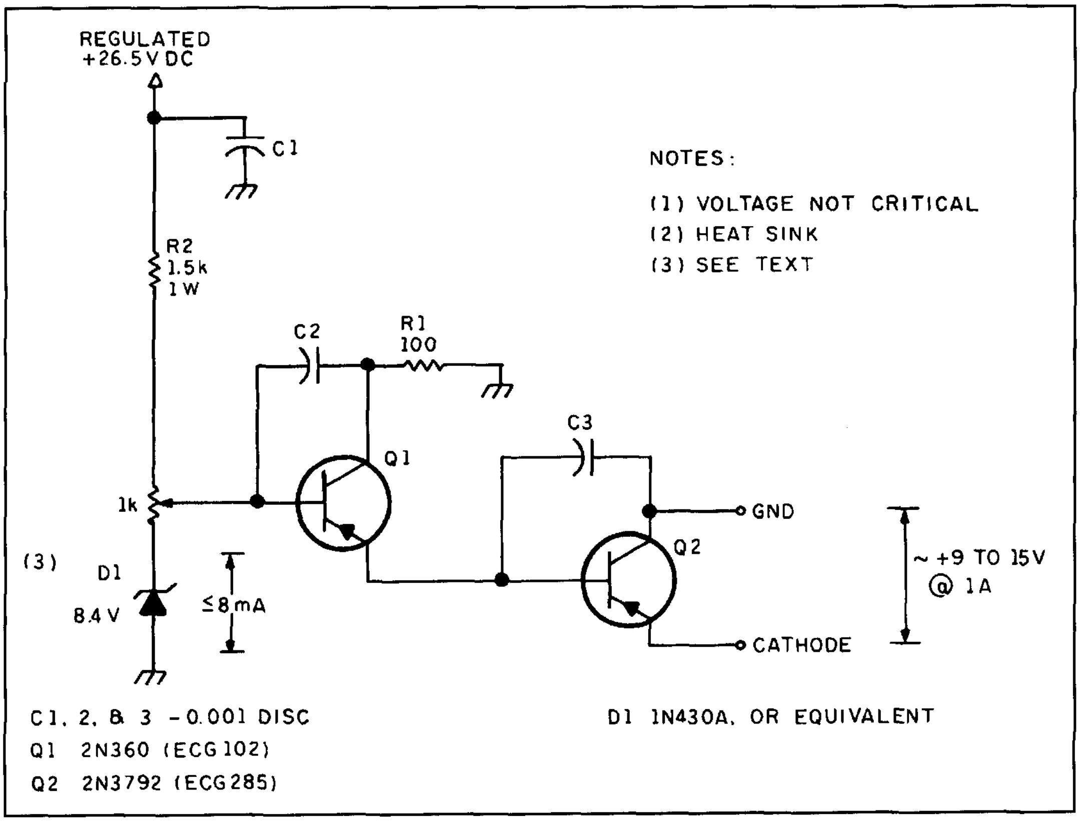

Figure 1. Circuit schematic.

from 3.3 to 5.6 volts! Trying another tack, I took a TO-3 packaged 1N2811B 13-volt 50-watt Zener that was well-heatsunk and supplied with forced-air cooling. The bias voltage rose approximately 0.49 volts under the same operating parameters noted previously.

While still trying to overcome the positive bias voltage shift problem, I tried placing two 6.8-volt 50-watt 1N2840B TO-3 packaged Zeners in series for a 100-watt capability. The diodes were heatsunk and placed in the forced air cooling path of the amplifier's plenum. Surprisingly, the shift was unacceptable: plus 1.38 volts! I concluded that the voltage shift was not heat related, but due instead to a source-impedance problem (internal resistance) common to Zener diodes.

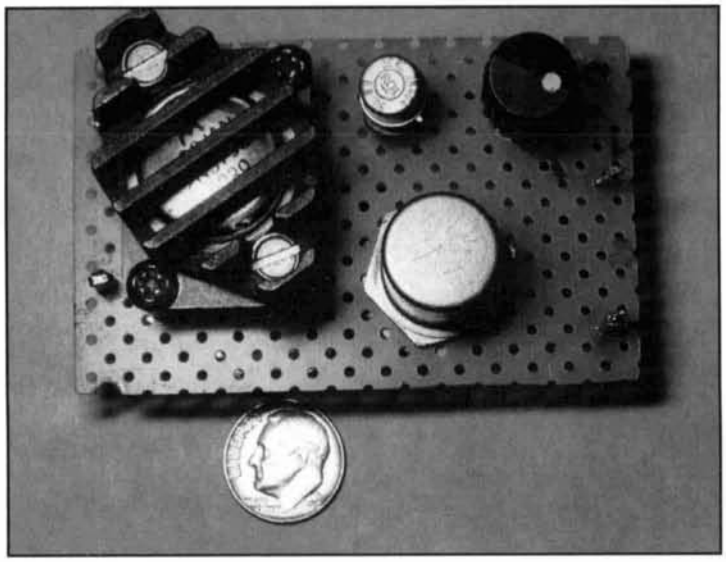

Photo A. Bias module. W6FR photo.

The solution!

Figure 1 shows the biasing circuit that satisfied all my requirements. Its evolution is based on the considerable time I spent breadboarding and investigating various bias circuits.

Two PNP transistors are used in an emitter-follower Darlington pair. The circuit yields a bias voltage at its output that is essentially the same as the voltage applied to the input. The purist could use a PNP Darlington at Q1 to drive Q2. This would lower the source impedance significantly. It would also improve the bias regulation throughout the voltage range (for example, at the higher bias voltage settings).

Photo A shows my bias board, with Q2 heatsunk and ready to be placed in the path of the amplifier's forced air plenum for optimum cooling. Or, the TO-3 power transistor (Q2) could be heatsunk to a chassis or other suitable heatsink. Note that the PNP TO-3 transistor case is the collector and may be directly grounded! Thus, the TO-3 case may be affixed directly to a metal chassis for best thermal performance. Using a thermal compound, such as Wakefield's, will help here.

Test data

I started with a quiescent anode power amplifier current of 180 mA with the bias voltage at near its maximum setting (the worst case, being

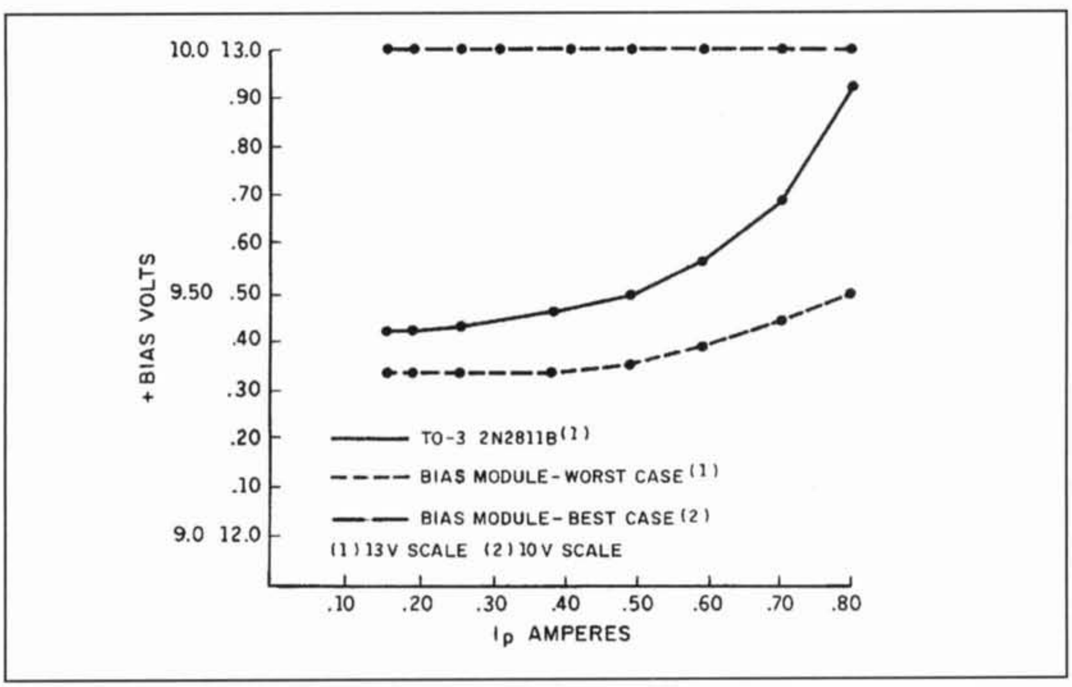

Figure 2. Performance data.

C1, C2, C3, C4	0.001 µF disc ceramic
R1	100 ohms
R2	1500 ohms, 1 watt
R3	1000 ohms variable
D1	1N430A, NTE 5016A
Q1	2N360 PNP, TO-5 package, NTE 102 or ECG 102
Q2	2N3792 PNP, TO-3 package, NTE 285

Table 1. Schematic Values

furthest from the lowest source impedance). When the amplifier was driven to an anode current of 800 mA, there was an instantaneous bias voltage increase from 12.36 to 12.44 volts (as measured on a Fluke 8800A DMM and verified on an oscilloscope). This bias shift was in a positive direction, but not in as substantial a manner as a 50-watt Zener. At the lower end of the bias range, the outcome was beyond all expectations! My test results are shown in **Figure 2**. Remember this data is based upon a sample of one.

Device selection

Neither of the PNP transistors nor the layout is critical for the bias circuit shown in Figure 1. For kilowatt-level power amps, a TO-3 size device, or equivalent, will suffice for Q2. Resistor R1 in the collector of Q1 prevents any tendencies toward instability in the Darlington. My tests revealed no evidence of instability when resistor R1 was in or out of the circuit. I used an 8.4-volt true-precision 1N430A reference diode from my junkbox (shown in Photo A). It may be replaced by a comparable 5- or 10-watt unit, although there could be a slight loss of stability. NTE Electronics' general replacement line shows their NTE 5016A as a substitute for the 1N430A. Other NTE or ECG substitutions are given for the schematic semiconductors in **Table 1**.

Many other suitable true reference diodes are available. One is the 8.8-volt 1N3154A. To obtain a different bias voltage range, simply change diode D1 and resistor R2 accordingly. Diode D1 establishes the low-end voltage range. The regulated input voltage, along with resistor R2, sets the upper limit. The available low-end voltage will be that of the reference diode, minus the voltage drop developed across the base-emitter junctions of germanium transistors Q1 and Q2.

Conclusion

The results speak for themselves. I'd be interested to learn about this circuit's performance in other applications.

Acknowledgment

My thanks to Tiff, W6GNX, for providing the results of his tests on pass-transistor and diode string bias generation methods. Those data saved considerable time and effort. ■

PRODUCT INFORMATION

New World-Wide Wireless Support from Cylink

Cylink Corporation has announced the availability of the AirLink VF-E wireless modem for local loop voice and data.

The VF-E is a complete wireless local loop (WLL) solution, providing instant wireless communication for outdoor applications utilizing spread spectrum technology. It comes in AC and DC models, with or without battery backup, and can operate at distances in excess of 20 miles depending on antenna choice, orientation, and feed cable length. The VF-E is based on Cylink's current VF wireless modem, including it's use of 32 kbps ADPCM (Adaptive Differential Pulse Code Modulation)voice compression. The weatherproof enclosure adheres to the most stringent telco requirements for outdoor use and mounts to any structure. The Air-Link VF-E removes the need for wire in numerous applications.

The AirLink VF-E Voice Radio Extended temperature modem is a single-channel, full duplex point-to-point voice communication

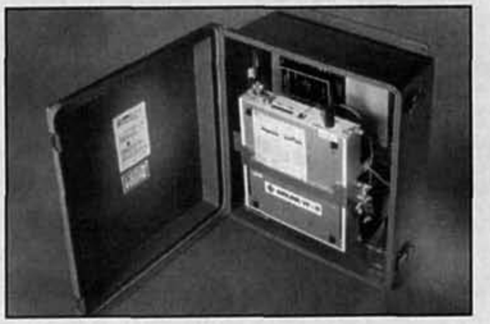

system. Operation is in the L-band with a maximum range of over 20 miles depending on terrain and obstructions. The interface is a two-wire loop start using industry standard RJ-11 connectors. Data is supported up to 4800 bps by using standard V.22 or V.32 external modems. The system can be powered by either 110/220 Vac or by solar power 12, 24, or 48 Vdc. Temperature range is –30 to +60°C. Models optionally can include battery backup.

For further information, call Cylink Corp. at 408-735-5817; or Breakthru Communications at 408-777-9364.

L.B. Cebik, *W4RNL*
1434 High Mesa Drive
Knoxville, Tennessee 37938-4443
Internet: CEBIK@UTKVX.UTK.EDU

MODELING AND UNDERSTANDING SMALL BEAMS: PART 4

Linear-loaded Yagis

The most common reason for designing and building a small, 2-element beam or array is size. Whether for home or portable field use, small antennas have a niche in the ham world.

There is a second, often overlooked, reason for building antennas with reduced dimensions relative to a standard 2-element Yagi: increased front-to-back ratio. Standard, closed spaced (approximately 1/8 wavelength) Yagis aren't capable of large front-to-back ratios because the parasitic reflector won't be positioned or sized for the correct current level and phase angle for maximum rejection off the rear. Most notably, the Moxon rectangle achieves close to optimal reflector conditions. Its altered geome-

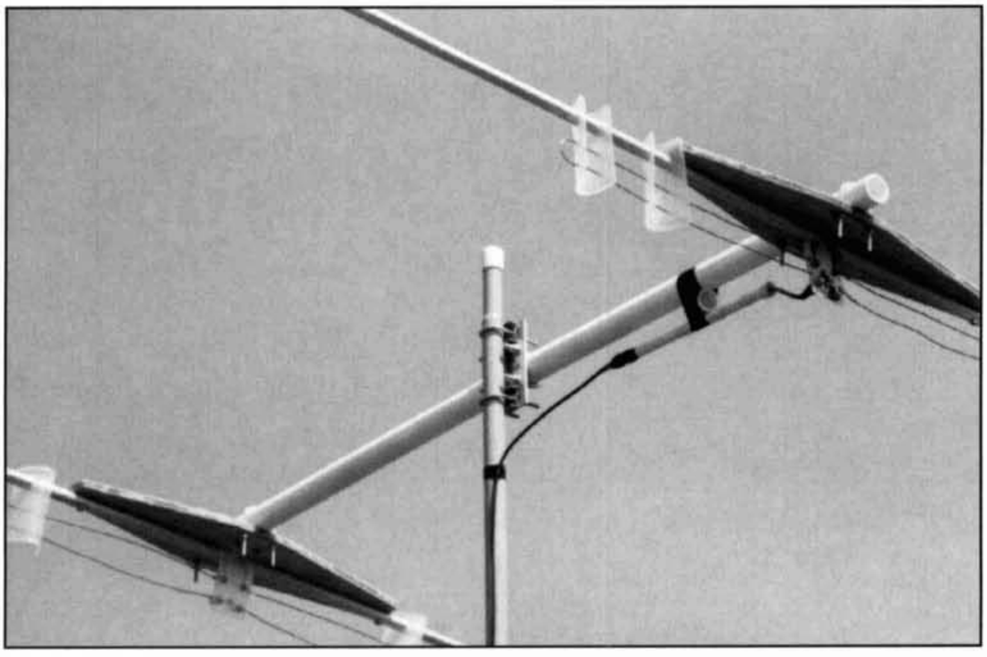

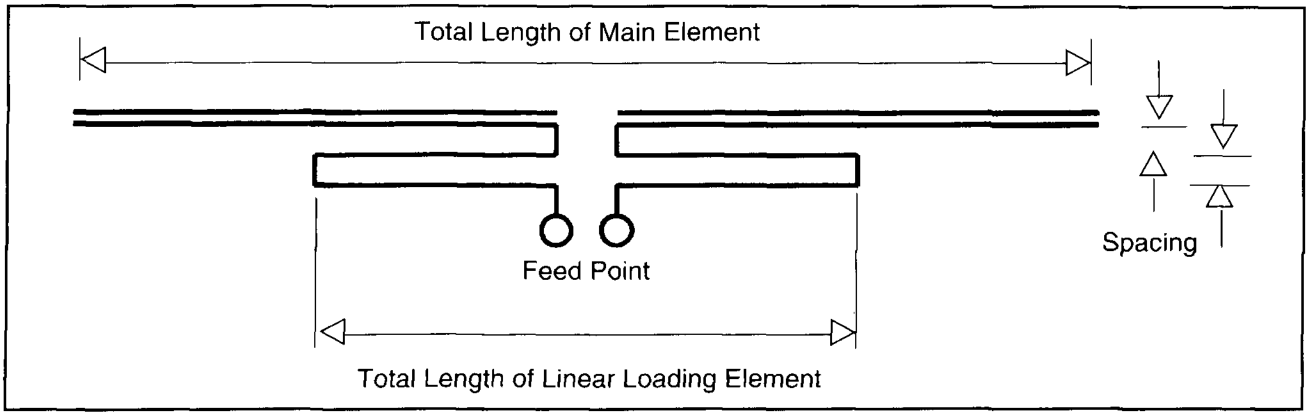

Figure 1. A schematic diagram of a dipole element with linear loading.

try attains a very high front-to-back ratio for a 2-element array. The cost is about a half dB of forward gain.

A second strategy that will also improve the front-to-back ratio is to shorten the Yagi elements while maintaining the close spacing. With center or linear-loading of both the driven element and the reflector of a 2-element Yagi with about 1/8-wavelength spacing, the front-to-back ratio increases from about 12 to about 18 dB—a full S-unit of improvement. Models of the beam show that the current amplitude and phase more closely approach values necessary for a complete rearward null than those for a full-size 2-element Yagi. As with the Moxon rectangle, the short beam's forward gain drops about a half dB in the process. Additionally, the bandwidth of the beam decreases.

The result of modeling and testing these ideas was a 2-element 10-meter Yagi with 12-foot elements—a 25 percent savings in size, turning radius, and weight. In addition, the antenna uses 6-foot lengths of hardware store aluminum tubing for the elements, making parts acquisition easier. (Note, however, that the aluminum tubing usually available at hardware centers doesn't have the strength and durability of tubing used by commercial antenna manufacturers. This factor has little affect on small, weight-balanced 2-element beams for

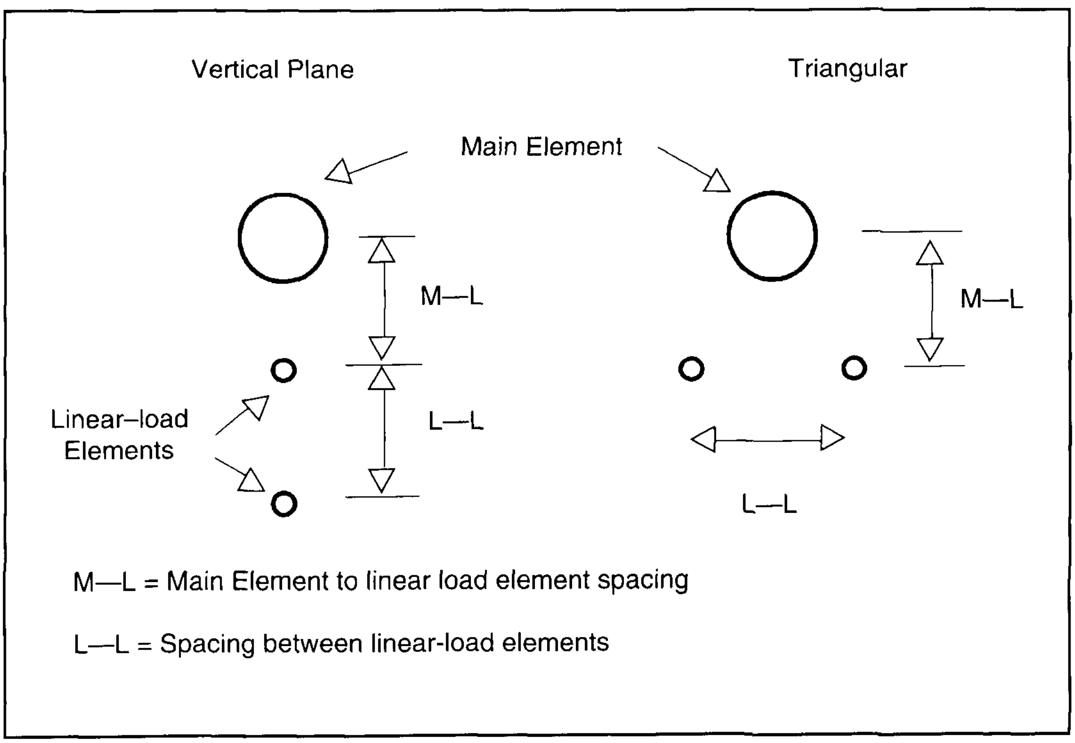

Figure 2. Vertical-plane and triangular geometries for linear-loading sections.

10 meters, but may be very significant in tapered-element 20-meter models.[1])

Linear-loading versus inductive loading

The principle of center loading is very old and well-understood. Center-loaded dipoles and Yagis have appeared in numerous antenna books over the decades. In such antennas, a coil at the center of a shortened inductor compensates for the capacitive reactance that results from shortening the element from its naturally resonant length (approximately 1/2 wavelength), thus restoring resonance. A parasitic element, such as a reflector, may be similarly shortened and an inductor used to compensate for the resultant capacitive reactance until its relationship to the driven element is optimal.

The performance of a center-load dipole or Yagi depends largely upon the Q of the inductor. A shortened antenna, solely by virtue of its shortening, will show a reduction in gain relative to an unshortened antenna used as the reference. We might let a center-loaded dipole or Yagi use theoretical inductors with infinite Q (that is, with no resistance) to form a base line for comparisons. Then, by selectively establishing values of Q for the inductors and modeling the result (via a program such as MININEC), some rough comparisons become possible.

Table 1 summarizes two such exercises—one for 12-foot aluminum dipoles at 28.5 MHz,

A Comparison of Gain and Other Properties of Center-Loaded and Linear-Loaded Dipoles and Yagis

1/2λ Dipole: 12' 0.75" diameter aluminum

Type	Q_{Load} dBi	Gain Maximum	% of R ± jX	Impedance
C-L	Inf.	1.93	100%	28 + 0.4
C-L	50	1.24	63%	33 + 0.5
C-L	100	1.57	80%	31 + 0.5
C-L	200	1.75	91%	30 + 0.5
C-L	300	1.81	91%	29 + 0.5
L-L	—	1.82	94%	29 + 0.3

2-Element Yagi: DE = 11.6' 0.75" diameter aluminum; RE = 12' 0.75" diameter aluminum

Type	Q_{Load}	Gain dBi	% of Maximum	Front-to-Back Ratio dB	% of Maximum	Impedance R ± jX
C-L	Inf.	6.20	100%	20.0	100%	17 – 0.7
C-L	50	4.21	68%	13.2	66%	22 – 3.9
C-L	100	5.14	83%	15.8	79%	19 – 2.4
C-L	200	5.65	91%	17.6	88%	18 – 1.6
C-L	300	5.83	94%	18.3	92%	18 – 1.3
L-L	—	5.82	94%	18.4	92%	17 – 2.8
C-L	DE=200 RE= 50	5.02	—	13.2	—	19 – 3.9
C-L	DE= 50 RE=200	4.84	—	17.6	—	22 – 1.6

Notes: C-L = center-loaded; L-L = linear-loaded. All values taken from models in free space and include materials losses (aluminum). As an indicator of loading coil losses, $Q_{Load}=X_L/R_L$. X_L for DE = 250Ω; for RE=257Ω. Antennas L-L are linear-load with a 4' loading element of #12 wire in a vertical plane, with the upper wire 1.2" below the main element and the lower wire 1.2" below the upper wire.

Table 1. A comparison of gain and other properties of center-load and liner-loaded dipoles and Yagis.

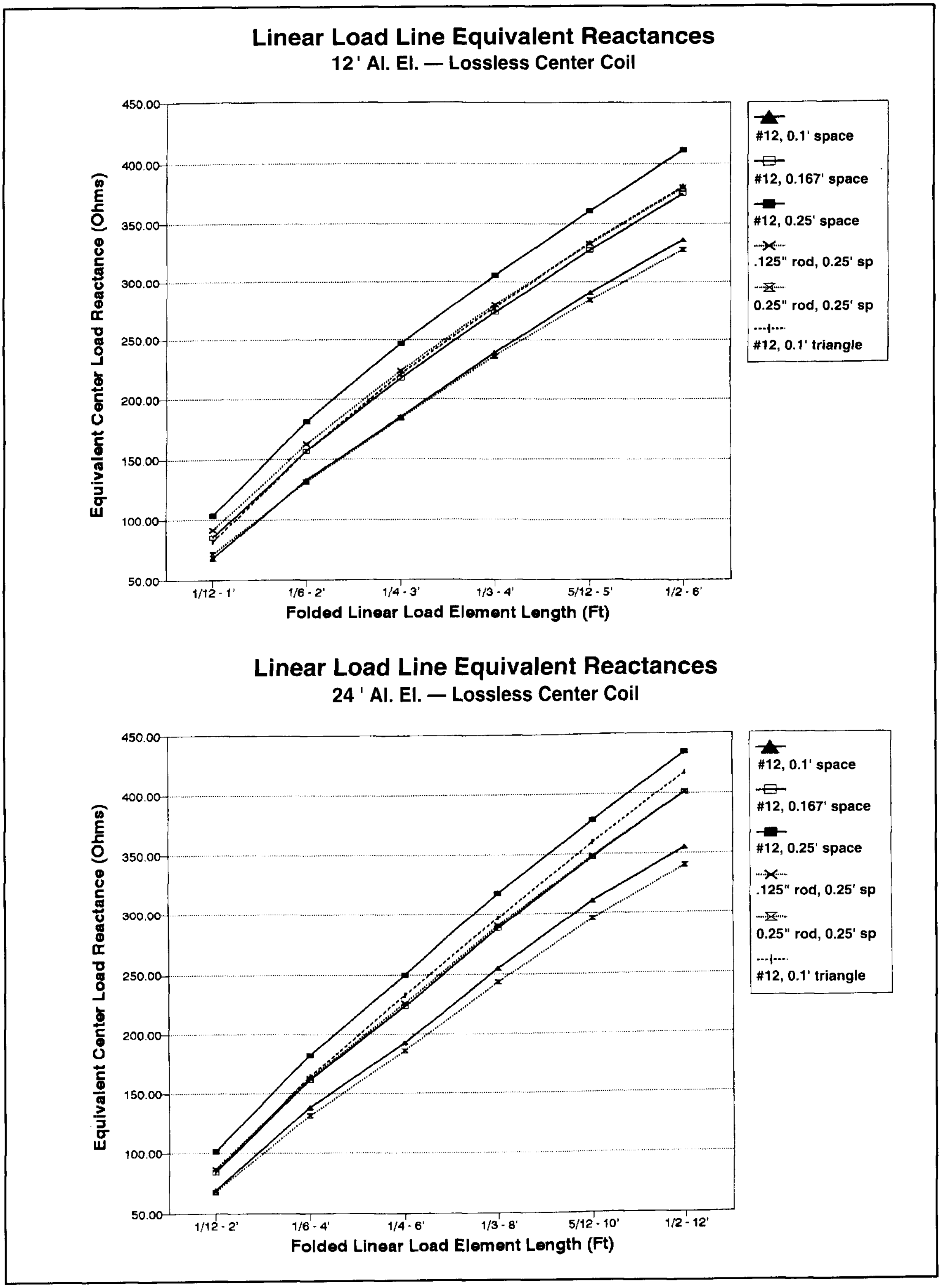

Figure 3. Linear load line equivalent reactances (to a lossless center loading inductor) between ratios of 1:12 to 1:2 for (A) a 12 foot 0.65 inch diameter aluminum main antenna element and for (B) a 24 foot 0.75 inch diameter aluminum main antenna element for 6 linear-load configurations.

Sample table of linear-loaded dipoles listing gain, feedpoint impedance, resonant frequency, equivalent center-load reactance, and approximate Q

Antenna element = 12' 0.75" diameter aluminum
Linear load = #12 wires spaced 2" (0.167') from antenna element; 2" (0.167') from each other
Antenna-to-linear load geometry: vertical plane

Linear load length - ft	Gain dBi	Z (R ± jX) ohms	Resonant Frequency MHz	Equivalent Center-load Reactance ohms	Approximate equivalent Q
0 (self-resonance)	2.13	72.2 + 0.01	38.94	——	——
1	2.01	49.4 + 0.00	35.04	85.4	225
2	1.94	37.4 – 0.02	31.84	157.7	303
3	1.85	29.6 – 0.00	29.34	217.4	294
4	1.78	24.4 – 0.01	27.12	273.9	326
5	1.69	20.7 – 0.00	25.20	327.2	327
6	1.60	18.0 – 0.02	23.58	375.8	334

Notes:

1. Antennas were considered resonant if the remnant reactance was less than 0.05Ω. Figures are rounded from 3- and 4-place decimal results.
2. Equivalent Q is determined by finding a value of resistance for the center load inductance at the given reactance that produces an antenna gain equal to that of the corresponding linear-loaded model. Q results are subject to variables of the modeling process and are likely no more reliable than 10 to 15 percent.

Table 2. Sample table of linear-loaded dipoles listing gain, feedpoint impedance, resonant frequency, equivalent center-load reactance, and approximate Q.

the other for a 2-element Yagi of similar element length at the same frequency. The table shows Qs of 300, 200, 100, and 50 as typically realizable values, although there is little likelihood of sustaining an inductor at a Q of 200 or more in outdoor conditions. A Q of 100 is more probable. Note the decrease in performance with the decrease in Q for both the dipole and the Yagi.

A linear load is simply a folded continuation of the main element, usually (but not necessarily) of a lighter (hence, thinner) material, as shown in the dipole sketch in **Figure 1**. Linear loading can be introduced anywhere along an antenna element, including current and voltage maxima points, but we'll restrict our focus here to current nodes; that is, to the center point of 1/2-wavelength elements. Although there are numerous reports of empirically generated antennas using linear loading, little has been quantified in amateur literature.[2] As a start toward remedying this deficiency, I decided to juxtapose linear-loaded dipoles and Yagis with their center-loaded counterparts. For comparison with the center-load models of both dipoles and Yagis in **Table 1**, I added a linear-load model with no. 12 wire extending 2-feet on either side of the element center in a vertical plane below the main element. The upper wire is 1.2 inches below the main element, and the lower wire is 1.2 inches below the upper wire.

A model of the linear-loading element is only approximately comparable to the model of the center-loaded element because of differences in modeling conventions. A loading inductor (or capacitor) is treated in both NEC and MININEC as a nonradiating item inserted into the structure. By contrast, the linear-loading structure is part of the overall radiating structure of the antenna. Moreover, because most versions of MININEC permit but one material, the models are all aluminum—even though in practice the linear-load element is usually copper. Nevertheless, figures for the linear-loaded model given in **Table 1** are roughly comparable with the center-loaded results and indicative of relative performance. In both cases, the material losses of the main aluminum element are included in the model.

Whether a dipole or a Yagi, the gain of linear-loaded elements tends to surpass that of the corresponding center-loaded elements by a significant amount. So, too, does the front-to-back ratio of the Yagi model. If we assume that a Q of 100 is a reasonable and sustainable figure for a center-loading inductor, then linear loading becomes a very attractive alternative in shortened horizontal antennas. It generally requires a center-loading coil Q of 300 or better to reach the performance of a linear-loaded Yagi.

The last two entries under the Yagis in **Table 1** are included to demonstrate the effects of losses should only one of the Yagi's two elements exhibit more than design losses, perhaps due to weathering. Reduction of reflector Q results in a lower front-to-back ratio and a higher reactive component to the feedpoint impedance. In contrast, reduction of the driven element Q results in a lower antenna gain and a higher resistive component of the antenna feedpoint impedance. Understanding these differences can be an aid to troubleshooting antenna problems.

A preliminary method of calculating linear loads

The resemblance of a centered linear-loading element to a transmission line is no accident. In fact, each half of the linear-loading element can be viewed as a shorted, inductive transmission line stub, and this view provides a basis for approximate calculations of the element length. Each half of the element represents a reactance, and the two halves are in series.

The designer can derive the required total reactance of a shortened dipole by simply using MININEC or NEC to model the short element at the desired frequency. Alternatively, one can measure the feedpoint impedance of an actual main element without loading. The capacitive reactance at the feedpoint requires exact compensation by an equal inductive reactance provided by either a center loading coil or, as here, a shorted length of transmission line.

Materials for a linear-loading element are a matter of designer preference within the limits of good structure. Given the selection of wire, rod, or tubing for the linear load, the process of calculating the linear load begins by determining the characteristic impedance, Zo, of the proposed load line, using the standard approximation:

$$Z_o = 276 \log\left(\frac{2S}{d}\right) \qquad (1)$$

where S is the spacing between the wire centers and d is the wire diameter, both in the same units.[3]

From the value of Z_o and the desired reactance, determine the line length in electrical degrees, L_E, from the equation:

$$Z_o = 120 \cosh^{-1}\left(\frac{S}{d}\right) \qquad (2)$$

where X_L is the total desired reactance. The doubling of Z_o in the denominator provides for the length of each half of the linear-loading element. Converting the length into feet requires the design frequency, F_R, the assumption of a velocity factor of 1, and the equation:

$$L_E = \arctan\left(\frac{X_L}{2Z_o}\right) \qquad (3)$$

Remember to double the length for the full element.

The utility of this calculation procedure is limited. There are two generally popular geometries for constructing linear-loaded center elements. **Figure 1** compares the "end-on" appearance of vertical-plane geometry with triangular geometry. Because the load lines of the triangular arrangement are usually equally spaced from the main element, the transmission-line calculation produces usable results as a first approximation for building. However, the vertical-plane geometry places one "side" of the transmission line closer to the main element, thus disrupting the presumed equal currents and voltages essential to the calculation's accuracy.

Calculations of triangular linear-load elements correspond in the main with models of fully structured antennas within about 2 to 3 percent. Because of limitations in modeling linear-loaded antenna structures, the calculations are as good as the model as a guide to building.[4] However, transmission-line calculations vary from modeling results for vertical-plane antennas by 15 to 30 percent, depending upon the particular line size and spacing. The calculations tend to call for radically shorter linear load elements than actually needed. To get a handle on vertical-plane linear loading arrangements requires a different technique.

Calibrating a vertical-plane linear load

A standard Yagi element or a dipole antenna shows a set of currents that decrease continuously, but not linearly, from the feedpoint because the elements are roughly resonant. An element with a linear-loading element has an overall wire length (counting both the element tube and the load wire) longer than a half wavelength. Hence, the current rises as one moves away from the feedpoint, reaching a secondary maximum over halfway out the loading element, and reaching a primary maximum on the way back in toward the junction with the tube. The inequality of currents in the outgoing and incoming wires of a vertical-plane linear-loading element verifies that the loading element isn't acting as a pure transmission-line element. The current along the element doesn't rise much and the tube-to-load element junction shows over 99 percent of the current. Essentially, the radiation produced by the currents in the loading element cancel, leaving the tube element radiation to dominate the far field

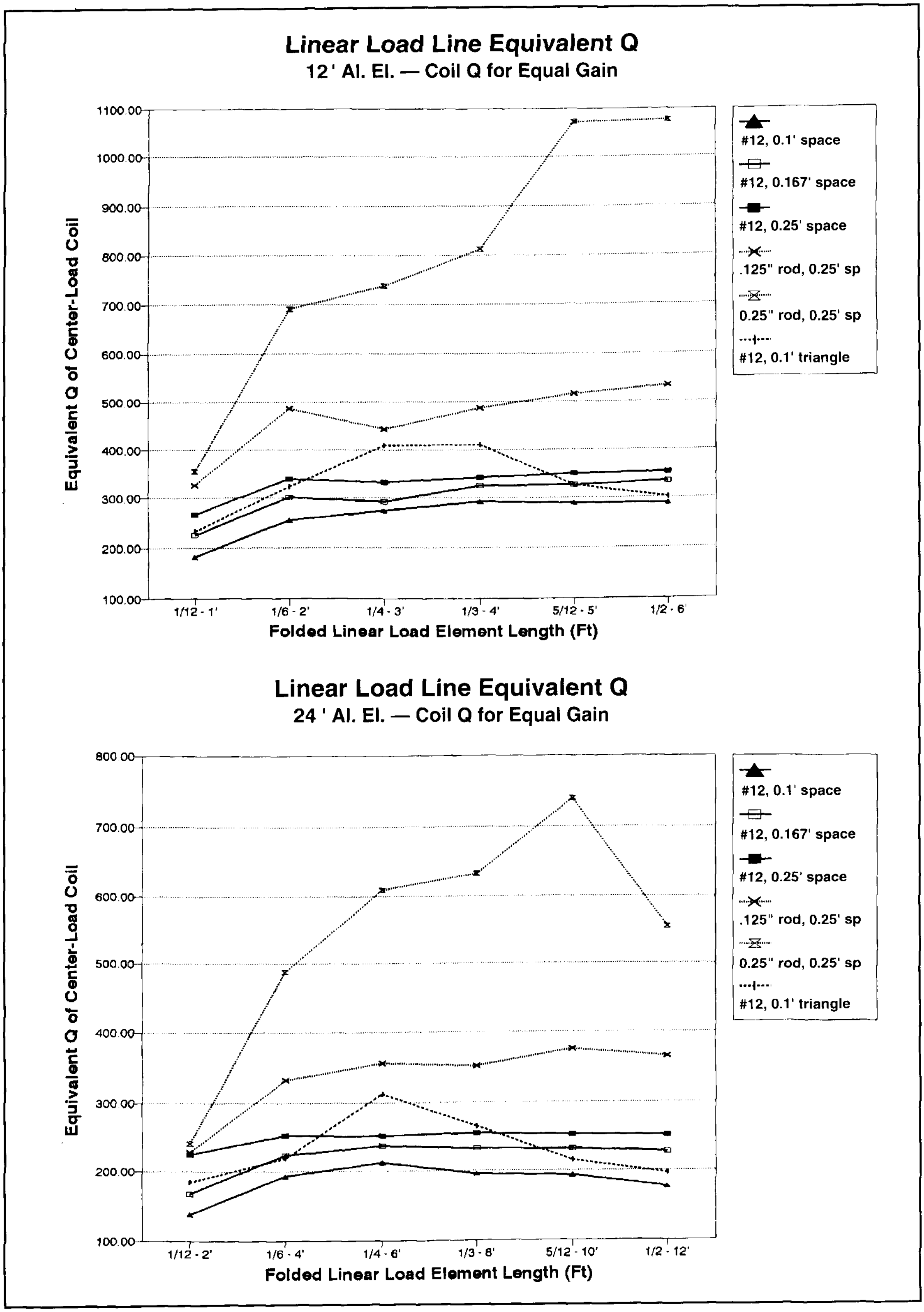

Figure 4. Equivalent Qs of linear load lines (relative to a center-loading inductor) between ratios of 1:12 to 1:2 for (A) a 12 foot 0.75 inch diameter aluminum main antenna element and for (B) a 24 foot 0.75 inch diameter aluminum main antenna element for 6 linear-load configurations.

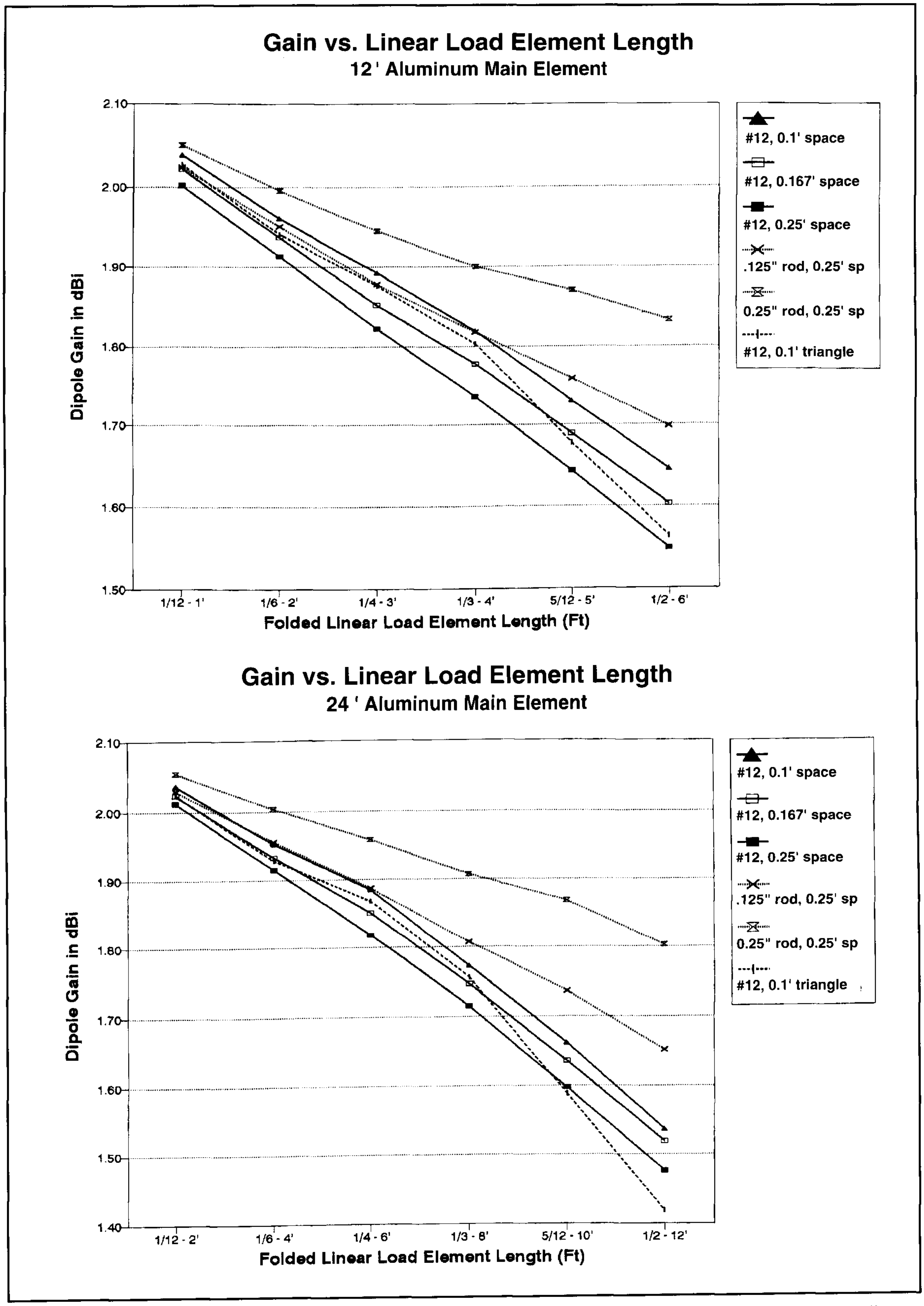

Figure 5. The gain of dipoles with varying lengths of linear-loading between ratios of 1:12 to 1:2 for (A) a 12 foot 0.75 inch diameter aluminum main antenna element and for (B) a 24 foot 0.75 inch diameter aluminum main antenna element for 6 linear-load configurations.

Antenna #	Geometry & Materials	Range of Q (1-6' length)	Gain with 4' linear section	Q with 4' linear section
	Antenna element = 12' 0.75" diameter aluminum; load length = 4'			
1	VP, 0.25" rod sp: 0.25'/0.25'	1075-355	1.90	812
2	VP, 0.125" rod sp: 0.25'/0.25'	532-328	1.82	487
3	VP, #12 wire sp: 0.25'/0.25'	355-267	1.74	343
4	VP, #12 wire sp: 0.167'/0.167'	334-224	1.78	326
5	VP, #12 wire sp: 0.1'/0.1'	293-183	1.82	293
6	Tri, #12 wire sp: 0.1'/0.1'	411-233	1.80	411
Antenna #	**Geometry & Materials**	**Range of Q (1-12' length)**	**Gain with 8' linear section**	**Q with 8' linear section**
	Antenna element = 24' 0.75" diameter aluminum; load length = 8'			
1	VP, 0.25" rod sp: 0.25'/0.25'	739-600	1.91	632
2	VP, 0.125" rod sp: 0.25'/0.25'	375-229	1.81	352
3	VP, #12 wire sp: 0.25'/0.25'	256-225	1.72	256
4	VP, #12 wire sp: 0.167'/0.167'	238-168	1.75	232
5	VP, #12 wire sp: 0.1'/0.1'	213-138	1.77	196
6	Tri, #12 wire sp: 0.1'/0.1'	313-185	1.76	266

Note: VP = linear load elements in vertical plane with antenna element; Tri = linear elements in triangular configuration with antenna element.

Table 3. A comparison of linear-loaded dipoles listing geometry, materials, Q range (for all load lengths), and gain and Q (with a 4' or 8' load length).

pattern. Cancellation isn't perfect, leaving a high current level over a greater length of the antenna element than with lower-Q center-loading schemes.

Correlating models of linear-loaded dipoles with center-loaded counterparts permits a rudimentary calibration of linear-loaded dipoles of both vertical-plane and triangular geometries. Free space models of fixed-length main elements with variable linear loads were checked for resonant frequency, as indicated by a near-zero reactance. Then, using the same frequency, an equivalently long dipole of the same material was center loaded to resonance by the same test. The requisite reactance became the center-load lossless-inductor reactance for the linear load. Flipping between copper and aluminum elements (both tubing and linear-load wire) produced no change in the resonant point. As noted above, the modeling process is subject to certain limitations of both MININEC and NEC.

Table 2 provides a sample of the data developed for just one linear-load configuration: a vertical-plane arrangement with a no. 12 wire spaced about 2 inches from the main element and 2 inches apart for a 12-foot element. The table clearly shows the decrease of gain as the linear element is lengthened, along with the increase in equivalent reactance and the decrease in resonant frequency. Because the goal was to develop dimension figures ade-

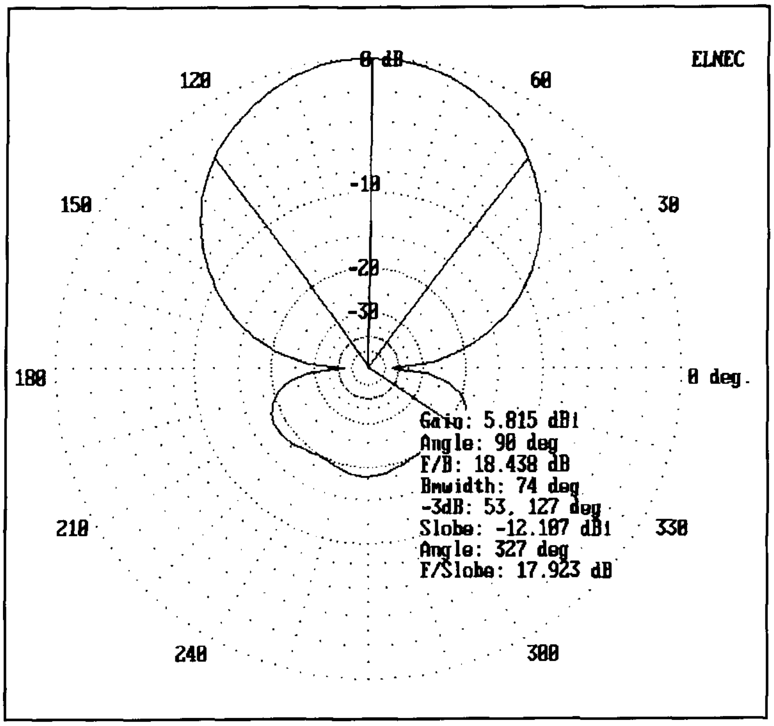

Figure 6. Free space azimuth pattern for a linear-loaded 2-element beam with close-spaced elements.

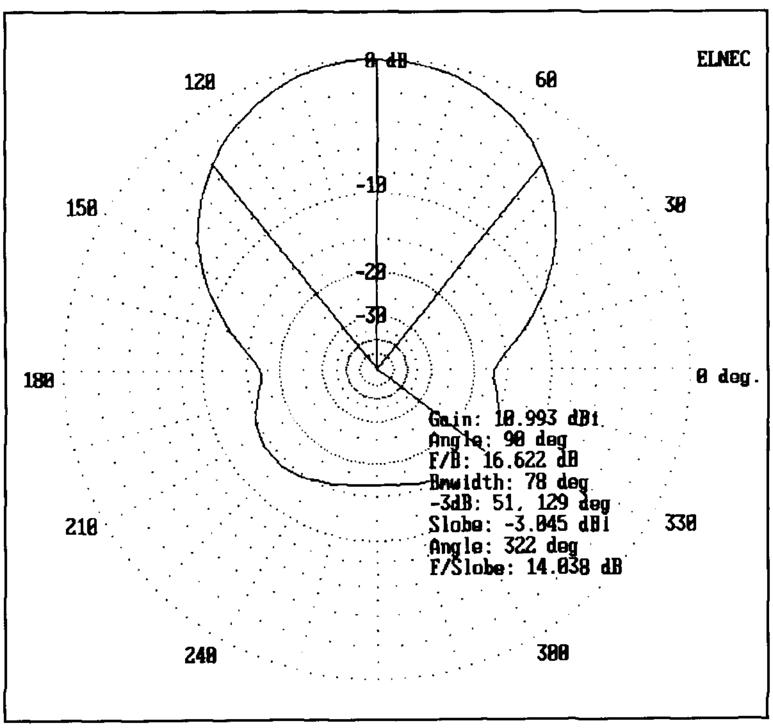

Figure 7. Azimuth pattern at 23 degrees elevation for the 2-element linear-loaded beam at a height of 20 feet above medium real ground.

quate to the start of home construction, resonance was defined as a remnant feedpoint reactance of less than 0.05 ohms.

Figures 3A and **3B** show the results of six dual runs on linear elements (1/2-wavelength dipoles) of different lengths, materials, and spacing. Each type of element shows a reasonably linear increase in equivalent reactance with increases in length. (Note that the element length is for the folded element; the actual wire length is twice that amount plus connecting leads.) Extrapolation to intermediate lengths and similar but deviant linear-load configurations is possible for other required values of reactance.

Although the equivalent reactance was derived using zero-loss center-loading inductors, an indication of equivalent Q was derived by adding resistance to the inductor until the antenna gain was the same as the linear-loaded model. **Table 3** provides the data on equivalent Q ranges for the linear-load geometries shown in the graphs in **Figures 4A** and **4B**, with specific data on gain and Q for one typical linear section length. **Figures 5A** and **5B** provide gain profiles for six variations each using 12-foot and 24-foot 0.75-inch diameter aluminum main elements.

Triangular geometry loads don't fully overlap their vertical-plane counterparts. As shown in **Figures 3A** and **3B**, the close-spaced triangular arrangement of no. 12 wire turns out to parallel closely the reactance progression of vertically planed no. 12 wire spaced more widely (0.167 foot versus 0.1 foot), or 1/8-inch rod spaced at 0.125 foot. However, the equivalent Q of the triangular configuration shows a clear peak at midlength load element sizes, as shown in **Figures 4A** and **4B**. In common with the vertical plane no. 12 linear-load configuration, the no. 12 triangular configuration shows a more rapid fall-off in gain after the 4-foot point with 12-foot main elements and after the 6-foot point with 24-foot main elements (see **Figures 5A** and **5B**). The rapid reduction in gain for close-spaced no. 12 linear-load elements suggests that the break points on the graph represent the limit of their effective use compared to other configurations.

Besides the linear relationship between element length and equivalent center-loaded lossless-inductor reactance, certain other trends in **Figures 3, 4**, and **5** are noteworthy:

1. **Spacing.** For a given geometry, load-length, and wire size, antenna element gain decreases and Q increases as spacing increases.
2. **Wire size.** For a given geometry, load-length, and spacing, antenna element gain and Q increase as the wire size increases.
3. **Geometry.** For a given load length, spacing, and wire size, a triangular geometry yields a higher Q than the vertical-plane geometry, but provides less antenna element gain.
4. **Diameter.** As main element and linear section wire diameters decrease relative to a wavelength at the signal frequency, reactance increases slowly and Q decreases.

5. **Long linear elements.** As the ratio of linear-load length to main element length exceeds 5:12, both the equivalent center-load reactance and Q tend to depart from a relatively linear curve. Note that, although the Q curves for 0.125 and 0.25-inch diameter linear-load elements seem to depart radically from the no. 12 vertical-plane models, a closer examination of the curves shows they are topographically similar, with a fairly complex magnitude adjustment factor.

6. **Short linear elements.** As the ratio of linear-load length to main element length falls below 1:6, both the equivalent center-load reactance and Q tend to depart from a linear curve, with the Q falling off rapidly.

7. **Recommended linear element lengths.** Between ratios of 1:6 and 5:12 of the linear-load element to the main element, equivalent reactance and Q curves are nearly linear, as is the rate of decrease in antenna element gain with increased linear-load length. As noted, close-spaced no. 12 linear-load elements depart from this near-linearity of gain and Q beyond certain "break" points, which limit their applicability.

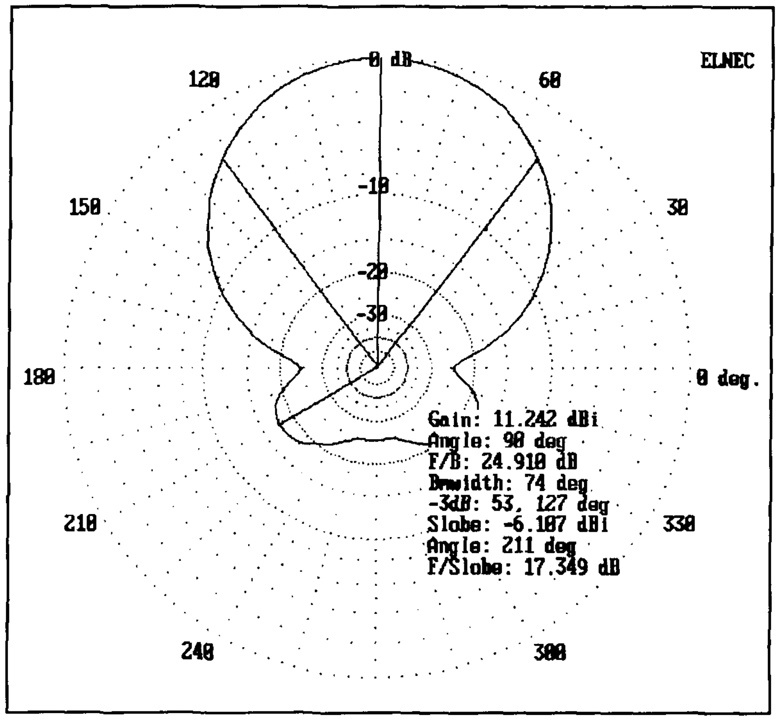

Figure 8. Azimuth pattern at 14 degrees elevation for the 2-element linear-loaded beam at a height of 35 feet above medium real ground.

One additional trend also deserves notice: the longer the loading element (or the higher the reactance of any center-loading means), the lower the resistive feedpoint impedance. Linear-loading elements in the vicinity of one-third the total length of the main element show a resistive component between 20 and 30 ohms, depending upon design. A direct match to 50-ohm coaxial cable, accordingly, isn't feasible—although simple beta, gamma, balun, and transformer matching systems are available. For anyone concerned about the small mismatch that exists between a full-size dipole (72 ohms nominal) and 50-ohm coax, a short linear load of one twelfth the main element length is a solution. The result is, in almost any construction mode, a feedpoint impedance within ±5 ohms of the coaxial cable's Z_0. Of course, the main element must be shortened from full size, but the decreased size produces negligible gain loss (less than 0.1 dB).

For shortened Yagi designs or portable field dipoles, a close-spaced linear element approximately one third the length of the main element represents a good compromise among a number of factors to consider when designing a shortened antenna. It maintains element gain at a high level, while effecting a significant shortening of the overall element length. Specific design objectives, of course, may require a departure from these very general recommendations.

The linear-loading section curves developed for 12 and 24-foot main elements can be used directly for 10- and 20-meter beams by extrapolation. Extrapolations for other bands will be less precise, but sufficient for reasonable construction estimates. A recommended alternative is to create a set of curves for the specific materials to be used in a given project. With almost any antenna modeling program, the task is an evening's work. In the end, no matter how extensive the modeling, home construction techniques will rarely be exact enough with respect to replicating the modeled spacing among the parts of a linear-loaded element to permit building without adjustment. However, the tables and graphs do provide some initial quantitative guidance. For those who prefer to use the transmission-line stub calculations as a foundation for building, **Table 4** provides a set of generalized deviance factors for correcting the calculations to correspond with each of the types of linear loads described here. The averaged factor holds for linear-load lengths between about 15 and 40 percent of the main element length. The progressions of correction factors may also serve as a guide to builders using load dimensions outside the range of those analyzed here.

Designing a 2-element linear-loaded Yagi

The technique of using center-load reactance as a substitute for a linear-loaded ele-

Correction Factors for Using Transmission Line Calculations with Some Lengths of Vertical-Plane Linear-Loading Elements.

12' Aluminum Main Element Models

Linear-Load Characteristics: Diameter	Spacing from Main Element	Spacing Between L-L Elements	Multiply Transmission-Line Calculations by this Value to Agree with Modeling Results
#12 (.0808")	0.1' (1.2")	0.1' (1.2")	1.30
#12	0.167' (2")	0.167' (2")	1.23
#12	0.25' (3")	0.25' (3")	1.15
0.125	0.25'	0.25'	1.18
0.25	0.25'	0.25'	1.24
#12	0.1'	0.1' (triangular)	1.05

24' Aluminum Main Element Models

Linear-Load Characteristics: Diameter	Spacing from Main Element	Spacing Between L-L Elements	Multiply Transmission-Line Calculations by this Value to Agree with Modeling Results
#12 (.0808")	0.1' (1.2")	0.1' (1.2")	1.27
#12	0.167' (2")	0.167' (2")	1.23
#12	0.25' (3")	0.25' (3")	1.18
0.125	0.25'	0.25'	1.21
0.25	0.25'	0.25'	1.27
#12	0.1'	0.1' (triangular)	1.03

Note: Because MININEC models return slightly long dimensions, correction factors may be reduced by up to 3%.

Table 4. Correction factors for using transmission line calculations with some lengths of vertical-plane linear-loading elements.

ment for dipole modeling carries over into the design of 2-element Yagis. Choosing a set of main element lengths, center-loading them for the desired antenna performance (within the limits imposed by shortening the elements), and replacing the center loads with their equivalent linear-loading elements can produce buildable models. Because changing the magnitude of a center-load inductive reactance is far quicker in all antenna modeling programs than changing the complex dimensions of a linear loading element, the design process is significantly shortened.

As a design example, let's select 12-foot main elements of 3/4-inch diameter aluminum as the main elements for a 2-element shortened Yagi for a center frequency of 28.5 MHz. A little element juggling, along with the addition of center loads for the elements of about 250 ohms, each produced a reasonable design with the following properties: Driven element, 11.6 feet; reflector, 12.16 feet; spacing, 4.25 feet. The extension of the reflector didn't violate my intention to use 6-foot lengths of hardware store aluminum tubing, because construction would place the two lengths about 2 inches (0.167 foot) apart. The anticipated gain of the array (using a Q of 300 for both loading coils) was 5.8 dBi, with a front-to-back ratio of about 18 dB. The feedpoint impedance of the center-loaded beam calculated by the modeling program was about 17 ohms.

The chart for 12-foot aluminum elements shows a linear-loading element of no. 12 wire, spaced 0.1 foot (about 1.2 inches) and 4-foot long corresponds closely to the 250-foot center-loading inductors. Substituting the required linear sections into the model yielded a 2-element beam with the same gain, front-to-back ratio, and feedpoint impedance as the center loaded model. **Figure 6** shows the free space azimuth pattern of the beam design. Since modeling an antenna with linear-loading sections requires extensive and careful element segment tapering techniques with MININEC programs, the resultant antenna description is quite large. Those with slower computers or restricted RAM may wish to skip this step and go directly from the graphs to the shop. However, it pays to check an extrapolated design to ensure against errors.

A 2-element beam, like every other array, will tend to vary in gain and front-to-back ratio

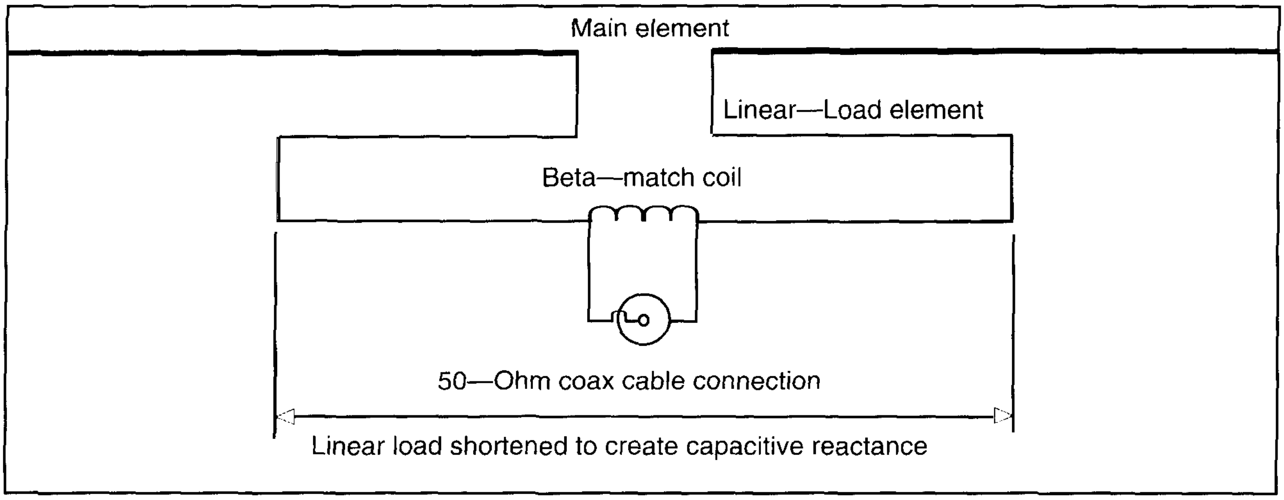

Figure 9. General scheme of the beta match used with the 2-element linear-loaded beam.

at heights above real ground below about 2 wavelengths. As a check on the design, patterns were run at the angle of maximum radiation for heights of 20 and 35 feet, with the results shown in **Figure 7** and **Figure 8**. However, as usable as these performance expectations are, this step didn't end the design process.

Because one of the main uses for shortened antennas is for portable field operations, I anticipated building the linear-loaded Yagi to make it transportable. Under these conditions, it's possible to add, to the reflector, a tuning capacitor remotely placed some multiple of a half-wavelength from the antenna and connected by a suitable length of parallel feeder (450 ohms, in this case). This required lengthening the linear element of the reflector purposely to make it inductive. Lengthening the linear section of the reflector to 5 feet (2.5 feet either side of center) permitted the use of loading capacitance between about 50 and 95 pF to retune the reflector back to maximum front-to-back ratio.

A second design modification was required by the use of a beta-match to convert the 17-ohm feedpoint impedance to the 50-ohm coax value. Shortening the driven element linear section to 3.7 feet (1.85 feet either side of center) yielded the requisite 23 ohms of capacitive reactance in the driven element to go with the 32.7-ohm inductive reactance across the feedpoint terminals (0.18 μH or about 4 turns of no. 12 copper wire, 1/2 inch in diameter and 1/2 inch long at 8 turns per inch).[5] **Figure 9** shows the general scheme of the beta match applied to the linear-loaded antenna.

These modifications for portable use actually improve one aspect of the antenna's performance—the SWR bandwidth. **Figure 10** is a graph of the SWR bandwidth of several antennas, all of which use the same main element dimensions: center-loaded Yagis with Qs of 300 and 100, the unmodified linear-loaded antenna, and the modified version for portable use. That the linear-loaded antenna is equivalent to a center-loaded beam with a Q well over 300 is obvious from the steepness of the SWR curve below the design frequency. The curve for the remotely tuned portable version shows a greater symmetry, with about 700 kHz of usable (<2:1) SWR bandwidth at optimum front-to-back ratio.

Actually, the antenna will tune within a 2:1 SWR across the entire first MHz of 10 meters. However, the front-to-back ratio will degrade at the band edges. **Figure 11** is a composite pattern of a fixed-reflector model between 28 and 29 MHz. **Figure 12** shows the composite free space azimuth pattern of the remotely tuned version over the same spectrum. The minor retuning required for bringing the SWR into the 2:1 range at the band edges doesn't reduce the front-to-back ratio very much.

Tuning the reflector actually improves the front-to-back ratio over real ground relative to a fixed-reflector free-space-derived model. **Figures 13** and **14** show composite patterns for the first MHz of 10- for 20 and 35-foot elevations, respectively, with the reflector in each case tuned for maximum front-to-back ratio. These patterns and numbers, of course, are anticipations bred from models. The final question is whether they can be realized.

Constructing and checking a test model

Building a linear-loaded beam for portable field use (10-meter hilltopping) isn't difficult, because the elements are light. The basic dimensions are: Driven element, 11.6 feet;

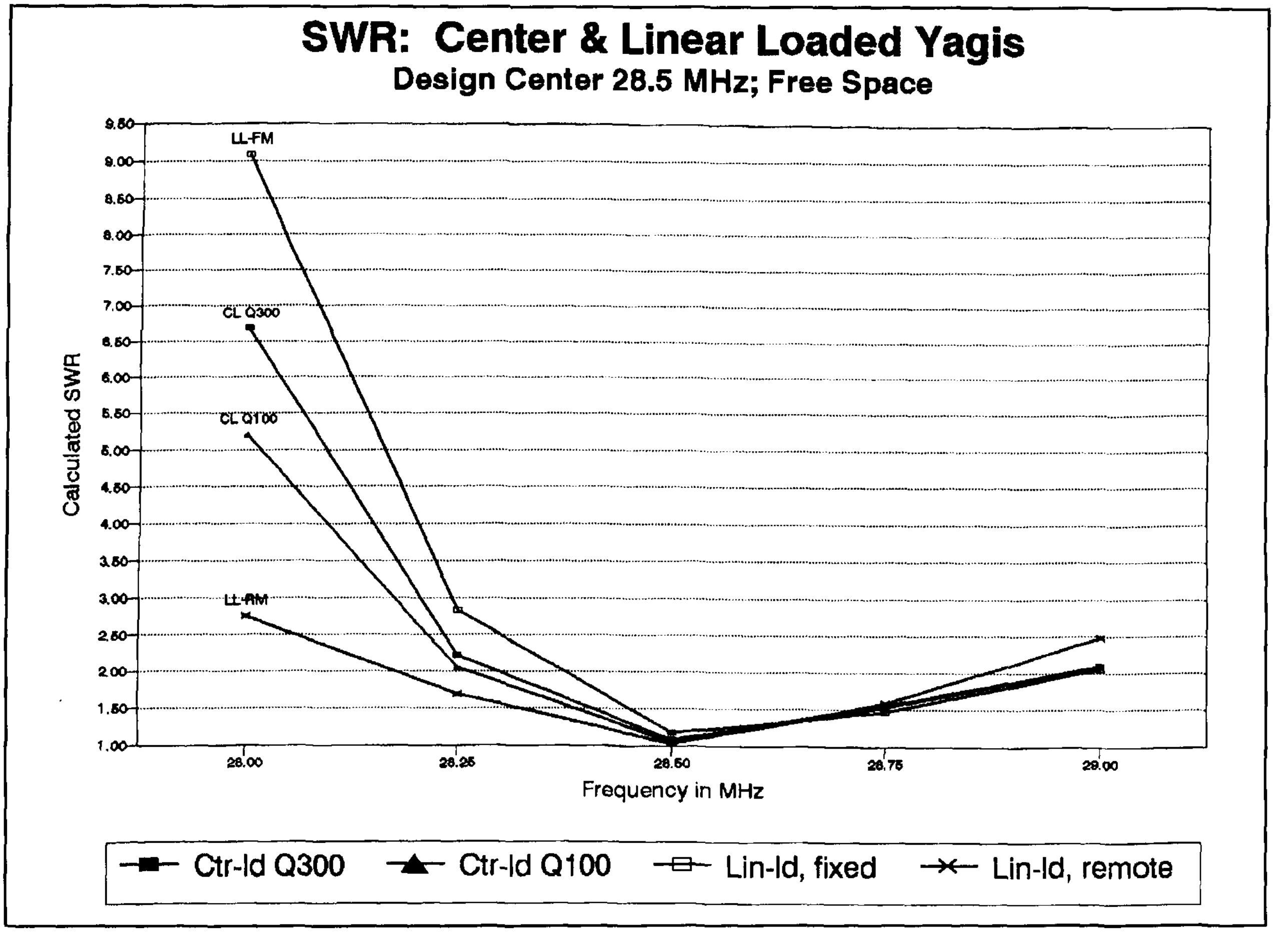

Figure 10. Calculated SWR bandwidth for center- and linear-loaded Yagis.

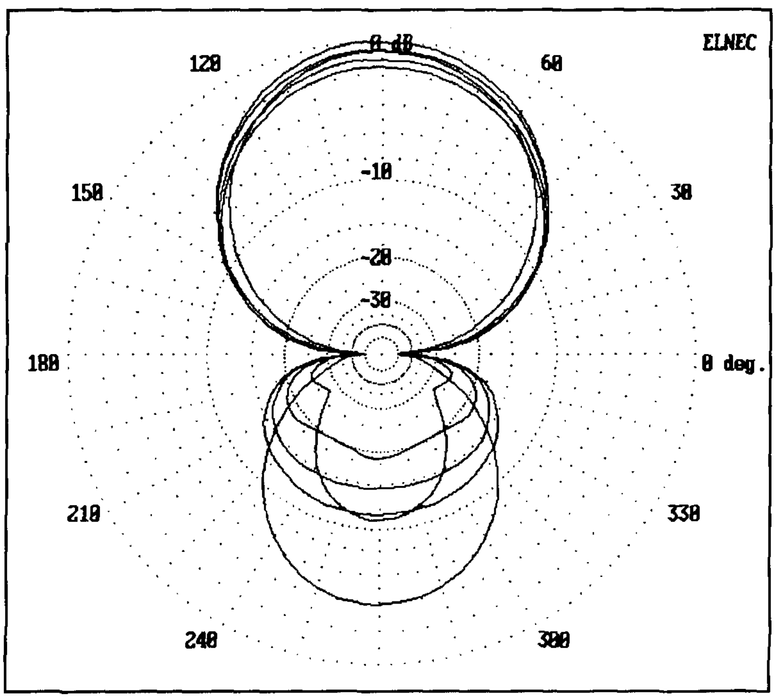

Figure 11. Composite free space azimuth pattern for a fixed reflector linear-loaded 2-element Yagi from 28.0 to 29.0 MHz.

reflector, 12.16 feet; spacing, 4.25 feet. Four 6-foot lengths of 0.75-inch diameter tubing from the local hardware outlet provided the main elements. With a 2-inch center spacing, the reflector lengths are correct as purchased, but the driven elements were cut to 5 feet 8 inches each.

The element-to-boom plates are 1/2-inch plywood, about 6 to 7 inches wide and 2 feet long. As shown in **Figure 15**, excess wood was removed from the corners for minimum weight. Each plate was coated with car-repair epoxy for fiberglass patching. This material is more weather-resistant than any other I have found. Number 10 stainless steel nuts, bolts, and lock washers fasten the element to the plate. (Small U-bolts are recommended for larger antennas.) Because the boom is a 5-foot section of 1-1/4 inch nominal diameter Schedule 40 PVC, 1-1/2 inch U-bolts are used for the plate-to-boom connection.

The plate-to-boom U-bolts also hold another fixture—the center supports for the linear-loading wire. The test antenna uses no. 12 solid copper wire linear sections in two pairs: two 2 foot 6 inch sections for the reflector and two 1 foot 5 inch sections for the driven element.

Each section attaches to a thick plastic plate angled from the outer U-bolt inward, as shown in **Figure 15**. A heavy plastic freezer box a little over 4 inches square and 1 inch high provided two plates with the correct angle to place the linear-load wires directly under the main element when mounted to the outer U-bolts. The composition of the plastic ensures good weathering characteristics, and no RF problems have surfaced.

Wires a little over twice each section length were straightened and then bent over a piece of 1-1/4 inch mast to establish the spacing. Before mounting, I slipped midlength and end supports over each wire loop. I cut eight 4 by 4 inch squares from the corners of a squared-off half-gallon plastic jug. On each side of each corner, I used a hole-saw to cut 3/4-inch circles for the main elements and then drilled 1/8-inch holes for the linear-load wires. Squeezing the corners allows the wire and the main element to pass through each pair of holes. Releasing the corners places the assembly under tension, which keeps the main element and the linear-loading wires aligned. Local storm winds haven't moved this assembly, but something stronger is recommended for larger or more permanently mounted antennas.

Solder rings on the ends of the linear-load wires attach the section to bolts (no. 10 stainless steel) on the center plastic plate. Short no. 12 wires, also with solder rings, provide a junction between the wire assembly and the main aluminum element. Before attaching solder rings to wires, I usually let solder flow all over the ring, as many types will rust in the weather.

The driven element linear section terminates its lower center in a coaxial chassis connector mounted on the plastic plate with the threads facing the mast. A ferrite bead or shield 1:1 balun taped to the boom allows the coax to be run inside or outside the mast—in my case, sections of TV mast. The beta match coil mounts across the plate-to-linear-wire bolts with solder rings. The reflector section center terminates in two pin jacks. For initial testing, a capacitor with mating pins connects at the element. For field use, a half-wavelength of 450-ohm parallel feeder terminated at one end with pins and at the other with pin jacks places the capacitor within easy reach for remote adjustment with 20 feet of mast. A series of plastic spray can tops, each punched with four holes for cable ties that clamp the mast and the feeder, space the feeder from the mast.

For testing, solder rings can be omitted from the linear section wires until the correct length is determined. Clamping the wires under washers at the plate will suffice for initial tests. The object is to obtain the lowest possible SWR at the center design frequency by first tuning the reflector capacitor for a minimum reading and then spreading or compressing the beta match turns for a final null. Adjust the length of the wire section to bring the null frequency to the design center. If initial tests are close, minor

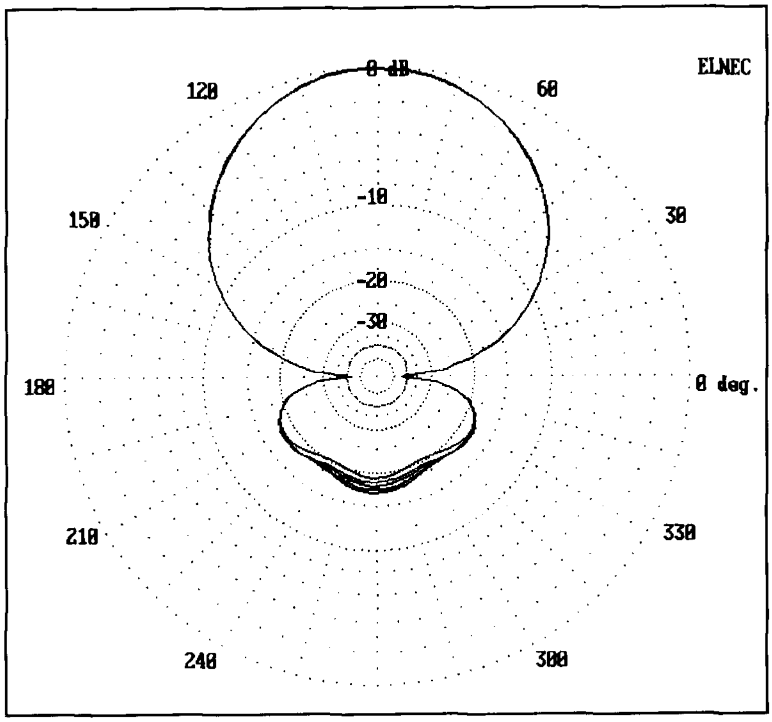

Figure 12. Composite free space azimuth pattern for a remotely tuned reflector linear-loaded 2-element Yagi from 28.0 to 29.0 MHz.

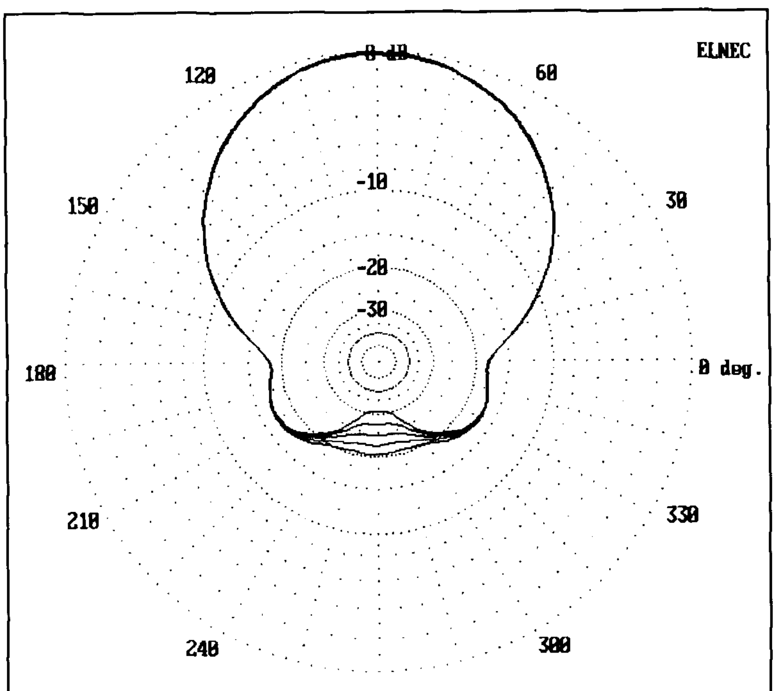

Figure 13. Composite 20-foot height azimuth pattern for a remotely tuned reflector linear-loaded 2-element Yagi from 28.0 to 29.0 MHz.

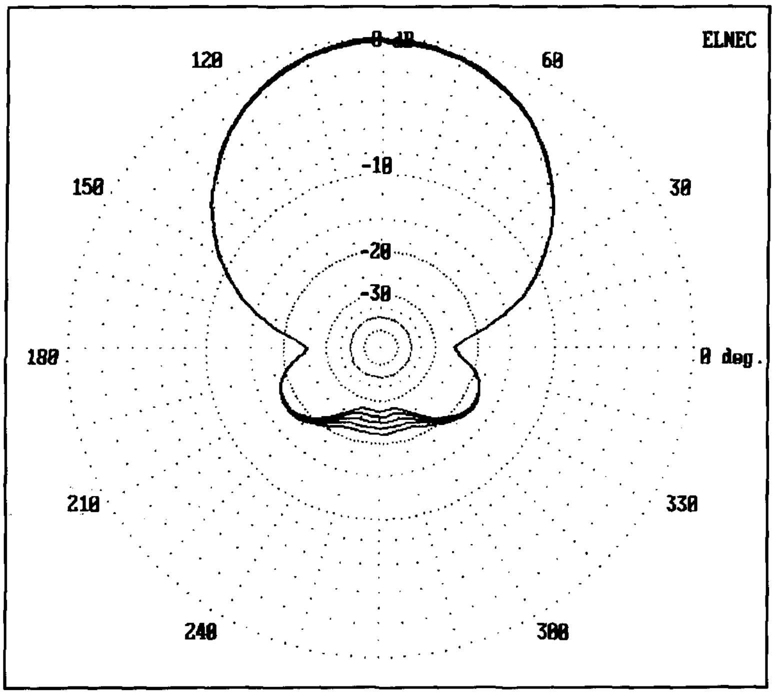

Figure 14. Composite 35-foot height azimuth pattern for a remotely tuned reflector linear-loaded 2-element Yagi from 28.0 to 29.0 MHz.

adjustments can be made by squeezing or spreading the linear wire sections (using the bottom wire only). Squeezing lowers reactance and raises the frequency, while spreading increases reactance and lowers the frequency. If significant wire deforming is required, adjust the length instead.

Off center frequency, do not adjust the reflector capacitor for absolutely the lowest SWR. Instead, find the lowest SWR point and then slightly off-tune the capacitor (within a 2:1 SWR ratio) in the direction of the setting for the antenna's design center frequency. That will establish a point closer to maximum front-to-back ratio in the absence of a reference signal. Refer to the SWR bandwidth graph for guidance.

The test antenna, built to the specifications provided by the graphs and models, performed to expectations. As indicated, the linear-loading element on the driven element was somewhat long—partly because the models yield slightly long dimensions and partly because the spacing used was slightly wider than the model for horizontal plane no.12 wire elements at 0.1 foot spacing. Removing 3 feet of load wire on each

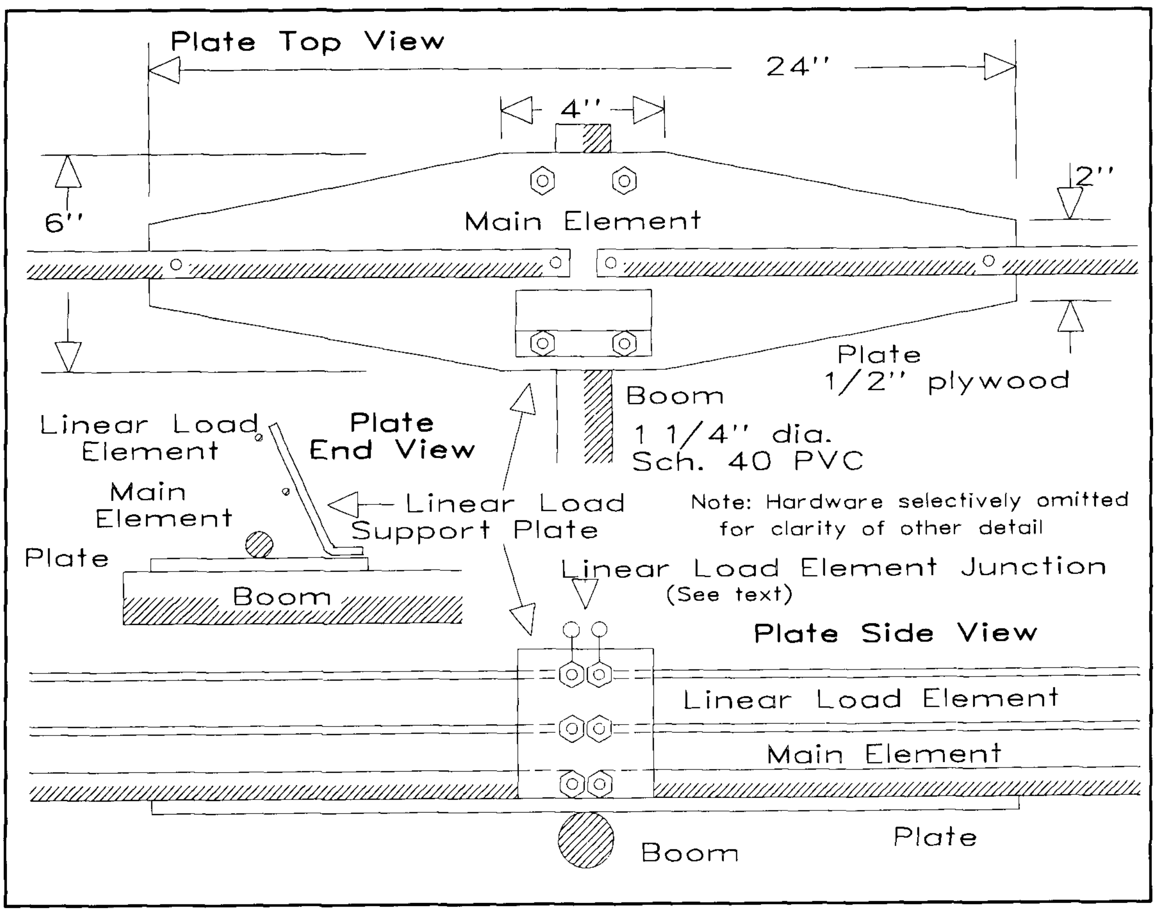

Figure 15. The basic element-to-boom assembly of the test 2-element linear-loaded Yagi with details of the linear load support plate at the main element center point.

side of center brought the antenna to resonance. The reflector element was also somewhat long, requiring less capacitance than specified. At the design center frequency of 28.5 MHz, 27 pF brought the antenna to maximum front-to-back ratio. Matching required only a small adjustment of the beta-match coil, a matter of squeezing the turns slightly.

With a fixed reflector loading capacitor, the 2:1 SWR bandwidth of the antenna was slightly over 300 kHz, confirming its high Q. A variable capacitor in the reflector increased the bandwidth to nearly 1 MHz, with over 750 kHz of that bandwidth at maximum front-to-back ratio. Performance tests at a 20-foot height with local line-of-sight signals confirmed about 3 S-units of front-to-back ratio—although these rough tests can't be equated with the elevated patterns shown in various figures. Nonetheless, they strongly suggest that the antenna performs close to its modeled specifications.

The 2-element linear-loaded Yagi has proven to be a most satisfactory field antenna. Although the linear load assembly on the elements requires some care, once assembled, it's almost as carefree as a full-size 2-element Yagi. The added front-to-back ratio shows up in practice, while the half-dB reduction in gain does not. In a fixed-tuned model, the chief drawback is the narrower usable bandwidth. That configuration is most useful where the operator tends to use a small portion of the band. The field version with a tunable reflector overcomes this limitation in large measure, making this antenna a good competitor with a full-size 2-element Yagi.

In addition to yielding a buildable antenna, the modeling that has gone into the development of the linear-loaded Yagi demonstrates something else. Antenna modeling programs aren't restricted to providing pattern-pictures of existing antennas. With proper care, they can be used to generate a considerable body of adjunct data helpful to antenna builders. The calibration of linear-loading elements is but one example of techniques that can expand the utility of such programs. The more we can interconnect the direct data produced by these programs with other collections of data that are important to antenna design, the better we can understand the antennas we use. Whether this result or the development of linear-loaded Yagis is the more important result of this investigation is a question for fireside, coffee-cup debate on cold evenings when the bands are closed.

REFERENCE NOTES

1. For more expert information on the construction of full size Yagis, see Leeson, *Physical Design of Yagi Antennas* (Newington: ARRL, 1992).

2. For example, see pages 6–7 and 6–8 of either the 16th or 17th Edition of the *ARRL Antenna Book*. See also pages 11–22 and 11–23 of the 16th Edition for W0YNF's linear-loaded 14-MHz driven-element-director Yagi, which uses triangular geometry. A linear-loaded 40-meter dipole also appears in Orr and Cowan, *Beam Antenna Handbook* (Radio Publications, 1990), pages 58–59. It uses vertical-plane geometry.

3. For somewhat greater accuracy, especially with large wires and close spacing, substitute for the given equation, the following:

$$L_F = \frac{L_E}{.366\ F_R}$$

4. Both MININEC 3.13 and NEC 2 are subject to systematic errors when combining elements of differential radii in complex geometries. The models used in this study are fully tapered MININEC models. By extensive comparisons with various modeling techniques, including the use of single-wire-size substitutes for various parameters, the utility and general validity of the MININEC models was established. However, the linear-loads called for by those models may be up to 2 to 4 percent long, which closes the apparent gap between transmission-line calculations and the models. Nevertheless, extensive modeling, including modeling the antennas listed in note 2 above, establishes that triangular and vertical-plane geometries aren't interchangeable without lengthening the linear-load element. Elements modeled in free space on W0YNF's dimensions and triangular geometry show a feedpoint reactance at 14.2 MHz of less than –10 ohms, although a similar close-space vertical geometry model with the same dimensions show nearly –60 ohm reactance (indicating a need to be longer to achieve resonance). Similarly, the vertical-plane geometry of the Orr dipole for 40 meters required a no. 12 wire linear load almost 8 feet longer than a no. 12 wire triangular linear load to achieve resonance with a 44.2-foot 1-inch diameter aluminum main element. The calculated triangular linear load modeled within 3-ohm reactance of resonance.

5. A beta match is a form of L-section match in which the series capacitor is created by shortening the antenna element. A shunt coil completes the section that matches an antenna impedance of less than 50 ohms to the higher impedance of the coaxial cable. Formulas for L-sections appear in almost any handbook. Designing an antenna for resonance on a modeling program and then shortening the driven element by an amount that yields the required value of capacitive reactance provides guidance for building the driven element, usually within limits that permit final adjustment by spreading or compressing turns in the shunt coil. A "hairpin" section of shorted transmission line can also make up the shunt inductor, usually with smaller losses, although the coil's lower Q permits a wider bandwidth. See the ARRL Antenna Book, 16th or 17th Edition, pp. 26–21 to 26–23, for further details, and be sure to read Thomas Cefalo, Jr., WA1SPI, "The Hairpin Match: A Review," *Communications Quarterly* (Summer, 1994), pages 9–54, and Gooch, Gardiner, and Roberts, "The Hairpin Match," *QST* (April, 1962), pages 11–14, 146, 156.

Appendix: How short can we go?

After developing the data and model antenna for linear loading, I ran across an article on a 10-meter 2-element Yagi that used 8-foot elements on a 4-foot boom with center loading and a beta hairpin match.[1] That led me to wonder how short we might make a Yagi, given that shortening elements permits an increase in front-to-back ratio at the expense of some gain. The results are interesting and worth passing on.

Beginning with center-loaded dipole performance, I modeled 0.75-inch aluminum elements ranging from full size (16.54 feet) down to the point where gain in dBi fell below zero (6 feet). **Table 1** summarizes the data, while **Figure 1** displays it in graphical form. The dipoles were initially modeled using infinite Q (0.0 ohms resistance) and then rechecked at Qs of 500 down to 100. The infinite-Q reading provides a

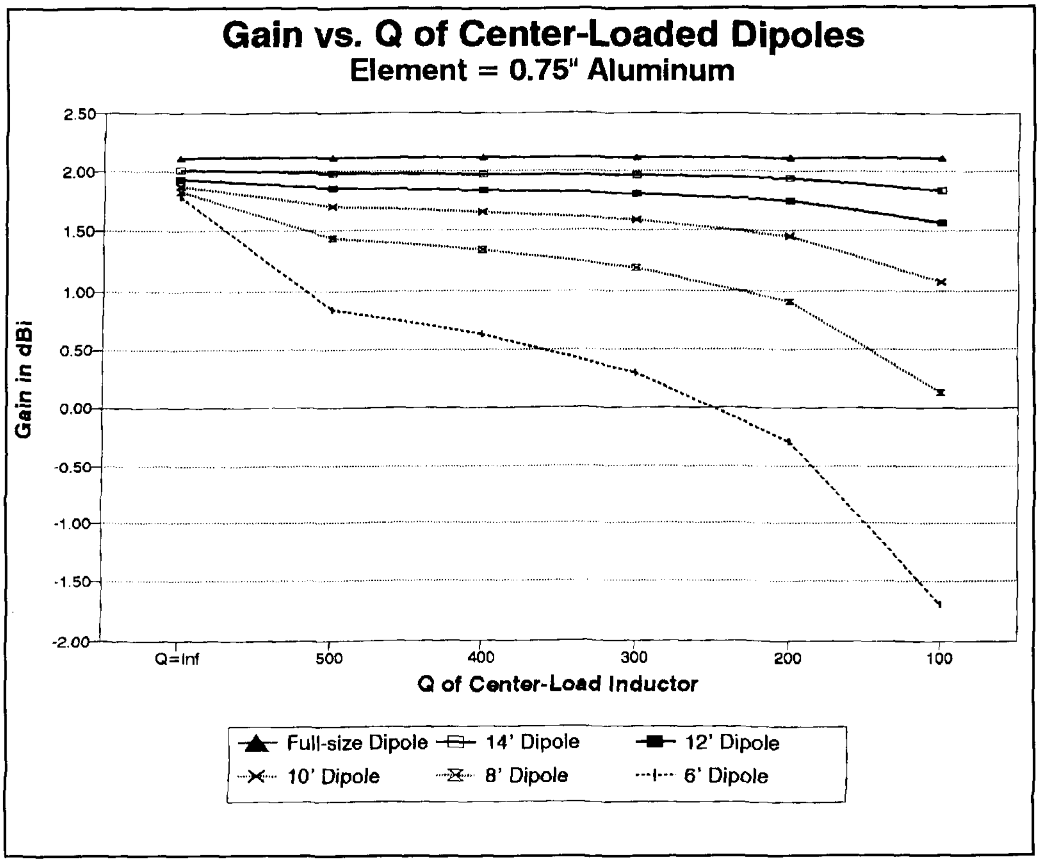

Figure 1. A comparison of the gain and the Q of a center-loading inductor for shortened 0.75-inch aluminum dipoles at 10 meters.

measure of the natural drop in basic gain as the antenna element becomes shorter. The finite Qs provide a measure of the losses incurred by center loading the element to resonance with an inductor (or even a linear-loading element). Note the shape of the curve as the Q decreases linearly.

Although conventional, registering comparisons in terms of one gain figure as a percentage of another may not be greatly informative when

Modeled Performance of Shortened 10-Meter Dipoles

Antenna Length (ft)	Load X_L (Ohms)	Feed Z (Ohms)	Q = —	Gain in dBi 500	400	300	200	100
16.54 (full size)	0	70.9	2.12					
14'	131	43.0	2.015	1.98	1.97	1.96	1.94	1.83
12'	247	28.4	1.93	1.86	1.84	1.81	1.75	1.57
10'	366	18.1	1.87	1.70	1.66	1.59	1.46	1.07
8'	510	10.7	1.83	1.43	1.34	1.19	0.90	0.14
6'	697	5.7	1.79	0.83	0.62	0.29	−0.29	−1.70

Table 1. A comparison of the modeled performance characteristics of shortened center-loaded dipoles on 10-meters.

making comparisons. Negative gains relative to an isotropic source are possible and do represent radiation by the antenna. The real question is whether the gain of any configuration is adequate for the job to which the antenna is assigned or whether something better may be available. The graph may give a better sense of the manner in which an antenna with decreasing length and centerload-Q may likely disappoint the builder, if a full-size dipole is the standard of comparison.

Applying the dipole data selectivity to full-size and shortened center-loaded 2-element Yagis produced the data in **Table 2**. The full-size Yagi used the 4-foot boom specified for the 8-foot model and is only a slight variation on the standard used throughout these tests. Models with 8-foot and 12-foot elements were run at Qs from infinity to 100 to gauge the performance possibilities of half- and three-quarter-size antennas. With both shortened antennas, the front-to-back ratio is superior to a full-size 2-element Yagi at a cost in gain and SWR bandwidth. However, the 12-foot model shows a decrease in front-to-back ratio as the Q decreases, while the 8-foot model increases the front-to-

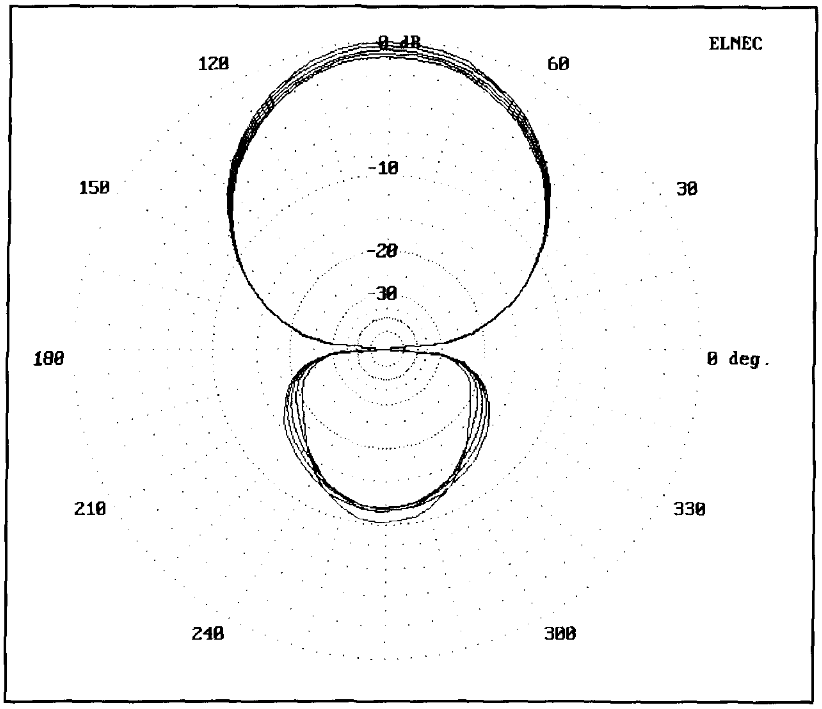

Figure 2. Free-space azimuth patterns for a full-size 2-element Yagi from 28 to 29 MHz.

Modeled Performance of Shortened 2-Element Yagis

Antenna and Load Q	Gain (dBi)	Front-to-Back Ratio (dB)	Feedpoint Impedance (Ohms)
Full-size Yagi[1]	6.63	11.27	29.9
12' Elements			
—	6.24	21.22	16.7
500	6.01	19.98	17.2
400	5.95	19.70	17.3
300	5.86	19.25	17.6
200	5.68	18.43	18.0
100	5.17	16.38	19.3
8' Elements			
—	5.76	13.69	11.0
500	4.88	16.93	12.1
400	4.68	17.92	12.4
300	4.36	19.80	12.8
200	3.78	24.96	13.7
100	2.34	21.83	16.2

Note 1: All antennas modeled with 0.75" aluminum elements and a 4' boom. Full size antenna: DE = 16.08'; Refl = 17.49'. All driven elements resonated, although in practice, the matching system may require a different length or load.

Table 2. A comparison of modeled performance characteristics of center-loaded shortened 2-element Yagis.

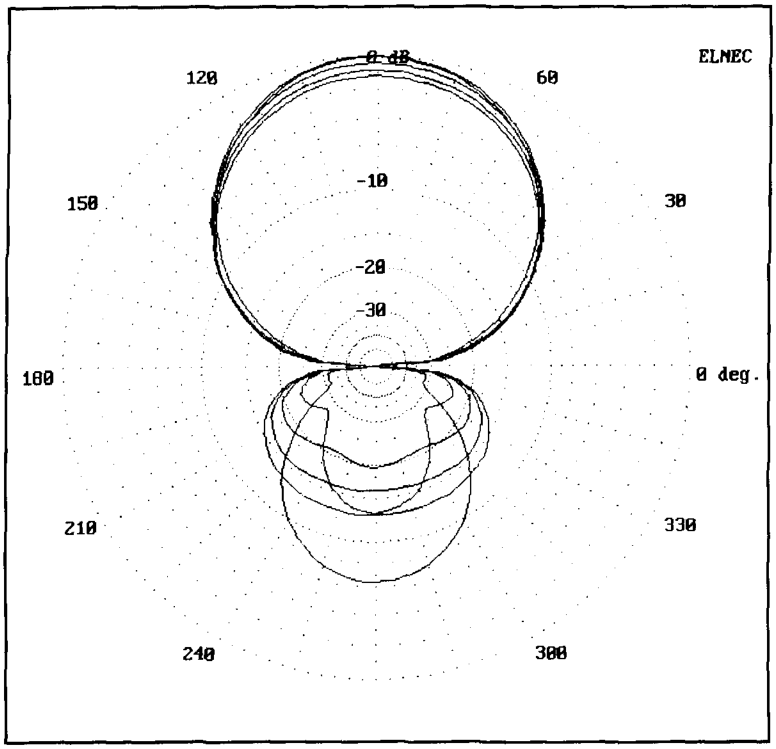

Figure 3. Free-space azimuth patterns for a shortened 2-element Yagi with 12-foot elements and inductive center loading having a Q of 300. The largest rearward lobe occurs at 28 MHz, with the smallest rearward lobe occurring at 28.5 MHz.

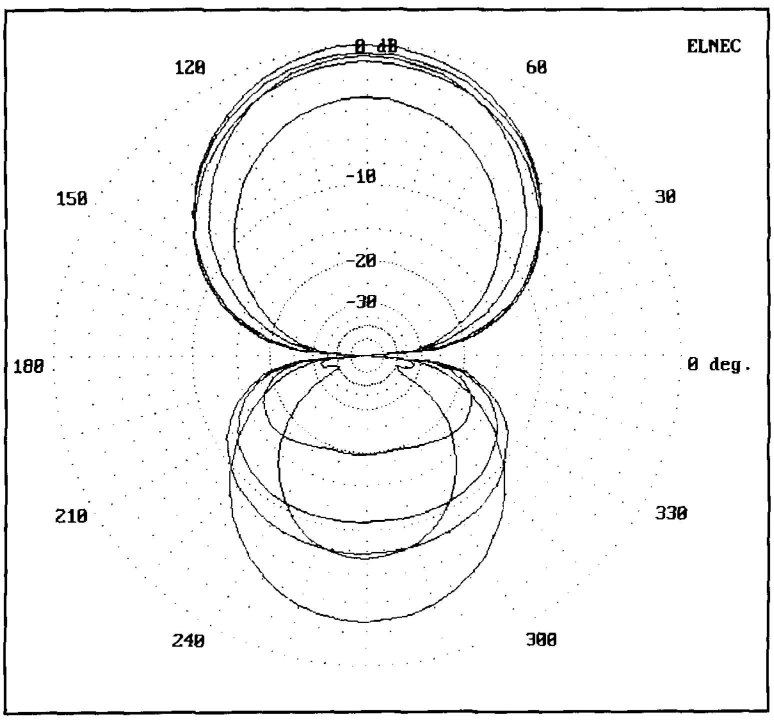

Figure 4. Free-space azimuth patterns for a shortened 2-element Yagi with 8-foot elements and inductive center loading having a Q of 300. The largest rearward lobe, along with the diminished forward lobe, occurs at 28 MHz, with the smallest rearward lobe occurring at 28.5 MHz.

back ratio with Q decreases down to 200.

Figures 2, 3, and **4** provide frequency-swept azimuth patterns in free space for the full-size, the 12-foot, and the 8-foot models, respectively. The full-size model, as expected, shows a consistent rear pattern throughout the 28 to 29-MHz range. In contrast, the rear pattern of the 12-foot model shows the narrow bandwidth of the maximum front-to-back ratio point, with usable front-to-rear ratios from 28.25 to 29 MHz, as compared to the full-size model. The rear pattern of the 8-foot model deteriorates much more quickly as the frequency departs from the 28.5-MHz design center. At 28.0 MHz, the antenna is essentially a lossy dipole.

That the patterns of the shortened Yagis degrade more quickly below design center is also reflected in the SWR bandwidth curves shown in **Figure 5**. Even the full-size Yagi shows a steeper SWR curve below design center than above. The 12-foot model is well off match at 28 MHz, while the 8-foot model reaches a similar departure from match only 250 kHz below design center. The curves suggest that the antennas are best designed for a lower center frequency, because the SWR increases slowly above that frequency. However sound that conclusion may be with respect to the full-size Yagi, it tells only part of the story with respect to the shortened models. One must also account for the degrading front-to-back ratio as the frequency departs upward from the center.

Do the numbers condemn the shortest model? Not necessarily. Whether a particular antenna is right to build depends upon a collection of factors that perhaps only the user can balance. A full-size 2-element Yagi exhibits good gain within its class, about 2 S-units of front-to-back ratio, and a broad bandwidth—all at the expense of a larger physical structure. The 12-foot model shows a decreased bandwidth with respect to front-to-back ratio and SWR, but it maintains reasonably good gain and up to 3 S-units of front-to-back ratio with a size only three-fourths that of the full-size Yagi. The 8-foot model holds the appeal of a truly portable Yagi with some gain and 3 S-units of front-to-back ratio at its design center frequency. However, its gain is significantly reduced and its bandwidth is quite narrow. Moreover, with a feedpoint resistance in the neighborhood of 12 ohms, the ratio of loss resistance to radiation resistance is much increased. Nevertheless, a small antenna with some gain over a dipole and a good front-to-back ratio over a narrow bandwidth can have many uses.

Both shortened antennas were modeled for patterns and SWR bandwidth curves at a center-load Q of 300, that obtainable on the 12-foot model with a linear-loading element. It is dubious whether such a Q could be sustained for

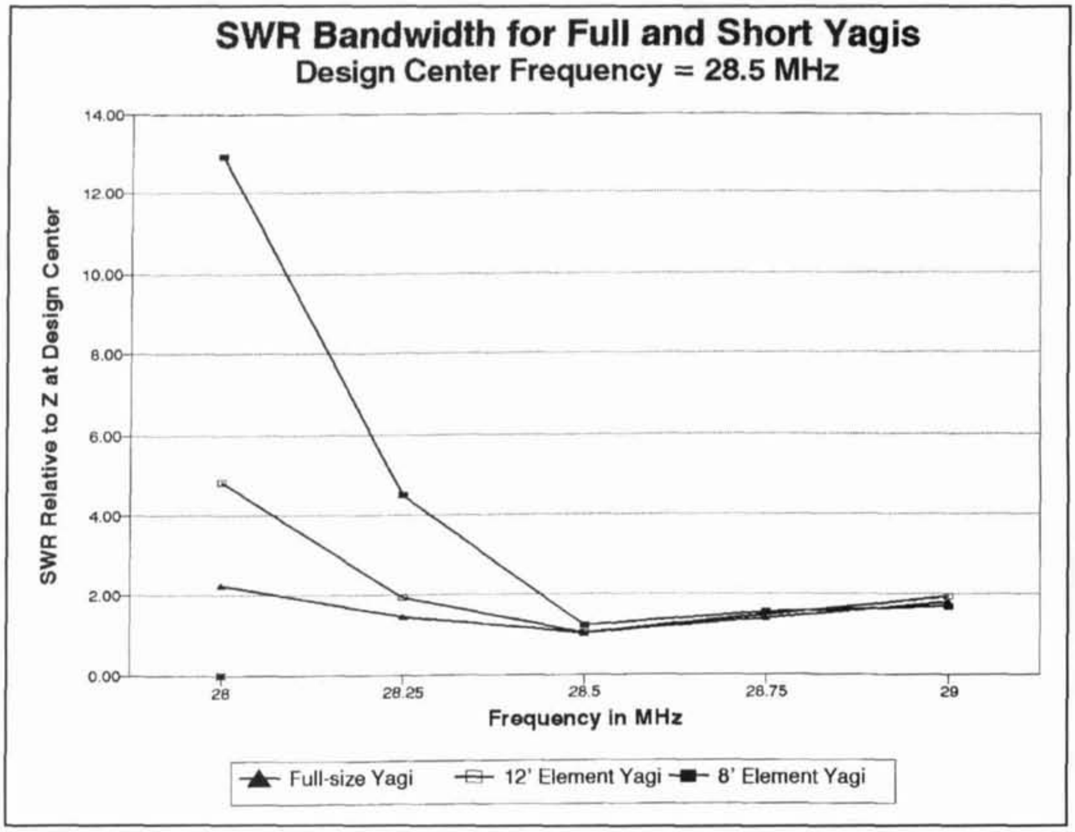

Figure 5. A comparison of the SWR bandwidths of full-size and shortened Yagis with 12 and 8-foot elements. The shortened Yagi loading coils are assigned a Q of 300.

either the 12 or 8-foot model with inductive loading. Connection losses, weathering losses, and other factors are likely to reduce the Q of even the most elegant loading coil assemblies to levels below 100 unless the antenna is often cleaned or is operated within a protected environment. Unfortunately, as **Table 2**'s data would suggest, these further reductions in gain might make the antenna less attractive as it weathers. However, for portable use—where assembly and disassembly provide reminders to clean all connections—the antenna may have its niche in the array of antennas in amateur use.

Like almost every other final evaluation question we have encountered, the inquiry, "How short can we go?", has no single reply. User needs, competing designs, parts availability, and building skills all contribute to the final answer for each ham.

REFERENCE

1. Glenn Blackwell, K4HJJ, "A Half-size Two-Element Beam with a Full Size Punch," *10-10 International News*, 33 (Spring 1995), 6.

PRODUCT INFORMATION

High Performance Digital Satellite Upconverter

RF Prototype Systems has a RFPS Digital Satellite Upconverter for testing multirate DVB/MPEG-2 compatible QPSK settop receivers and modems, in both the R&D and Production Test environments. It can also be used in analog DES receivers and PCS systems.

The Upconverter accepts digital or analog modulator outputs at 70 or 140 MHz, and translates them directly to the 950–2250 MHz input band of DBS/DSS receivers, eliminating the need to set up a complete C or Ku band upconverter to LNB conversion chain. It has been designed to provide the amplitude, group delay, phase noise and spurious output performance needed to support QPSK receiver testing at symbol rates between 1 and 45 MSPS. It offers several convenience features, including switchable IF inputs, an input for noise injection at the IF, and an auxiliary output at 480 MHz for demodulator testing at the Tuner IF output frequency.

For more information, contact RF Prototype Systems, 9400 Activity Road, Suite J, San Diego, CA 92126; phone 619-689-9715; fax 619-689-9733; or toll-free outside California 800-874-8037.

CQ Books

McCoy on Antennas, by Lew McCoy, W1ICP
This is truly a unique antenna book that's a must for every amateur. Unlike many technical publications, Lew presents his invaluable information in a casual, non-intimidating way for anyone! **Order No. MCCOY.....$15.95**

Building and Using Baluns and Ununs, by Jerry Sevick, W2FMI
This volume is the definitive source for the latest information and designs on transmission line transformer theory. Discover new applications for dipoles, yagis, log periodics, beverages, antenna tuners, and countless other examples.
Order No. BALUN.....$19.95

The NEW Shortwave Propagation Handbook, by W3ASK, N4XX & K6GKU
The most comprehensive source of information on HF propagation is available from CQ! Read about propagation principles, sunspots, ionospheric predictions with photography, charts and tables galore—it's all in this unique reference volume!
Order No. SWP....$19.95

The Packet Radio Operator's Manual, by Buck Rogers, K4ABT
CQ has published an excellent introduction and guide to packet operation. It's the perfect single source, whether you're an advanced user or just starting out.
Order No. PROM..... $15.95

1996 Amateur Radio Almanac, 3rd Edition, by Doug Grant, K1DG
This volume is filled with over 500 pages of ham radio facts, figures and information. CQ's almanac is a resource you'll refer to over and over again. If it's ham radio, it's in The Source! **Order No. BALM96.....$19.95**

Available from CQ

Title	Order No.	Price
ARRL Antenna Book	ARRLAB	$30
ARRL Handbook (1996 Ed. w/software)	ARRLHB	$38
ARRL Operating Manual (New Ed.)	ARRLOM	$22
ARRL Repeater Directory ('95-'96)	ARRLRD	$7
ARRL Antenna Compendium Vol. 1	ARRANT1	$10
ARRL Antenna Compendium Vol. 2	ARRANT2	$12
ARRL Antenna Compendium Vol. 3	ARRANT3	$14
ARRL Antenna Compendium Vol. 4	ARRANT4	$20
ARRL Weather Satellite Handbook	ARSAT	$20
ARRL FCC Rule Book (new)	ARFCC	$12
ARRL World Map	ARMAP	$12
ON4UN Antennas and Techniques for Low Band DXing	LOWDX	$20
1996 NA Callbook	NACB	$35
1996 Int'l Callbook	INTCB	$35
1996 Callbook Pair	NAICB	$65
1996 Callbook on CD-ROM (New)	CBCD	$49
Gordon West No-Code Technician Plus License Manual	GWTM	$10

We carry all ARRL products!

CQ Books

The Quad Antenna, by Bob Haviland, W4MB
This is the authoritative book on the design, construction, characteristics and applications of quad antennas.
Order No. QUAD..... $15.95

Keys, Keys, Keys, by Dave Ingram, K4TWJ
Enjoy nostalgia with this visual celebration of amateur radio's favorite accessory.
Order No. KEYS.....$9.95

The VHF"How-To" Book, by Joe Lynch, N6CL
This book is the perfect operating guide for the new and experienced VHF enthusiast.
Order No. BVHF.....$15.95

The Vertical Antenna Handbook, by Paul Lee
Learn basic theory and practice of the vertical antenna. Discover easy-to-build construction projects for anyone!
Order No. VAH..... $9.95

For Faster Service Fax (516)-681-2926

CQ's Video Library

Also in PAL format

Getting Started in Ham Radio
This is an excellent video introduction to ham radio. CQ's experts show how to select equipment and antennas, which bands to use, how to use repeater stations, the importance of grounding and the basics of soldering.
Order No. VHR $19.95

Getting Started in Packet Radio
This video will help de-mystify packet radio for you. Get started using your computer on the radio. Included are step-by-step instructions on making packet contacts and using packet bulletin boards, networks and satellites.
Order No. VPAC.. $19.95

Getting Started in Contesting
For the newcomer to contesting or experienced veteran, this video is for you! You'll get advice and operating tips from contesting's most successful competitors, including Ken Wolff, K1EA, and CQ's own contest columnist, John Dorr, K1AR. **Order No. VCON $19.95**

Getting Started in Amateur Satellites
Learn how veteran operators set up their satellite stations. Locate and track ham satellites with ease. Watch operators access current satellites and make contacts around the world. **Order No. VSAT..... $19.95**

Getting Started in DXing
Top DXers share their experience with equipment, antennas, operating skills, and QSLing. You'll see hams work rare DX. If you're new to DXing, this video is for you! **Order No. VDX..... $19.95**

Getting Started in VHF
This is the ideal introduction to VHF. See demonstrations of the latest radios. Also, learn about repeater usage, packet, satellites as well as the more exotic VHF operating modes. **Order No. VVHF....$19.95**

Ham Radio Horizons: The Video
Discover all aspects of ham radio ranging from what it takes to get started to how to get your ham license. Ideal for public events or as an opening to your club's licensing courses! **Order No. VHOR.....$19.95**

YES! I want to learn from the experts. Rush me my book(s), video(s) right away!

Qty	Item #	Description	Price	Total Price
		Please add $4 shipping & handling. FREE shipping & handling for orders $50 and over.	Shipping/Handling	
		NY State Residents add applicable sales tax.	Total	

Name ____________________ Callsign ____________

Address ____________________

City ____________ State ________ Zip ________

Form of payment: ☐ MC ☐ VISA ☐ AMEX ☐ Discover ☐ Check ☐ Money Order

Credit Card # ____________________ Expires ________

Please mail your orders to: **CQ Communications, Inc., 76 North Broadway, Hicksville, New York 11801-9962 • Phone 516-681-2922**

ADVERTISER'S INDEX

We'd like to see your company listed here too. Contact Arnie Sposato, N2IQO, at (516)681-2922 or FAX at (516)681-2926 to work out an advertising program to suit your needs.

ASTRON CORPORATION
9 Autry
Irvine, CA 92718
(714) 458-7277 • FAX (714) 458-0826


MODEL VS-50M

ASTRON POWER SUPPLIES

• HEAVY DUTY • HIGH QUALITY • RUGGED • RELIABLE •

SPECIAL FEATURES

- *SOLID STATE ELECTRONICALLY REGULATED*
- FOLD-BACK CURRENT LIMITING Protects Power Supply from excessive current & continuous shorted output
- CROWBAR OVER VOLTAGE PROTECTION on all Models except RS-3A, RS-4A, RS-5A, RS-4L, RS-5L
- MAINTAIN REGULATION & LOW RIPPLE at low line input Voltage
- HEAVY DUTY HEAT SINK • CHASSIS MOUNT FUSE
- THREE CONDUCTOR POWER CORD except for RS-3A
- ONE YEAR WARRANTY • MADE IN U.S.A.

PERFORMANCE SPECIFICATIONS

- INPUT VOLTAGE: 105-125 VAC
- OUTPUT VOLTAGE: 13.8 VDC ± 0.05 volts (Internally Adjustable: 11-15 VDC)
- *RIPPLE Less than 5mv peak to peak (full load & low line)*

SL SERIES

• LOW PROFILE POWER SUPPLY

MODEL	Colors Gray	Colors Black	Continuous Duty (Amps)	ICS* (Amps)	Size (IN) H × W × D	Shipping Wt. (lbs)
SL-11A	•	•	7	11	2 5/8 × 7 5/8 × 9 3/4	12
SL-11R	•	•	7	11	2 5/8 × 7 × 9 3/4	12
SL-11R-MC		•	7	11	5 3/4 × 7 1/4 × 9 3/4	13
SL-11R-GE	•		7	11	5 3/4 × 7 × 9 3/4	13
SL-11R-RA		•	7	11	4 3/4 × 7 × 9 3/4	13
SL-11R-EFJ		•	7	11	5 1/8 × 7 1/4 × 9 3/4	13
SL-11MG		•	7	11	5 1/8 × 7 1/16 × 9 3/4	13
SL-15R	•	•	12	15	2 5/8 × 7 × 9 3/4	13
SL-15R-GE	•		12	15	5 1/8 × 7 5/8 × 9 3/4	14
SL-15R-RA		•	12	15	4 3/4 × 7 1/4 × 9 3/4	14
SL-15R-EFJ		•	12	15	5 1/8 × 7 1/16 × 9 3/4	14

RS-L SERIES

• POWER SUPPLIES WITH BUILT IN CIGARETTE LIGHTER RECEPTACLE

MODEL		Continuous Duty (Amps)	ICS* (Amps)	Size (IN) H × W × D	Shipping Wt. (lbs)
RS-4L	•	3	4	3 1/2 × 6 1/8 × 7 1/4	6
RS-5L	•	4	5	3 1/2 × 6 1/8 × 7 1/4	7

RM SERIES

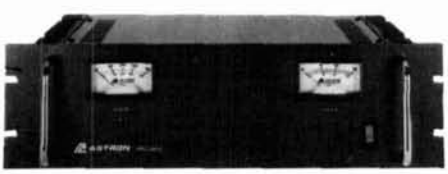
MODEL RM-35M

• 19" RACK MOUNT POWER SUPPLIES

MODEL	Continuous Duty (Amps)	ICS* (Amps)	Size (IN) H × W × D	Shipping Wt. (lbs)
RM-12A	9	12	5 1/4 × 19 × 8 1/4	16
RM-35A	25	35	5 1/4 × 19 × 12 1/2	38
RM-50A	37	50	5 1/4 × 19 × 12 1/2	50
RM-60A	50	55	7 × 19 × 12 1/2	60
• Separate Volt and Amp Meters				
RM-12M	9	12	5 1/4 × 19 × 8 1/4	16
RM-35M	25	35	5 1/4 × 19 × 12 1/2	38
RM-50M	37	50	5 1/4 × 19 × 12 1/2	50
RM-60M	50	55	7 × 19 × 12 1/2	60

RS-A SERIES


MODEL RS-7A

MODEL	Colors Gray	Colors Black	Continuous Duty (Amps)	ICS* (Amps)	Size (IN) H × W × D	Shipping Wt. (lbs)
RS-3A		•	2.5	3	3 × 4 3/4 × 5 3/4	4
RS-4A	•	•	3	4	3 3/4 × 6 1/2 × 9	5
RS-5A		•	4	5	3 1/2 × 6 1/8 × 7 1/4	7
RS-7A	•	•	5	7	3 3/4 × 6 1/2 × 9	9
RS-7B	•	•	5	7	4 × 7 1/2 × 10 3/4	10
RS-10A	•	•	7.5	10	4 × 7 1/2 × 10 3/4	11
RS-12A	•	•	9	12	4 1/2 × 8 × 9	13
RS-12B		•	9	12	4 × 7 1/2 × 10 3/4	13
RS-20A	•	•	16	20	5 × 9 × 10 1/2	18
RS-35A	•	•	25	35	5 × 11 × 11	27
RS-50A	•		37	50	6 × 13 3/4 × 11	46
RS-70A	•		57	70	6 × 13 3/4 × 12 1/8	48

RS-M SERIES


MODEL RS-35M

MODEL	Continuous Duty (Amps)	ICS* (Amps)	Size (IN) H × W × D	Shipping Wt. (lbs)
• Switchable volt and Amp meter				
RS-12M	9	12	4 1/2 × 8 × 9	13
• Separate volt and Amp meters				
RS-20M	16	20	5 × 9 × 10 1/2	18
RS-35M	25	35	5 × 11 × 11	27
RS-50M	37	50	6 × 13 3/4 × 1	46
RS-70M	57	70	6 × 13 3/4 × 12 1/8	48

VS-M AND VRM-M SERIES


MODEL VS-35M

• Separate Volt and Amp Meters • Output Voltage adjustable from 2-15 volts • Current limit adjustable from 1.5 amps to Full Load

MODEL	Continuous Duty (Amps) @13.8VDC	Continuous Duty (Amps) @10VDC	Continuous Duty (Amps) @5VDC	ICS* (Amps) @13.8V	Size (IN) H × W × D	Shipping Wt. (lbs)
VS-12M	9	5	2	12	4 1/2 × 8 × 9	13
VS-20M	16	9	4	20	5 × 9 × 10 1/2	20
VS-35M	25	15	7	35	5 × 11 × 11	29
VS-50M	37	22	10	50	6 × 13 3/4 × 11	46
VS-70M	57	34	16	70	6 × 13 3/4 × 12 1/2	48
• Variable rack mount power supplies						
VRM-35M	25	15	7	35	5 1/4 × 19 × 12 1/2	38
VRM-50M	37	22	10	50	5 1/4 × 19 × 12 1/2	50

ICS - Intermittent Communication Service (50% Duty Cycle 5 min. on 5 min. off)

"I never opened the manual for my HP 8920A."

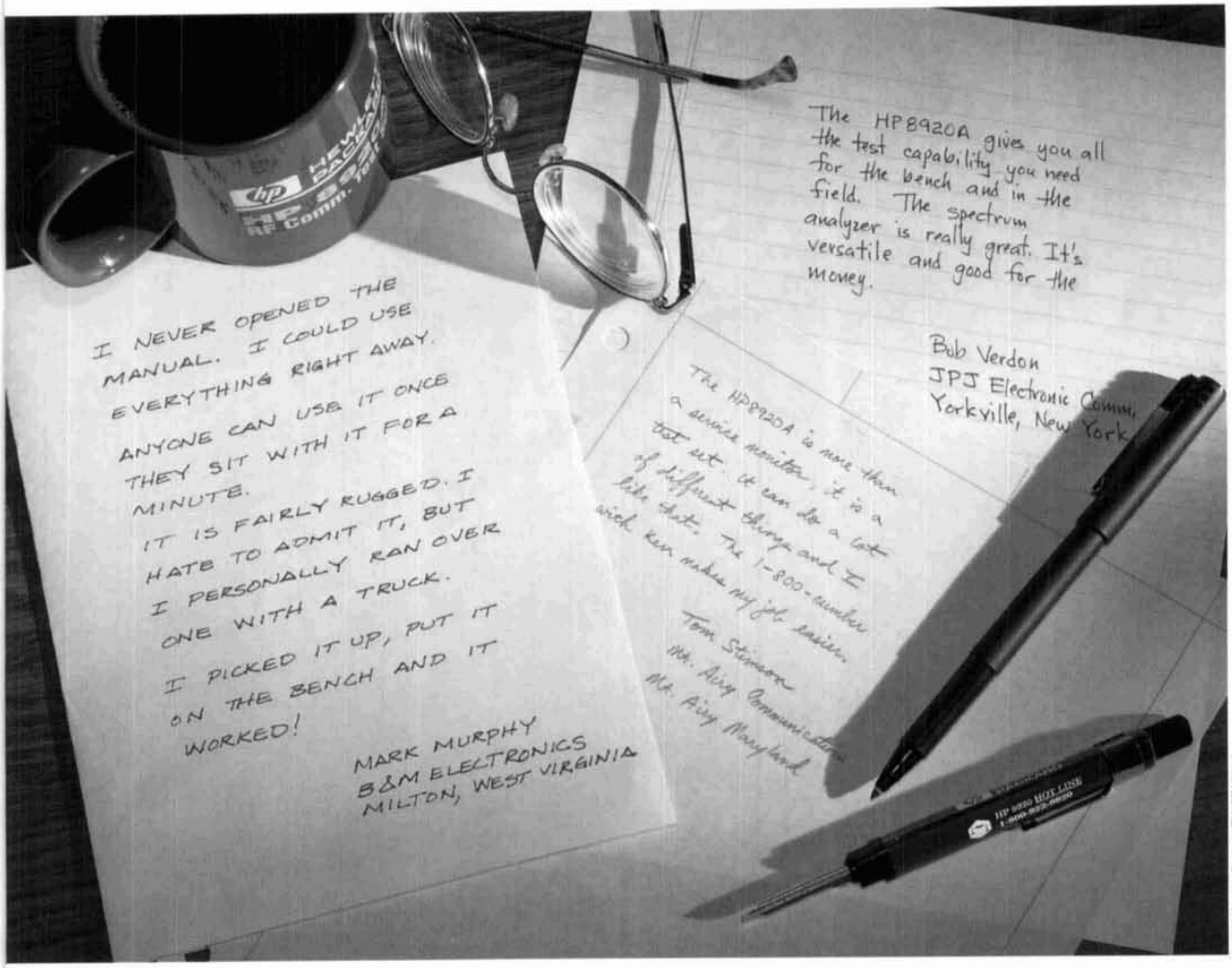

Either the new HP 8920A RF Communications Test Set is easy to use, or the people who use it are particularly intuitive.

We can't vouch for the latter, but there's a lot we can offer about the former. Like what, you ask? Like the fact that virtually every RF test you'll ever need to do is available at the push of a front-panel button.

The result? You get your job done faster. And better. Because the HP 8920A provides high-performance spectrum analysis, built-in encode/decode capabilities for paging and trunking, and easy-to-use software for fast, repeatable, documented results.

Speaking of pushing buttons, just push **1-800-344-3802** and ask for **Charlie**. There are many seasoned vets who can answer all your questions. They can also give you the details on how to get the HP 8920A for under $12,500.

The HP 8920A — the end of manual labor.

Latest Enhancements

- Variable frequency notch filter for SINAD (300 Hz to 10 kHz)
- 5% power measurement accuracy
- Signal/noise ratio measurement
- Adjacent channel power measurement

There is a better way.

HEWLETT® PACKARD